Examining Mechanisms of Altered Skeletal Muscle Cellular Passive Mechanics in the Context of Acute Fatigue and Age

by

Grace Elise Privett

A dissertation accepted and approved in partial fulfillment of the

requirements for the degree of

Doctor of Philosophy

in Human Physiology

Dissertation Committee:

Damien Callahan, Ph.D., Chair

Michael Hahn, Ph.D., Core Member

Mark Miller, Ph.D., Core Member

Karina Nakayama, Ph.D., Core Member

Robert Guldberg, Ph.D., Institutional Representative

University of Oregon

Summer 2024

Dissertation Abstract

Grace Elise Privett

Doctor of Philosophy in Human Physiology

Title: Examining Mechanisms of Altered Skeletal Muscle Cellular Passive Mechanics in the Context of Acute Fatigue and Age

Skeletal muscle stiffness influences locomotor function and may predict soft-tissue injury risk. Recent literature suggests fatiguing exercise transiently reduces whole skeletal muscle stiffness, yet the underlying mechanisms remain unclear. Therefore, the **purpose** of this dissertation was to i) determine whether fatiguing exercise reduces cellular passive stress and Young's Modulus in conjunction with altered phosphorylation of the sarcomere protein titin, ii) extend these measures to samples of composite tissue, and iii) assess whether aging mediates the effect of fatigue on skeletal muscle passive mechanics. **Methods**: 9 young and 8 older males and females completed unilateral fatiguing exercise followed by biopsy of the fatigued and non-fatigued Vastus Lateralis. In younger adults, passive stress and strain were compared in fatigued versus non-fatigued single fibers and titin phosphorylation was quantified via liquid chromatography mass spectrometry (LC-MS, Aim 1). Cellular measures were then translated to bundles of 12-14 fibers with intact extracellular matrix (ECM, Aim 2). Finally, cellular and tissue-level mechanical measures were compared in young versus older adults (Aim 3). **Results**: We observed that fatiguing exercise reduced passive stress and Young's Modulus in myosin heavy chain (MHC) IIA and IIA/X fibers from young and older males, but not females. Titin phosphorylation was altered by fatiguing exercise, with no apparent sex-based differences. In-vitro treatments to phosphorylate or dephosphorylate titin did not support a direct link between titin phosphorylation and altered cellular passive mechanics. In bundles, fatiguing exercise only affected passive modulus in young females, and this fatigue-induced difference was at least partially due to titin. Aging did not affect cellular or bundle passive measures, nor did aging mediate the response to fatigue. **Discussion**: These data suggest that fatiguing exercise reduces cellular passive stress and modulus in muscle from older and younger males, in conjunction with altered titin phosphorylation. Furthermore, intracellular proteins appear to contribute to tissue mechanics, though their relative influence is unclear. Ultimately this study contributes to efforts aimed at understanding the chronic and acute mediators of skeletal muscle mechanics.

Publications

Privett, G. E., Ricci, A. W., Ortiz-Delatorre, J., & Callahan, D. M. (2024). Predicting myosin heavy chain isoform from postdissection fiber length in human skeletal muscle fibers. *American Journal of Physiology-Cell Physiology*, *326*(3), C749-C755.

Privett, G. E., Ricci, A. W., David, L. L., Wiedenfeld Needham, K., Tan, Y. H., Nakayama, K. H., & Callahan, D. M. (2024). Fatiguing exercise reduces cellular passive Young's modulus in human vastus lateralis muscle. *Experimental Physiology*.

Privett, G. E., Ricci, A. W., Wiedenfeld Needham, K., & Callahan, D. M. (2024). Chronic and Acute Mediators of Passive Viscoelasticity in Human Skeletal Muscle Fibers. *bioRxiv*, 2024-08. *Submitted to The Journal of Physiology August 24, 2024.

Acknowledgments

This project would not have been possible without Dr. Damien Callahan, who consistently provided patient guidance and invaluable feedback regarding technical skills, study design, presentation skills, professional skills, and writing. Thank you for taking a chance on the Kinesiology student who was once told she wasn't cut out for work requiring fine motor skills. I am also thankful for the support of my committee: Dr. Mike Hahn, Dr. Karina Nakayama, Dr. Mark Miller, and Dr. Robert Guldberg. Thank you for taking the time to share your knowledge and expertise throughout this process. Additionally, I thank the Wu Tsai Human Performance Alliance and the National Institute on Aging for supporting this research. For supporting my studies, I thank the Harvey E. Lee Graduate Scholarship, the Marthe E. Smith Memorial Science Scholarship, the Ursula Moshberger Scholarship, the Shapiro Family Scholarship, the Joseph K. Starr Scholarship, the Hill Fund Graduate Award, and the Leon Culbertson Scholarship.

Many thanks are due to Austin Ricci for his role in collecting, analyzing, and interpreting data that contributed to this dissertation. These assays are best conducted by a team, and I am so grateful for the awesome synergy that we developed over our years working together. Similarly, I am indebted to Karen Needham, who generously shared her time and expertise with me over the years. Karen, your insight was invaluable to me, the person who changed her major in undergraduate to avoid taking more chemistry classes. Thanks are due to Julissa Ortiz-Delatorre, Wesley Force, Meherbaan Khalsa, Jordan Cooper, Joshua Jaffe, and Mason Vaughn Brown for their contributions to this work. I would also like to thank Dr. Kiisa Nishikawa, whose insight regarding titin mechanics was crucial to these studies. Finally, I would like to thank members of the UO community who made this work possible: UO librarians (especially Annie Z-K) and members of the Hazardous Materials Group (especially Seth Sponcey).

I would like to recognize the support of my friends and family, especially my parents, sisters, grandparents and in-laws. Our regular phone calls and your visits to Eugene kept enthusiasm and motivation for this work high throughout this long but rewarding journey. Last, but certainly not least, I would like to thank my husband Scott and our small pack of pups (Sunny, Dustin, Bodie, Bailey) for their unending support and love through every single day spent earning this doctoral degree. You make the bright days brighter and the tough days lighter, and I will forever be grateful to have you on my team.

Dedication

Dedicated to Grandpa John, the original “Dr. Privett”. Thank you for teaching me to “never stop learning”.

Table of contents

Chapter Page

List of Figures

Figure Page

List of Supplementary Figures

Supplementary Figure Page

List of Tables

Table Page

List of Supplementary Tables

Supplementary Table Page

1. Introduction and Statement of the Problem

Although prior investigations have predominantly focused on active contractile performance, skeletal muscle passive stiffness has emerged as an important mediator of muscle function (Gajdosik, 2001; Azizi & Roberts, 2010; Marcucci & Reggiani, 2020). Through influence on rate and efficiency of force transduction from muscle to the tendon (Wilson & Flanagan, 2008), joint range of motion (Wilson *et al.*, 1991) and joint stability (Blackburn *et al.*, 2011), muscle stiffness impacts locomotion and functionality in everyday tasks. Indeed, some studies have linked altered musculotendinous stiffness to increased risk for soft tissue injury in athletes (Myer *et al.*, 2008*a*; De Ste Croix *et al.*, 2015) and changes to locomotor function and joint range of motion in older adults (Marcucci & Reggiani, 2020). Muscle stiffness is mediated by chronic factors such as aging (Eby *et al.*, 2015; Lim *et al.*, 2019; Noonan *et al.*, 2020*b*) and resistance training (Noonan *et al.*, 2020*a*), but acute modifiers are less understood. Previous studies using shear wave elastography (Andonian *et al.*, 2016; Siracusa *et al.*, 2019; Chalchat *et al.*, 2020) and B-mode ultrasound (Kubo & Ikebukuro, 2019) suggest that fatiguing exercise reduces whole skeletal muscle stiffness in passive and active conditions. Given that fatigue also affects joint kinematics (Kernozek *et al.*, 2008), and neuromuscular recruitment (Bouillard *et al.*, 2014; De Ste Croix *et al.*, 2015), fatigue-induced reduction of skeletal muscle stiffness may contribute to knee joint destabilization and subsequent soft tissue injury in athletes (Myer *et al.*, 2008*b*; Watsford *et al.*, 2010; Blackburn *et al.*, 2011). Specifically, reduced muscle stiffness decreases the amount of strain elastic energy that can be absorbed by a tissue before injury occurs (Mair *et al.*, 1996). When experienced in older adults, fatigue-induced muscle compliance may reduce joint stability and impair the ability to instantly adjust muscle function in response to perturbation, collectively contributing to increased falls risk following repeated and/or prolonged muscle activation (Morrison *et al.*, 2016). Despite the clear clinical implications of reduced musculotendinous stiffness following fatiguing exercise, the underlying mechanisms of this phenomenon, and whether they are mediated by biological sex, are not yet known.

Previous studies of fatigue-induced reductions of whole-muscle stiffness included exclusively (Siracusa *et al.*, 2019; Chalchat *et al.*, 2020) or predominantly (Andonian *et al.*, 2016) male participants. However, musculotendinous stiffness appears to be influenced by biological sex, with females exhibiting reduced passive stiffness of the gastrocnemius (Morse, 2011) and reduced active stiffness of the medial gastrocnemius tendon (Kubo *et al.*, 2003)

compared to males. These divergent mechanical properties have been attributed to the effects of sex hormones on whole-muscle (Chidi-Ogbolu & Baar, 2019; Ham *et al.*, 2020) and tendon (Hansen & Kjaer, 2016) stiffness. In muscle, estrogen appears to support the maintenance of mass and strength, metabolic function, and connective tissue collagen turnover and incorporation (Chidi-Ogbolu & Baar, 2019). Estrogen also renders ligaments and tendons more compliant in females compared to males (Hansen & Kjaer, 2016). More compliant connective tissues increase joint laxity, which likely increases risk of anterior cruciate ligament (ACL) injury (Myer *et al.*, 2008*a*). In fact, female athletes are more susceptible to knee injuries (Deitch *et al.*, 2006), commonly to the ACL (Arendt *et al.*, 1999; Matzkin & Garvey, 2019) than age-matched male athletes. By contrast, males experience greater inflammation following extreme muscle loading (Stupka *et al.*, 2000) and greater incidence of muscle strains in practice and competition (Cross *et al.*, 2013; Dalton *et al.*, 2015). To complicate matters further, the effect of the menstrual cycle on skeletal muscle stiffness is unclear, with some studies demonstrating varied active and passive whole-muscle stiffness throughout the menstrual cycle (Ham *et al.*, 2020) and others demonstrating no change (Bell *et al.*, 2011). Oral contraceptive (OC) use significantly attenuates cyclical estrogen fluctuations, and has therefore been studied as a possible approach to minimizing soft-tissue injury risk (Morse *et al.*, 2013; Konopka *et al.*, 2019). However, to date, consensus has not been reached, with some studies demonstrating altered muscle stiffness during OC use (Morse *et al.*, 2013), and others reporting no change (Bell *et al.*, 2011). Collectively, these studies suggest that biological sex does impact skeletal muscle stiffness, but the underlying mechanisms are poorly understood. Whether biological sex mediates acute reduction of muscle stiffness following fatiguing exercise is also unclear.

Skeletal muscle stiffness is impacted by intracellular (sarcomere proteins) and extracellular (extracellular matrix, ECM) elements, both of which are dynamic. In cases of chronic effectors of stiffness, such as aging (Wood *et al.*, 2014; Noonan *et al.*, 2020*b*; Pavan *et al.*, 2020) and physical exercise training (Noonan *et al.*, 2020*a*), altered stiffness is commonly attributed to the remodeling of ECM collagen. Interestingly, differences in cellular stiffness have been observed in chemically permeabilized single skeletal muscle fibers across age (Lim *et al.*, 2019; Noonan *et al.*, 2020*b*) and training status (Noonan *et al.*, 2020*a*), suggesting that intracellular proteins also contribute to chronic stiffness adaptations. Within muscle fibers,

passive stiffness is primarily determined by the viscoelastic protein titin (Ottenheijm *et al.*, 2012; Lim *et al.*, 2019). All three titin isoforms – two cardiac (N2B and N2BA) and one skeletal (N2A) – contain extensible (I-band) and non-extensible (A-band and M-band) regions. Titin isoform distribution can shift as a mechanism for tuning the stiffness of a muscle tissue. In cardiac muscle, shifts occur between N2B and N2BA isoforms (Bupha-Intr *et al.*, 2011), and in skeletal muscle the N2A isoforms vary in terms of titin splice variants that differ in size (Prado *et al.*, 2005). Acutely, titin extensible regions are subject to post-translational modifications (PTMs), many of which have the potential to alter titin-based stiffness in response to stimuli such as fatiguing exercise (Müller *et al.*, 2014).

Titin-based mechanisms of altered passive stiffness have been extensively studied in cardiac muscle, due to the clinical implications of altered cardiac titin for cardiomyopathies (Fukuda et al., 2005; Granzier & Irving, 1995; LeWinter & Granzier, 2014; Müller et al., 2014; Yamasaki et al., 2002). However, titin's role in modulating skeletal muscle stiffness has been of growing interest, revealing altered titin-based stiffness in conditions such as cerebral palsy (Mathewson *et al.*, 2014) and Ehler's Danlos Syndrome (Ottenheijm *et al.*, 2012). In both skeletal and cardiac muscle, the most studied titin PTM is phosphorylation. Phosphorylation sites have been identified in the immunoglobulin (Ig), PEVK, and unique sequence regions of the elastic I-band of titin, yet the locations of these phosphorylation sites vary across titin isoforms (Hamdani et al., 2017). One group (Müller *et al.*, 2014) demonstrated that a single bout of exercise was sufficient to modify titin phosphorylation in association with altered myocyte stiffness in murine cardiac muscle. These results suggest that altered titin phosphorylation may contribute to acute, exercise-induced changes in muscle stiffness. Furthermore, such changes may have implications for whole-muscle stiffness, given titin's influence on whole-muscle mechanical properties (Brynnel *et al.*, 2018).

A growing body of literature supports the notion that titin influences cardiac (Granzier & Irving, 1995; Yamasaki *et al.*, 2002; Fukuda *et al.*, 2005; Müller *et al.*, 2014; LeWinter & Granzier, 2014) and skeletal (Ottenheijm *et al.*, 2012; Mathewson *et al.*, 2014; Müller *et al.*, 2014; Brynnel *et al.*, 2018) muscle stiffness under passive conditions. Our overall approach was to leverage prior investigations that suggest fatigue, as a physiological stimulus, may alter titin phosphorylation and that modifications to titin may impact tissue stiffness. The contribution of

acute titin phosphorylation to regulation of skeletal muscle stiffness in humans remains unclear and, to our knowledge, has never been assessed at the cellular level. Therefore, the purpose of this study was to compare cellular passive stress and stiffness, quantified as passive Young's Modulus to account for potential variation in single fiber size, in skeletal muscle samples obtained from non-fatigued and fatigued vastus lateralis muscles of healthy young and older males and females. To interrogate potential mechanisms contributing to altered stiffness following fatigue, titin phosphorylation was compared in non-fatigued versus fatigued skeletal muscle samples using liquid chromatography coupled with high resolution mass spectrometry (LC-MS). We hypothesized that fatiguing exercise would reduce passive modulus in single fibers from males and females in conjunction with increased titin phosphorylation. Finally, passive modulus was measured in bundles of fibers with intact ECM from non-fatigued and fatigued skeletal muscle samples from a subset of older and younger participants to test the hypothesis that the effect of fatigue on skeletal muscle passive mechanics is evident at the tissue level. Furthermore, a subset of the included bundles was treated to chemically eliminate intracellular contributors to passive modulus to assess the extent to which intracellular mechanisms contribute to observations of altered bundle passive modulus after fatiguing exercise. We hypothesized that any effect of fatiguing exercise on measures of bundle stiffness would be abolished by elimination of intracellular contributors to passive modulus.

Ultimately, these studies contribute to a growing body of literature seeking to understand chronic (age) and acute (fatiguing exercise) mediators of skeletal muscle mechanics.

2. Literature Review

2A. Skeletal muscle mechanical properties affect muscle function and appear to differ by biological sex.

Skeletal muscle active and passive mechanical properties influence the rate and efficiency of force transduction from muscle to the tendon (Wilson & Flanagan, 2008), joint range of motion (Wilson *et al.*, 1991) and joint stability (Blackburn *et al.*, 2011), thereby impacting locomotion and functionality in everyday tasks. Skeletal muscle stiffness, the ability to actively or passively deform in response to an applied force, is dynamic and is chronically altered by resistance training (Magnusson, 1998; Noonan *et al.*, 2020*a*) and aging (Marcucci & Reggiani, 2020; Noonan *et al.*, 2020*b*; Kennedy *et al.*, 2020). In both cases, altered stiffness is attributed to collagen remodeling. However, observations of altered stiffness at the cellular level, presumably devoid of extracellular matrix, have also been made in aged (Lim *et al.*, 2019; Noonan *et al.*, 2020*b*) and trained (Noonan *et al.*, 2020*a*) muscle, suggesting that intracellular mechanisms may also contribute to chronic stiffness alteration.

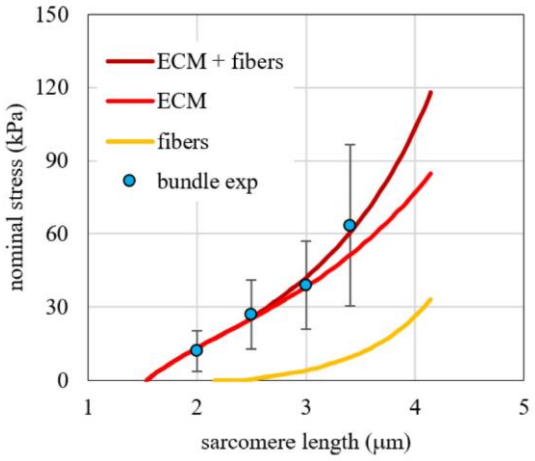

Figure 1. Marucci et al., 2019 demonstrated the differing mechanical properties of single fibers, fiber bundles, and extracellular matrix. Single fibers and fiber bundles will be utilized in these proposed studies.

The passive stiffness of whole skeletal muscle is provided by two primary, load-bearing structures: muscle fibers, the passive properties of which are attributed to the giant elastic protein titin, and the extracellular matrix (ECM) of connective tissue that surrounds the muscle fibers (Lieber & Binder-Markey, 2021). The relative contribution of these two elements to skeletal muscle passive stiffness has been contested in recent years. The consensus appears to be that ECM is the primary source of whole muscle and fascicle stiffness (Ward *et al.*, 2020), whereas titin dominates single fiber stiffness (Ottenheijm *et al.*, 2012; Lim *et al.*, 2019). However, these elements are not mutually exclusive. Recent evidence suggests titin can directly modify whole-muscle stiffness in mice (Brynnel *et al.*, 2018). Another study suggests single fiber stiffness is predominantly determined by ECM (Noonan *et al.*, 2020*c*), though these later results must be interpreted with caution, as methods of single fiber

preparation (mechanical fiber dissection followed by chemical permeabilization) are understood to leave little more than basement membrane remaining. For this reason, studies seeking to measure ECM stiffness on the cellular level utilize samples of muscle fibers dissected along with intact extracellular elements (Meyer & Lieber, 2011; Marcucci *et al.*, 2019). Such studies have produced passive stress measures for single fibers, bundles of fibers, and ECM allowing for comparison of relative mechanical properties (Figure 1). Interestingly, single fibers and bundles of fibers with intact ECM exhibit stress-length curves that are similar in shape to each other yet distinct from that of ECM alone, which may suggest that single fiber properties are evident at the tissue level.

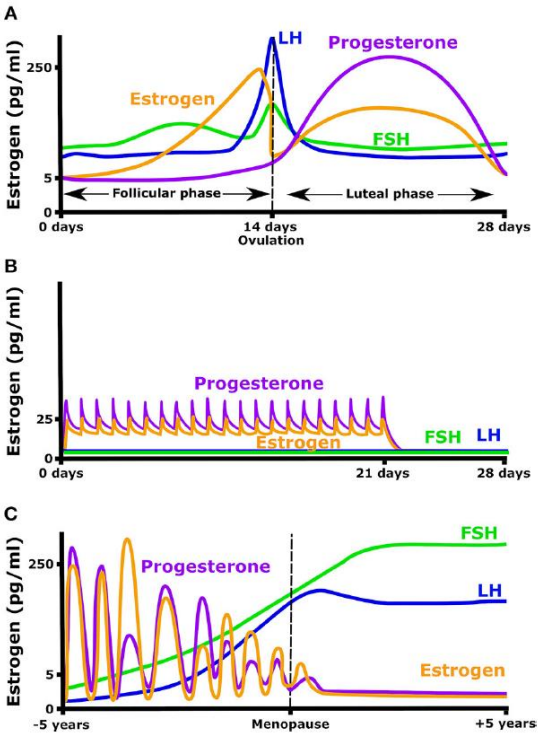

Figure 2. Chidi-Ogbolu & Baar, 2019 illustrated the changes in circulating hormone concentration during normal menstruation (A), oral contraceptive use (B) and menopause (C). Of these hormones, estrogen has been extensively studied due to its impact on musculotendinous mechanical properties.

Muscle stiffness appears to be influenced by biological sex, with females exhibiting markedly reduced muscle stiffness compared to males (Kubo *et al.*, 2003; Morse, 2011). These divergent mechanical properties have been attributed to the effects of sex hormones on whole-muscle (Chidi-Ogbolu & Baar, 2019; Ham *et al.*, 2020) and tendon (Hansen & Kjaer, 2016) stiffness. The effects of biological sex hormones on muscle and connective tissue properties have been well described by a recent review (Chidi-Ogbolu & Baar, 2019) in which authors conclude that estrogen impacts muscle metabolic function and connective tissue collagen turnover and incorporation. In muscle, estrogen appears to support the maintenance of muscle mass and strength (Chidi-Ogbolu & Baar, 2019). Furthermore, age-related decline in estrogen (Figure 2) contributes to the loss of muscle mass and strength. Regarding musculotendinous stiffness, estrogen appears to render ligaments and tendon more compliant in females compared to males. More compliant connective tissues increase joint laxity, which was demonstrated to contribute to increased risk injury to the anterior

cruciate ligament (ACL, Myer *et al.*, 2008*a*). In fact, female athletes do experience ACL tears at a higher rate than male athletes (Arendt *et al.*, 1999). To complicate matters further, the effect of the menstrual cycle on whole-muscle stiffness is unclear, with some evidence of stiffness variation throughout the menstrual cycle (Ham *et al.*, 2020) and other evidence of no change (Bell *et al.*, 2011). Oral contraceptive (OC) use appears to ameliorate cyclical estrogen fluctuations (Figure 2), and has therefore been studied as a possible approach to minimizing soft-tissue injury risk (Morse *et al.*, 2013; Konopka *et al.*, 2019). While some studies have demonstrated altered muscle stiffness during OC use (Morse *et al.*, 2013), other studies have observed no change in stiffness during OC use (Bell *et al.*, 2011). During menopause, females experience precipitous declines in circulating estrogen (Figure 2), which may compound age-related increases in musculotendinous stiffness (Eby *et al.*, 2015; Marcucci & Reggiani, 2020). In fact, one study (Eby *et al.*, 2015) utilized shear wave elastography to demonstrate increased shear modulus in females compared to males aged 60 years and older, suggesting a reversal of the effect of estrogen on stiffness in younger males and females (Kubo *et al.*, 2003; Morse, 2011). Collectively, these studies suggest that biological sex does impact whole-muscle stiffness, but the underlying mechanisms are poorly understood.

Female athletes are at higher risk for knee injuries (Deitch *et al.*, 2006), especially to the ACL (Arendt *et al.*, 1999; Matzkin & Garvey, 2019), whereas males experience males experience greater inflammation following extreme muscle loading (Stupka *et al.*, 2000) and greater incidence of muscle strains in practice and competition (Cross *et al.*, 2013; Dalton *et al.*, 2015). Because risk of soft tissue injury increases during game play (Gleim & McHugh, 1997; Witvrouw *et al.*, 2004; Watsford *et al.*, 2010; De Ste Croix *et al.*, 2015), further study into the sex-based differences in mediators of skeletal muscle stiffness during fatiguing exercise is critical.

2B. Intra-cellular mechanisms may contribute to changes in muscle stiffness.

The intracellular protein titin is 3.4-3.7 MDa (Krüger & Kötter, 2016) and spans the half sarcomere from Z-disc to M-band (Tonino *et al.*, 2017). Cellular stiffness is largely determined by titin (Ottenheijm *et al.*, 2012; Lim *et al.*, 2019), and there is evidence to support its role in mediating whole-muscle passive stiffness (Brynnel *et al.*, 2018). Titin contains extensible (I-band) and non-extensible regions (A-band and M-band) regions. The functionally stiff (Prado *et al.*, 2005) A- and M-bands of titin reside within the thick filament and therefore do not contribute

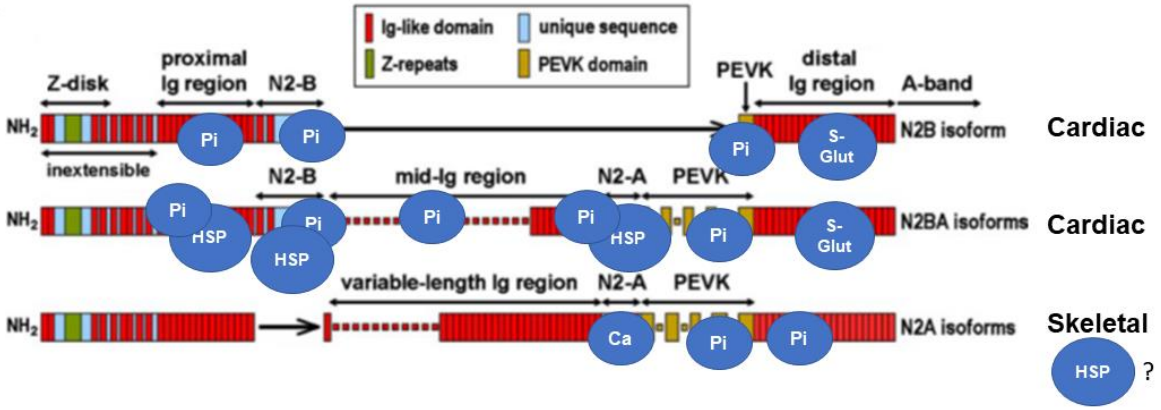

Figure 3. Titin post-translational modifications have been well characterized in cardiac muscle. Emerging evidence suggests extensive post-translational modification to skeletal titin, as well. It is unclear where HSP interacts with skeletal titin. Graphic depicting the I-band titin region adapted from Linke & Grützner, 2008. Pi = phosphorylation, S-Glut = glutathionylation, HSP = heat shock protein, Ca = calcium binding.

to titin-based stiffness. On the other hand, the differentially spliced domains of the titin I-band region (Figure 3) act as molecular springs that are unique to cardiac or skeletal muscle. Titin domains common to both tissues include proximal immunoglobulin (Ig) domains, PEVK domain, and the distal Ig domains (Linke & Grützner, 2008). Structural diversity arises from inclusion of N2B unique sequences (cardiac), N2A elements (skeletal and one cardiac isoform), and the variable length of the mid-Ig region (Prado *et al.*, 2005; Linke & Grützner, 2008). Consistent across isoforms is the contribution of the viscoelastic I-band (Linke & Grützner, 2008) to titin-based mechanical properties (Hamdani *et al.*, 2017; Tonino *et al.*, 2017). The characteristic viscoelastic nature of titin is attributed to Ig domains, with some contribution from the PEVK segment (Minajeva *et al.*, 2001; Herzog *et al.*, 2015). Specifically, proximal Ig domains unfold up to sarcomere lengths of ~ 2.7 µm, after which the PEVK segment extends, and this unfolding is believed to be highly viscoelastic (Nishikawa, 2020). This unfolding behavior explains the stress-relaxation observed during length hold maneuvers (Figure 10) as well as the hysteresis observed when a stretched muscle is returned to original length (Figure 4).

Titin stiffness is chronically altered by differential isoform expression (Prado *et al.*, 2005) and transiently altered by binding of heat shock proteins (Kötter *et al.*, 2014) or calcium (Nishikawa, 2020), through S-Glutathionylation (Alegre-Cebollada *et al.*, 2014; Watanabe *et al.*, 2020), or other post-translational modifications (PTM, Hamdani *et al.*, 2017) to the protein. Cardiac and skeletal titin are acted upon by multiple PTMs, the most studied of which is

phosphorylation. Phosphorylation sites have been identified in the immunoglobulin (Ig), PEVK, and unique sequence regions of the elastic I-band of titin (Hamdani *et al.*, 2017). The double negative charge of inorganic phosphate is speculated to inhibit Ig domain re-folding when bound, thereby reducing titin stiffness (Hamdani *et al.*, 2017). Support for this working hypothesis stems from the observation that S-Glutathionylation inhibits Ig domain refolding (Alegre-Cebollada *et al.*, 2014) thereby reducing skeletal myocyte passive stiffness (Watanabe *et al.*, 2020). Perhaps the same phenomenon occurs following Ig domain phosphorylation. However, few phosphorylation events have been experimentally demonstrated to alter titin-based passive stiffness, to date (Krüger & Linke, 2006*a*; Müller *et al.*, 2014; Hamdani *et al.*, 2017).

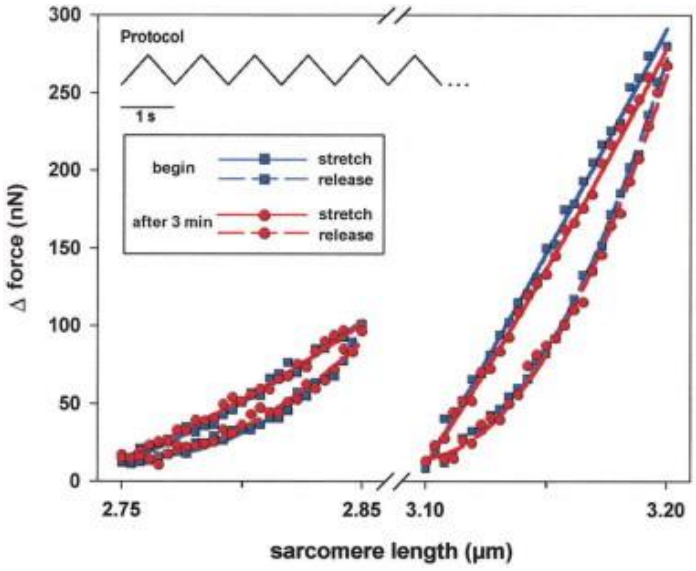

Figure 4. Figure from Minajeva et al., 2001 demonstrating the non-linear return of force during a repeated stretch-release maneuver of a single psoas muscle fiber. Observed hysteresis is attributed to the kinetics of Ig domain re-folding.

The effects of titin phosphorylation have been extensively studied in cardiac muscle due to implications for cardiac myopathies. Cyclic adenosine monophosphate (c-AMP)-dependent protein kinase A (PKA) (Yamasaki *et al.*, 2002; Fukuda *et al.*, 2005; Krüger & Linke, 2006*a*; Müller *et al.*, 2014) and cyclic guanosine monophosphate (c-GMP)-dependent protein kinase G (PKG) (Krüger *et al.*, 2009) phosphorylate the cardiac N2Bus region, thereby decreasing titin-based stiffness. Ca^{2+}/calmodulin-dependent protein kinase II δ (CaMKIIδ) phosphorylates the PEVK region to decrease titin-based passive stiffness (Hamdani *et al.*, 2013). Conversely, Ca^{2+}-dependent protein kinase C (PKC) (Hidalgo Carlos *et al.*, 2009; Müller *et al.*, 2014; Hamdani *et al.*, 2017) phosphorylates the PEVK region of cardiac titin to increase titin-based stiffness.

Less is known about phosphorylation of human skeletal muscle titin, but emerging evidence suggests it may be mediated by exercise. Increased phosphorylation of the PEVK region has been demonstrated in chronic (Ottenheijm *et al.*, 2012) and acute (Müller *et al.*, 2014)

conditions. Notably, differential phosphorylation of the PEVK region has been demonstrated in exercised murine skeletal muscle (Müller *et al.*, 2014; Hidalgo *et al.*, 2014). Hyperphosphorylation was observed at serine 12022, believed to be regulated by CaMKIIδ signaling yet decreased phosphorylation was observed at serine 11878, a site believed to be regulated by PKC (Müller *et al.*, 2014; Hidalgo *et al.*, 2014). LC-MS data from our lab suggest exercise-induced phosphorylation of distal Ig domains in human vastus lateralis muscle (Figure 13). These results demonstrate that a single, acute bout of exercise is sufficient to trigger signaling pathways that affect titin. Furthermore, they highlight the complexity of PTM-driven changes to titin, due to the large number of PTM events that can occur along the giant protein. In another study, cAMP-dependent PKA was shown to phosphorylate titin in rat diaphragm (Krüger & Linke, 2006*a*), demonstrating another signaling mechanism, present during exercise, that can potentially tune titin-based stiffness. Collectively, many signaling pathways, including β-adrenergic pathways activated during exercise, appear to trigger phosphorylation events along the titin molecule. These acute modifications render titin an intriguing candidate for a mediator of transient changes to skeletal muscle stiffness. Our preliminary evidence of titin phosphorylation in human skeletal muscle warrants further investigation into the possible role of titin phosphorylation in mediating fatigue-induced changes in skeletal muscle stiffness.

2C. Fatiguing exercise alters muscle stiffness.

Recent reports using shear wave elastography (Andonian *et al.*, 2016; Siracusa *et al.*, 2019; Chalchat *et al.*, 2020) or B-mode ultrasound (Kubo *et al.*, 2001) suggest that a single bout of fatiguing exercise reduces the passive stiffness of skeletal muscle and tendon structures (vastus lateralis tendon and aponeurosis), respectively. In athletes, fatigue-induced stiffness reduction contributes to joint instability, thereby increasing risk of soft tissue injury during game play (Gleim & McHugh, 1997; Witvrouw *et al.*, 2004; Watsford *et al.*, 2010; De Ste Croix *et al.*, 2015). In adults, fatigue has been linked to increased falls risk (Morrison *et al.*, 2016) due to altered locomotor control and joint range of motion (Marcucci & Reggiani, 2020). In whole muscle, the mechanisms underlying fatigue-induced muscle compliance are unclear due to the multitude of systemic inputs. For example, exercise increases body temperature, which increases intramuscular connective tissue compliance (Strickler *et al.*, 1990). Additionally, fatigue-induced

buildup of inorganic phosphate may impair the attachment of myosin heads to the thick filament (Debold, 2012; Debold *et al.*, 2016), reducing the contribution of residual crossbridge formation to skeletal muscle passive stiffness (Campbell & Lakie, 1998). Fatigue-induced changes to motor control impact the distribution of activation across a muscle group (Bouillard *et al.*, 2014), thereby diversifying fatigue-induced mechanical alterations across the muscles. In short, the multitude of inputs contributing to whole-muscle stiffness alteration complicates the understanding of underlying, intrinsic mechanisms of fatigue-induced compliance.

Considering the effect of single muscle fiber function on whole muscle performance (Miller *et al.*, 2014; Callahan *et al.*, 2015*b*), the impact of cellular level function on whole-muscle performance must be considered. There are logical connections between whole-muscle fatigue and changes to cellular stiffness via titin modification (Figure 5). In whole-muscle, exercise upregulates calcium cycling which increases the likelihood that titin will bind to the thin filament, thereby shortening the length of titin's extensible region and increasing titin-based stiffness (Dutta *et al.*, 2018). Additionally, exercise-induced β-adrenergic signaling, coupled with increased concentration of inorganic phosphate, will contribute to titin phosphorylation (Krüger & Linke, 2006*b*; Müller *et al.*, 2014; Hamdani *et al.*, 2017), which has potential to alter titin-based stiffness as previously discussed. Reduced pH within exercising muscle promotes aggregation of titin Ig domains, which would reduce titin elasticity, yet increased muscle temperature upregulates heat shock protein (HSP) 27 expression and subsequent binding to titin (Kötter *et al.*, 2014), thereby preventing Ig domain aggregation. Finally, exercise induces oxidative stress, which results in S-Glutathionylation to titin and subsequent compliance of muscle cells (Alegre-Cebollada *et al.*, 2014; Watanabe *et al.*, 2020). Though there are numerous potential sources of fatigue-induced alteration to titin stiffness, whether these modifications are present in experimental preparations used in our lab remains to be seen. In our hands, phosphorylation is the predominant PTM evident in our flash-frozen biopsy sample. For this reason, phosphorylation will be examined as a potential mechanism of fatigue-induced titin modification in these proposed studies.

The possibility that fatigue-induced compliance is in part due to extracellular mechanisms was considered. After all, collagen content is the strongest predictor of whole muscle passive function (Ward *et al.*, 2020) and most intramuscular collagen resides outside the

sarcolemma. In general, changes to ECM stiffness arise from changes in collagen content or altered collagen cross linking. Substantial changes to collagen content in the time between our fatiguing protocol and biopsy of the fatigued limb (~10 minutes) are unlikely. In fact, a previous study utilizing an hour of intense cycling coupled with an hour of intense running only saw upregulation of genes related to ECM remodeling after 96 hours of recovery (Neubauer *et al.*, 2014). Collagen cross-linking is also unlikely to be altered by our fatiguing protocol, since changes are typically observed on the order of weeks (Zimmerman *et al.*, 2001). However, our fatiguing protocol may cause acute re-alignment of collagen fibrils that alter ECM mechanical properties (Stromberg & Wiederhielm, 1969). What's more, repeated large-strain loading appears to shift the mechanical response of fibrin and collagen type 1 networks (Münster *et al.*, 2013). Using confocal microscopy, authors confirmed that this shift is indeed the result of relaxed network stress absent any form of structural damage to the network. Rather, fibers appear to buckle when the network is returned to its original length, creating delayed engagement during the subsequent stretch. This effectively reduces the stress produced during elongation of the network (Münster *et al.*, 2013). Altered ECM stiffness would very likely impact whole-muscle stiffness and was therefore considered in these proposed studies by inclusion of bundle measures.

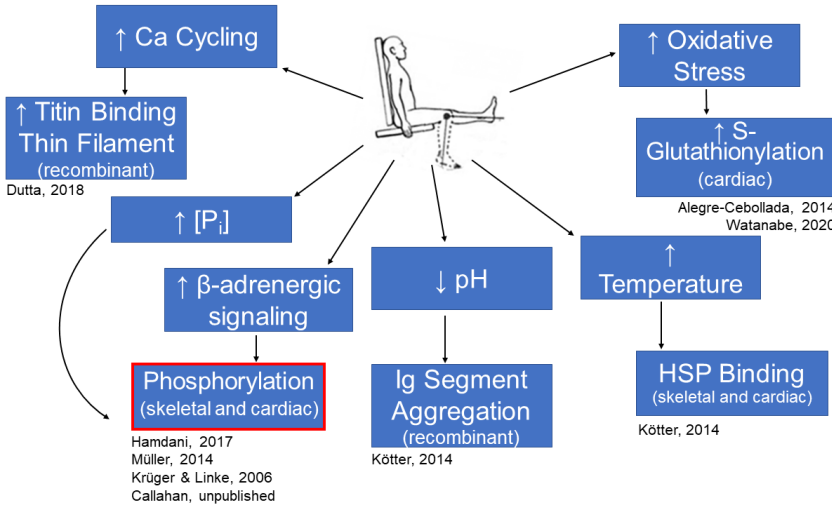

Figure 5. Fatigue results in metabolic end products that are evidenced to modify titin stiffness. Experimental preparations used previously are shown in parenthesis. Phosphorylation (outlined red) is the titin modification evidenced in our experimental preparations.

2D. Age-related changes to beta adrenergic signaling suggest the possibility of age-mediated stiffness response.

As humans age, changes to skeletal muscle mechanical properties (Wood *et al.*, 2014; Eby *et al.*, 2015; Lim *et al.*, 2019; Noonan *et al.*, 2020*b*; Kennedy *et al.*, 2020) and neural function (Aagaard *et al.*, 2010; Piasecki *et al.*, 2016*b*, 2016*a*, 2018) contribute to limitations in joint mobility and slowing of angular velocity during activities of daily living (Marcucci & Reggiani, 2020). In addition to the well-defined increase of ECM stiffness (Wood *et al.*, 2014), skeletal muscle fibers (Lim *et al.*, 2019; Noonan *et al.*, 2020*b*) and whole muscle (Eby *et al.*, 2015; Marcucci & Reggiani, 2020) also become stiffer in older versus younger adults, presumably through accumulation of intramuscular connective and adipose tissue (Cawthon *et al.*, 2009; Aagaard *et al.*, 2010; Ismail *et al.*, 2015; Aas *et al.*, 2020). Increased skeletal muscle stiffness limits joint range of motion and alters force transduction to the skeleton (Marcucci & Reggiani, 2020). Additionally, age-related neuromuscular changes may contribute to differential modification of the stiffness response of older versus younger skeletal muscle. Specifically, age-related reduction in central activation has been suggested to occur with aging (Aagaard *et al.*, 2010), but this is not always observed (Suetta *et al.*, 2009). Similarly, motor neuron dysfunction (Campbell *et al.*, 1973) and reduced peripheral nerve conduction speeds (Aagaard *et al.*, 2010) may contribute to age-related changes in skeletal muscle function. Peripherally, resting peak twitch torque and rate of force development in response to surface electrode stimulation are reduced in older versus younger adults (Suetta *et al.*, 2009), suggesting that mechanisms of age-related contractile dysfunction may reside within the muscle. Possible mechanisms include

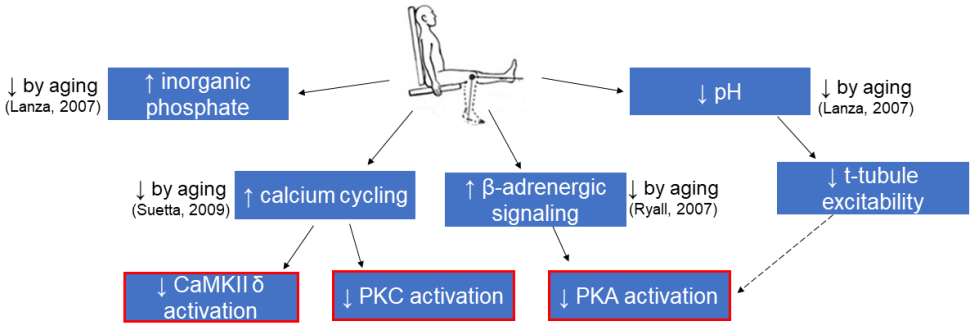

Figure 6. Age-related changes to metabolic outcomes during fatiguing exercise may alter downstream signaling pathways (outlined red) that are reported to alter titin phosphorylation.

decreased calcium sensitivity or reduced muscular post-synaptic excitability. There is some debate whether aging is accompanied by changes in the force-calcium relationship, with some studies suggesting no change (Hvid *et al.*, 2011, 2013, 2017) and other work demonstrating decreased calcium sensitivity (Straight *et al.*, 2018). Post-synaptic excitability, an upstream regulator of β-adrenergic activation (Young *et al.*, 2000), does appear to diminish with aging (Suetta *et al.*, 2009) and likely contributes to observed reductions of β-adrenergic signaling (Ford *et al.*, 1995; Ryall *et al.*, 2007), which may affect phosphorylation of proteins such as titin in aged muscle (Salcan *et al.*, 2020).

The physiological response to fatiguing exercise also changes with age (Figure 6), as evidenced by greater fatigue resistance in older versus younger females during maximal voluntary isometric contraction (Callahan & Kent-Braun, 2011). An age-related difference in the fatigue response may be attributed to reduced accumulation of inorganic phosphate and reduced acidosis (Lanza *et al.*, 2007), altered calcium cycling (Suetta *et al.*, 2009), and/or reduced β-adrenergic signaling (Ryall *et al.*, 2007). Since inorganic phosphate is necessary for protein phosphorylation, reduced phosphate production is likely to limit phosphorylation capability. Exercise-induced acidosis has been linked to increased T-tubule excitability (Pedersen *et al.*, 2004), an upstream component of β-adrenergic PKA signaling (Lynch & Ryall, 2008). Therefore, decreased exercise-induced acidosis in older skeletal muscle, even during repeated contraction to extreme fatigue (Lanza *et al.*, 2007) may hinder titin phosphorylation via PKA. Calcium stimulates phosphorylation via the CaMKII δ and PKC pathways, so reduced exercise-induced calcium cycling may alter titin phosphorylation. Collectively, age-related changes to neuromuscular function coupled with changes to native titin phosphorylation (Salcan *et al.*, 2020) and signaling pathways (beta-adrenergic and metabolic) likely contribute to age-mediated differences in the stiffness response of skeletal muscle to fatiguing exercise.

Importantly, decreased muscle stiffness at the whole-muscle level has also been observed in older versus younger adults (Kennedy *et al.*, 2020), in contrast with other reports (Eby *et al.*, 2015; Lim *et al.*, 2019; Noonan *et al.*, 2020*b*). This apparent divergence may stem from varying measurement techniques or perhaps an incomplete understanding of the relative contributions of extracellular (ECM) and intracellular (titin) components to skeletal muscle stiffness (Lieber & Binder-Markey, 2021). To address this gap in knowledge, these proposed experiments explored potential intracellular and extracellular mediators of skeletal muscle stiffness in the context of

aging using the proposed passive mechanical measurements in bundles. Furthermore, the scalability of skeletal muscle mechanical properties from cellular to tissue-level organization non-linear (Ward *et al.*, 2020), prompting the question of whether fatigue-induced changes to cellular mechanics might persist at the tissue level, the mechanical properties of ECM have more influence (Meyer & Lieber, 2011; Ward *et al.*, 2020). Previous studies have used in-vitro treatment of skeletal muscle samples with potassium iodide (KI) and potassium chloride (KCl) to isolate the influence of titin-based stiffness (Ottenheijm *et al.*, 2012; Brynnel *et al.*, 2018). As such, this approach was utilized to assess the impact of titin-based stiffness on tissue-level mechanics in our bundle assays. Ultimately, these assays sought to address a lack of literature regarding the origin of fatigue-induced reductions to skeletal muscle stiffness, and to determine whether changes to titin-based stiffness impact tissue-level mechanics.

3. Aim 1: To determine whether cellular passive stress or Young's Modulus is reduced following fatiguing exercise and assess potential intracellular mechanisms of this change.

3A. Introduction

Fatiguing exercise was shown to reduce whole muscle passive stiffness in human vastus lateralis (Andonian *et al.*, 2016; Siracusa *et al.*, 2019; Chalchat *et al.*, 2020), though the underlying cellular mechanisms are not yet understood. As a first step, we measured passive stress and Young's Modulus in single, permeabilized muscle fibers from non-fatigued and fatigued skeletal muscle from sedentary younger males and females to test the hypothesis that i) acute in-vivo fatigue would reduce in-vitro single fiber measures in all participants. When this study was initially proposed, there were no hypotheses considering the effect of biological sex on fatigue-induced reductions to cellular passive stress and modulus. However, the opportunity to include males and females presented itself; therefore, the inclusion of biological sex became an exploratory component of this aim. The measurement of passive mechanics in permeabilized single fibers allowed for focused study of how cellular passive mechanics are affected by altered sarcomere protein structure and function. The sarcomere protein of interest in this study was the viscoelastic protein titin. Titin stiffness can be dynamically modified via phosphorylation (Krüger & Linke, 2006*a*; Müller *et al.*, 2014; Hamdani *et al.*, 2017) and, as a result, has been implicated in acute, exercise-induced changes to muscle stiffness modification exercise in mice (Müller *et al.*, 2014). Therefore, Aim 1 measured titin phosphorylation in fatigued and non-fatigued human skeletal muscle fibers to test the hypothesis that ii) titin phosphorylation would be higher in fatigued versus non-fatigued muscle. Finally, titin was treated in-vitro with alkaline phosphatase (AP) (Franssen *et al.*, 2017; Krysiak *et al.*, 2018) to test the hypothesis that iii) de-phosphorylation of titin in fatigued muscle fibers would increase cellular passive stress and modulus to resemble that of non-fatigued. Although not initially proposed, in-vitro treatments to phosphorylate titin with protein kinase A (PKA) (Yamasaki *et al.*, 2002) were also performed to test the hypothesis that titin phosphorylation would reduce cellular passive stress and modulus in non-fatigued fibers to mimic the effect of fatigue.

3B. Methods

Population: This protocol was approved by the Institutional Review Board at the University of Oregon. Nine young (21 ± 2 yrs.), males (n=4) and females (n=5) from the

University of Oregon and surrounding community consented to participate in this study. All participants were characterized as “untrained”. Specifically, included individuals were recreationally active, yet reported no participation in structured physical exercise and no resistance training. Self-reported physical activity was confirmed by ActivePal (Pal Technologies, Glasgow, UK) accelerometers affixed to the outer-mid thigh with an adhesive (Dowd *et al.*, 2012). Physical activity was monitored for an average of 8 ± 2 days, which exceeds the recommended 3 days (Tudor-Locke *et al.*, 2005). To limit the potential for menstrual cycle-dependent variation in circulating estradiol to contribute to variability in skeletal muscle mechanical properties, all female volunteers either reported use of hormonal contraceptive (n = 1) or were tested in the pre-follicular phase of the menstrual cycle (n=4), within 5 days of menses onset. Participants reported no orthopedic limitations (severe osteoarthritis, joint replacement or other orthopedic surgery in the previous six months), endocrine disease (hypo/hyperthyroidism, Addison’s Disease or Cushing’s syndrome), uncontrolled hypertension (>140/90 mmHg), neuromuscular disorder, significant heart, liver, kidney or respiratory disease, and/or diabetes. Participants were non-tobacco-smokers and had no current alcohol disorder. Finally, participants taking medications known to affect muscle stiffness or beta-adrenergic signaling of neuromuscular activation (including but not limited to beta blockers, calcium channel blockers, and muscle relaxers) or anabolic steroids were not included.

Study Design: A schematic of the study design is provided in Figure *7*. Participants visited the lab on 2 occasions separated by at least 1 week. During the first visit, volunteers habituated to measures of voluntary strength, power, and the fatigue of their dominant knee extensors (KE). During the second visit, volunteers performed measures of maximal voluntary isometric KE strength followed by fatiguing exercise to task failure. Fatiguing exercise was followed by bilateral, percutaneous needle muscle biopsies: one on the exercised limb

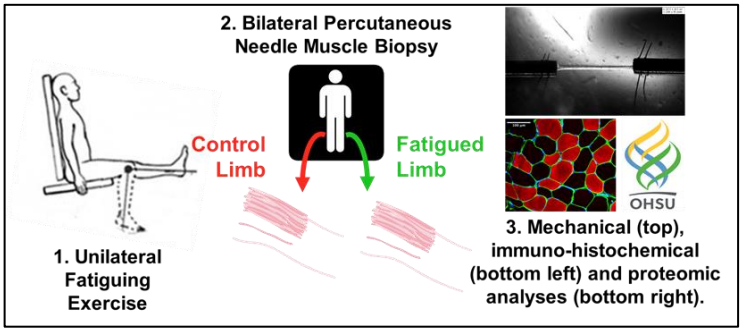

Figure 7. A schematic of the overall study design.

immediately following exercise ("fatigued") and the second on the contralateral, non-exercised limb ("non-fatigued").

Fatigue Protocol: Participants exercised the dominant limb on a Biodex System 3 dynamometer (Biodex Medical Systems, Shirley, NY). Participants were seated on the dynamometer with hips and knee flexed at 90° (180° = full extension). Prior to fatiguing exercise, participants completed three maximum voluntary isometric contractions (MVIC) of the knee extensors while analog voltage data for torque were sampled at 500 Hz. Analog data were converted to digital using an analog-to-digital converter (Cambridge Electronic Design, UK). Real-time visual feedback was provided to the participants to encourage maximal effort during the MVIC. The average torque value of the three MVICs was used to set the applied load to 30% MVIC maximal torque for the bout of fatiguing exercise. Following initial MVICs, participants performed repeated, voluntary knee extensions at this isotonic load until task failure. Task failure was identified as the inability to perform knee extension through at least 50% of the range of motion. For seven of the eight participants, fatigue was quantified as the Fatigue Ratio = $\frac{Final\ Power}{Initial\ Power}$, where "initial power" represents the average peak power of the first five knee extensions performed during fatiguing exercise, and "final power" represents the average peak power from the last five knee extensions. Due to a technical limitation, data were not appropriately transferred to allow assessment of fatigue ratio of one young female. Time to fatigue (task failure) was recorded for all eight participants.

Muscle Biopsy Procedure: Percutaneous biopsy of the vastus lateralis (VL) muscle was performed under sterile technique as previously detailed (Tarnopolsky *et al.*, 2011). After sterilization of the biopsy site and injection of local anesthetic (1-2% lidocaine HCL [Hospira Worldwide, Lake Forest, IL, USA]), a small incision was made in the skin and muscle fascia through which a 5 mm Bergstrom biopsy needle could be inserted to obtain VL muscle at a depth of ~2-3 cm. Time to collection of biopsy sample was recorded for 6/9 participants, averaging 10 ± 5 minutes.

Tissue Processing: VL biopsy typically yields between 100 and 150 mg (wet weight) of muscle tissue. After samples were removed from the biopsy needle, tissue was divided for proteomics (~30 mg), single muscle fiber mechanics (~40 mg), and electron microscopy (EM, ~10 mg) assays. Samples intended for proteomics analyses were immediately flash-frozen in liquid nitrogen and stored at -80°C. Sample intended for mechanical experimentation was placed in dissecting solution (MDS, 120.782 mM NaMS, 5.00 mM EGTA, 0.118 mM $CaCl_2$, 1.00 mM $MgCl_2$, 5.00 mM ATP-Na_2H_2, 0.25 mM KH_2PO_4, 20.00 mM BES, 1.789mM KOH) and parsed into bundles of ~50 fibers. Bundles were tied to glass rods, chemically skinned overnight, and advanced through solutions of increasing glycerol content before long-term storage in 50% glycerol solution (5.00 mM EGTA, 2.50 mM $MgCl_2$, 2.50 mM ATP-Na_2H_2, 10 mM imidazole, 170.00 mM potassium propionate, 1.00 mM sodium azide, 50% glycerol by volume) at -20°C. Sample apportioned for EM was tied to a glass rod, stretched slightly, and stored at 4ºC in Karnovsky's solution until embedding and sectioning (Miller *et al.*, 2009).

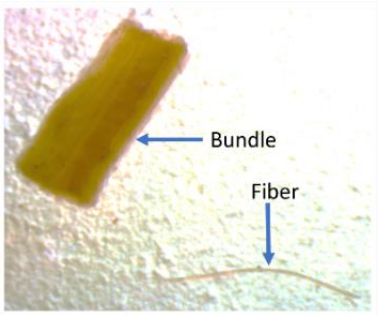

Figure 8. Annotated image of fiber dissection from a fiber bundle.

Single fiber morphology and contractile measures: Prior to mechanical assays, fiber bundles and dissected single fibers (Figure 8) were chemically skinned (MDS + 1% Triton X-100) before being transferred to plain MDS and kept on ice until experimentation. Prepared fibers were mounted in relaxing solution (67.286 mM NaMS, 5.00 mM EGTA, 0.118 mM $CaCl_2$, 6.867 mM $MgCl_2$, 0.25 mM KH_2PO_4, 20.00 mM BES, 0.262 mM KOH, 1.00 mM DTT, 5.392 mM Mg-ATP, 15.00 mM CP, 300 U/mL CPK) between a force transducer and a length motor (Aurora Scientific, Inc., Aurora, ON, Canada, Figure 9) using the Moss clamp technique (Moss, 1979) at 15ºC. Multiple wells are present under the mounting surface, allowing rapid transfer of the fiber between relaxing, pre-activating (81.181 mM NaMS, 5.00 mM EGTA,

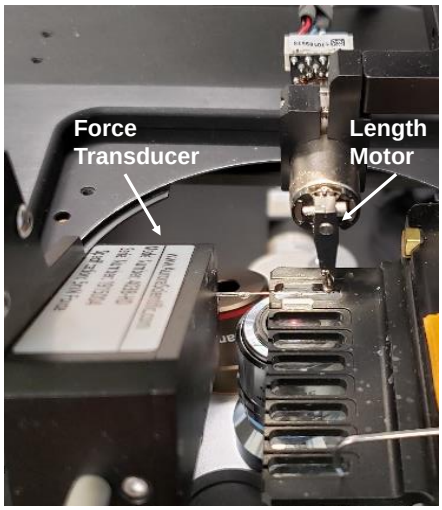

Figure 9. An image of the apparatus used to collect fiber mechanics data.

0.012 mM $CaCl_2$, 6.724 mM $MgCl_2$, 5.00 mM KH_2PO_4, 20.00 mM BES, 1.00 mM DTT, 5.397 mM Mg-ATP, 15.00 mM CP, 300 U/mL CPK) and activating (57.549 mM NaMS, 5.00 mM EGTA, 5.021 mM $CaCl_2$, 6.711 mM $MgCl_2$, 5.00 mM KH_2PO_4, 20.00 mM BES, 9.674 mM KOH, 1.00 mM DTT, 5.437 mM Mg-ATP, 15.00 mM CP, 300 U/mL CPK) solutions. The mounting chamber contains a glass bottom and two prisms mounted to the side walls to allow for viewing of the fiber in top-down and side-view orientations. Fiber dimensions were measured as follows: d_{top} = average of three diameter measures along the fiber using the top-down view; d_{side} = average of three diameter measures along the fiber using the side view; fiber length = distance between the two trough edges (Callahan *et al.*, 2015*a*). Diameter measures were used for calculation of stress (force per unit area, kPa), and fiber length was used to calculate passive strain (change in length divided by original length x 100, $\%L_0$). Sarcomere length was quantified using Aurora software and the inverted microscope mounted beneath the rig. Specifically, the Aurora software was used to measure the linear spacing between thick filaments, darkened in the view from the inverted microscope due to the lack of light passing through them. All mounted fibers were set to sarcomere length (SL) 2.65 µm. This SL is optimal for length-tension generation (Burkholder & Lieber, 2001). Active tension was measured at SL 2.65 µm by moving the fiber to pre-activating solution followed by activating solution until a steady state tension was recorded. All fibers were activated (pCa 4.5) prior to passive stretching to measure active tension and confirm fiber viability.

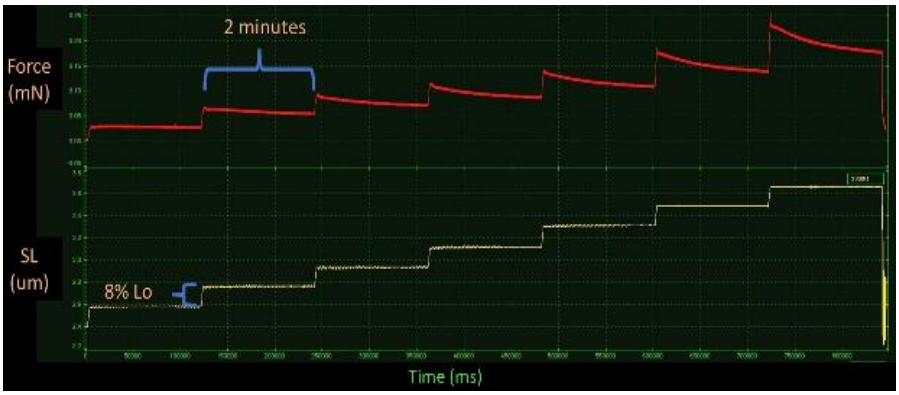

Figure 10. An annotated force and sarcomere length trace generated by the passive stiffness protocol. Each stretch step elongates the sample by 8% of initial length and holds this length for 2 minutes. At the end of the protocol, the sample is returned to initial length. The resulting trace is generally similar in fibers and fiber bundles.

Passive stretch protocol: Passive modulus measures were performed in 15ºC relaxing solution (pCa 8.0) using a passive stretch protocol adapted from previous work (Lim *et al.*, 2019). Initial sarcomere length was set to 2.4 µm, followed by 7 incremental stretches to reach a

final length of 156% of initial length (SL ~ 3.8 μm). Each stretch lengthened the sample 8% of initial length in 2 seconds and held this position for 2 minutes of stress-relaxation (Figure 10). Force response was measured by a force transducer and change in fiber length was measured by the displacement of the length motor. Sarcomere length was measured throughout the protocol using an inverted microscope located beneath the single fiber rig. To determine the extent to which actomyosin interactions contributed to measures of passive modulus, a subset of fibers from two males was subjected to the passive stretch protocol in relaxing solution with the addition of 40 mM 2,3-butanedione monoxime (BDM), a myosin inhibitor. Following the completion of the passive stretch protocol, each fiber was collected and placed in gel loading buffer (2% SDS, 62.5 mM Tris, 10% glycerol, 0.001% bromophenol blue, 5% β-mercaptoethanol, pH 6.8), centrifuged and heated at 65ºC for 2 minutes, then stored at -80°C until later assessment of myosin heavy chain (MHC) isoform. Any fibers failing to demonstrate an increased force in response to fiber stretch (i.e. the subsequent force value after stress-relaxation was less than that of the previous stretch step) were excluded from analyses. The measured stress at the end of stress-relaxation was used for subsequent calculations and analyses. Data files were analyzed using custom code in Matlab software (R2020b, The MathWorks, Inc., Natick, Massachusetts).

Incubation of single fibers in AP or PKA: AP - Following an initial (control) stretch, single fatigued fibers will be incubated in relaxing solution spiked with 4% v/v AP at 20ºC for 20 minutes, as these incubation conditions have been used successfully in our previous attempts to dephosphorylate myosin regulatory light chain. Following incubation, fibers will be stretched a second time. Successfully treated fibers will be collected and stored in sample buffer until later MHC identification. PKA – Single fatigued fibers were incubated in either relaxing solution spiked with PKA to a concentration = 2.4μg/μL or relaxing solution without PKA at 20ºC for 30 minutes. Following incubation, PKA-treated and sham fibers were passively stretched using the same protocol as described above. All fibers were collected and stored in sample buffer until later MHC identification.

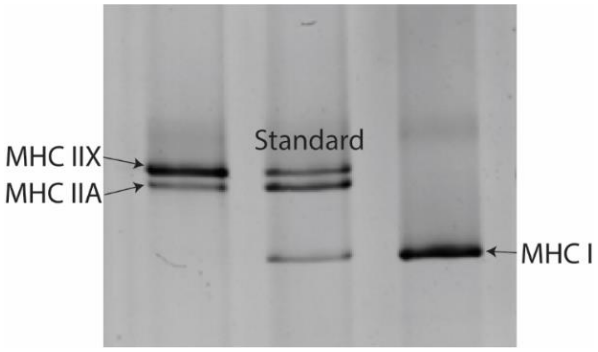

Figure 11. Sample image of silver-stained MHC bands. The left lane contains protein from a hybrid single fiber exhibiting both MHC IIA and MHC IIX isoforms. The middle band is a sample homogenate used to visualize all three MHC isoforms (I, IIA, IIX). The right lane contains protein from a single fiber expressing only MHC I isoform.

MHC isoform identification: Sodium dodecyl sulfate poly acrylamide gel electrophoresis (SDS-PAGE) was used to assess the MHC isoform of single muscle fibers. Sample from each fiber was loaded into its own well of a 4% stacking / 7% resolving polyacrylamide gel. The gel was run at 70 V for 3.5 hours followed by 200 V for 20 hours at 4°C (Miller *et al.*, 2010). Gels were stained with a silver stain kit (Pierce Biotechnology, Waltham, MA) and the resulting MHC isoform (I, IIA, and/or IIX) expression was determined by comparison to a standard made from a multi-fiber homogenate (Figure 11).

Mass spectrometry assessment of titin phosphorylation: Mass spectrometry was performed on skeletal muscle biopsy samples from individuals who were not included in the single fiber mechanics assays. This separate subset included four young (24.7 ± 5.7 years old), recreationally active individuals (2 males, 2 females) with a body mass index (BMI) of 24.4 ± 3.4 kg/m^2. Liquid chromatography followed by high resolution mass spectrometry (LC-MS) was performed as previously described (Paulo *et al.*, 2015) to determine which titin serine residues were differentially phosphorylated following acute fatigue. Briefly, samples were disrupted by shearing with glass beads, followed by protein digestion via trypsin and phosphopeptide purification by binding to TiO_2 beads. Phosphopeptides were then labeled with one of 10 different tandem mass tags, combined into a single sample, and run via the Orbitrap Fusion mass spectrometer. Informatics methods (Plubell *et al.*, 2017) were used to determine relative changes in phosphorylation of serine, threonine, and tyrosine residues.

Electron Microscopy: Electron microscopy was performed to assess sarcomere ultrastructure (Miller *et al.*, 2009). At the time of biopsy, samples apportioned for electron microscopy were fixed in Karnovsky's Solution (2.5% glutaraldehyde, 2.5% formaldehyde, 0.1M Sodium Cacodylate). Before imaging, samples were treated with 2% osmium tetroxide in 0.5 M sodium cacodylate buffer (Ted Pella, Redding, CA), stained with uranyl acetate, and embedded in epoxy resin. Cross sections (~100 nm) were then cut using an ultramicrotome and contrasted with uranyl acetate before mounting on copper grids and subsequent imaging with a FEI Tecnai™ with iCorr™ Integrated Light and Transmission Electron Microscope. Qualitative assessment of sarcomere ultrastructure was used to check for damage resulting from fatiguing exercise, however no extensive quantitative approach has been used as of yet.

Outcome Measures: Passive stress at each SL was calculated as $\frac{F}{CSA}$, where "F" indicates the measured force value at the end of stress relaxation (red asterisks, Figure 12) and "CSA" indicates fiber cross sectional area assuming elliptical shape. CSA $=\pi * (\frac{dtop}{2} * \frac{dside}{2})$, where "$d_{top}$" is the average of three top diameter measures, and "d_{side}" is the average of three side diameter measures. Strain was calculated as $\frac{\Delta L}{Lo}$, where "L_0" indicates initial length. Passive stiffness was quantified as Young's Modulus to account for potential differences in fiber size across samples. Passive Young's Modulus was calculated as the slope of the stress-strain relationship (using post-decay stress values) at shorter fiber lengths (strain = 1.0-1.24 %Lo) and at longer fiber lengths (strain = 1.32-1.56 %Lo). Separate slopes were calculated for shorter and longer fiber lengths to consider the length dependence of cellular passive modulus measures (Figure 14A-B, Noonan *et al.*, 2020*b*). Additionally, the response of cellular passive modulus to fatiguing exercise was quantified for each participant by expressing the average value for fatigued passive modulus as a percent of the mean value for non-fatigued modulus. Maximally activated tension was quantified as the measure of steady-state active force divided by fiber CSA. Titin phosphorylation, assessed via LC-MS, was quantified as fold-change ratio from non-fatigued.

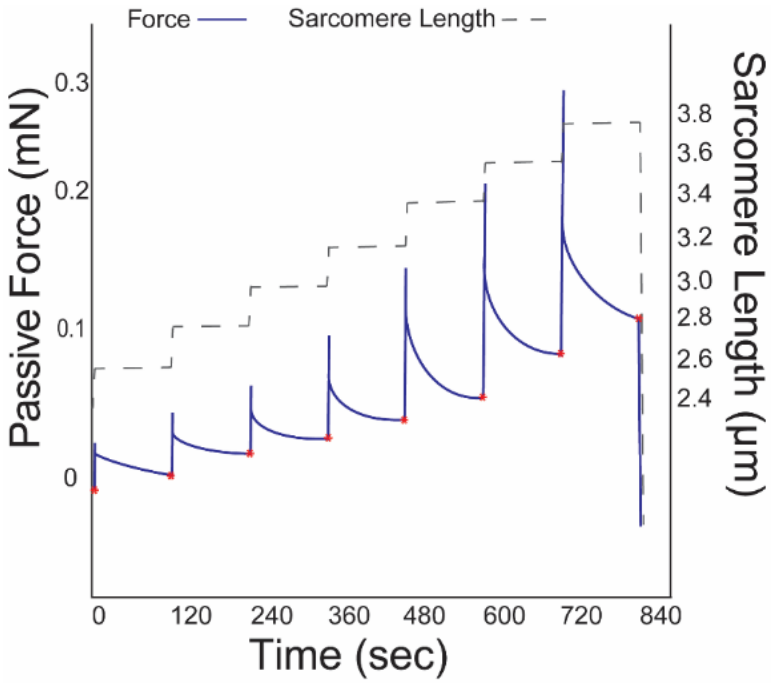

Figure 12. Sample force and sarcomere length traces produced during the passive stretch protocol. The force values measured at the end of each force decay, indicated by red asterisks, were used to calculate passive stress and, subsequently, passive Young's Modulus.

Statistical Analyses: Statistical testing was conducted using SPSS software package (SPSS, IBM Corp., Armonk, NY, USA), unless otherwise specified. Anthropometric measures and activity data were compared between males and females using a two-tailed, independent t-test. Differences in single fiber CSA and length were assessed using separate linear mixed models including biological sex and fatigue as main effects and participant as a random effect. To evaluate differences in single fiber passive stress and passive modulus (short and long lengths), separate linear mixed models were run with fatigue, biological sex, and interaction terms as fixed effects and participant ID as a random effect to account for fiber variation within individuals, as described previously (Callahan *et al.*, 2015*a*). Subsequent analyses to investigate an interaction between biological sex and fatigue did so using separate linear mixed models in males and females, each including fatigue as a fixed effect and participant ID as a random effect. To determine whether maximally activated tension, single fiber CSA, or fiber length differed by biological sex or fatigue condition, separate linear mixed effects models were run with sex, fatigue, and interaction terms as main effects and participant ID as a random effect. To test whether passive modulus was affected by treatment with BDM in a subset of fibers, a linear

mixed model was run with fatigue condition and BDM treatment as main effects and participant ID as a random effect. To test whether passive modulus was affected by treatment with AP or PKA within each fatigue condition, separate linear mixed models including treatment as a main effect and participant ID as a random effect were run in fatigued and non-fatigued fibers. To assess titin phosphorylation of fatigued versus non-fatigued sample using LC-MS, mean titin phosphorylation was quantified as fold change ratio, and any significant differences between fatigued and non-fatigued samples were identified by a false detection rate (FDR) lower than 0.05. These LC-MS statistics were conducted using EdgeR software, proprietary to the Orbitrap Fusion.

Table 1. Anthropometric and activity data of younger participants.

	N	BMI (kg/m^2) #	Height (cm) #	Weight (kg) #	Step Count (steps/day)	Light Activity (min./day)	Moderate Activity (min./day)	Vigorous Activity (min./day)
Males	4	24.4 ± 1.2	185.3 ± 13.0	84.0 ± 10.1	7108 ± 1525	37.6 ± 6.7	50.8 ± 14.7	1.1 ± 1.2
Females	5	20.9 ± 0.6	162.1 ± 6.1	55.0 ± 3.2	7274±2162	26.6 ± 9.1	56.5 ± 18.2	0.5 ± 0.6

# Indicates significant difference between biological sex groups ($p<0.05$). Data are shown as mean ± SD.

3C. Results

Participant anthropometrics and activity: The eight participants included were an average of 20.6 ± 1.7 years old. BMI (p=0.005), height (p=0.009), and weight (p<0.001) were higher in males versus females (Table 1). Participants were not engaged in structured exercise training, and activity levels of individuals were confirmed by accelerometry. There were no significant differences in step count (p=0.897), minutes spent in light (< 75 steps/minute, p=0.076), moderate (75-125 steps/minute, p=0.621) or vigorous (>125 steps/minute, p=0.444) activity between males and females (Table 1).

Fatiguing exercise and whole-muscle contractile measures: The average time to fatigue did not differ between males and females (74.6 ± 28.6 versus 68.3 ± 8.8 seconds, respectively, p=0.695, Table 2). In the 4 males and 4 females for which data were collected, there was no difference in fatigue ratio by biological sex (0.41 ± 0.2 versus 0.33 ± 0.1, respectively, p=0.462). Absolute peak power (p=0.011), absolute peak torque (p=0.007), and relative peak torque (p=0.002) were significantly higher in males versus females. Relative peak power (p=0.157) was not different between males and females.

Table 2. Fatigue data and whole-muscle performance

	Time to Fatigue (sec)	Fatigue Ratio	Absolute Peak Power (W) #	Relative Peak Power (W/kg)	Absolute Peak Torque (N) #	Relative Peak Torque (N/kg) #
Males	75±29	0.41±0.16	532±95	6.43±1.42	281±44	3.34±0.34
Females	68±8.8	0.34±0.10	295±33	5.43±0.32	140±8	2.54±0.12

Data are shown as mean ± SD.

Single fiber characteristics: Despite efforts to select comparable numbers of MHC I and MHC II (including IIA, IIX, and A/X) fibers (Privett *et al.*, 2024*b*), MHC I fibers were under-represented in this sample (10% of total sample), especially in the male participants (3% of fibers from males). However, fibers expressing MHC IIA or MHC IIA/X were similarly represented in samples from males and females (Table 3). Therefore, only fibers expressing MHC IIA and MHC IIA/X (n=140) were included in statistical analyses. In this subset, there was no effect of MHC isoform on passive modulus at short or long lengths (Supplementary Table 1). Therefore, MHC isoform was not included as a main effect in any subsequent analyses. There was no significant difference in single fiber CSA between fatigue conditions (p=0.579), but fibers were significantly larger in males versus females (0.0072 ± 0.0018 vs. 0.0042 ± 0.0013 mm^2, respectively, p=0.029). Fiber length did not differ by biological sex (p=0.087) or fatigue condition (p=0.056).

Table 3. Summary statistics of fibers analyzed in young adults.

					MHC				
		N	**CSA (mm^2) #**	**Length (mm)**	I (n)	I/IIA (n)	IIA (n)	IIX (n)	IIA/X (n)
Males	Non-fatigued	46	0.0071 ± 0.0020	1.7 ± 0.4	0	0	21	11	14
	Fatigued	44	0.0073 ± 0.0015	1.8 ± 0.5	3	0	23	10	8
Females	Non-fatigued	51	0.0039 ± 0.0013	1.3 ± 0.5	14	2	23	2	10
	Fatigued	56	0.0045 ± 0.0012	1.5 ± 0.3	9	6	27	0	14

# Indicates significant difference between biological sex groups ($p<0.05$). Data are shown as mean ± SD.

Assessment of passive stretch protocol and calculation of Young's Modulus: To address potential concerns regarding incomplete stress decay after each applied strain, a 3rd order polynomial function was used to perform a non-linear regression analysis, using the "fitnlm" function in MatLab, on the measured stress decay during the 112 seconds following applied strain. This produced a predicted final stress value that was compared to the measured stress at the end of each hold period. The difference between the measured stress and predicted stress, termed "missed stress", was calculated at each stretch step, for each fiber. Given the greater stress decay expected at longer lengths (Figure 12), the missed stress values were assessed at strains 1.32-1.56% Lo. Stress decay was greatest at longer lengths, suggesting the greatest potential for incomplete stress decay. However, measured stress at longer lengths was only different from predicted stress by 0.6-2.4%. Given this minimal variation, it is not likely that incomplete stress decay impacted the ability to draw meaningful conclusions from final measured stress, thus measured stress was used throughout. To assess the use of the dual-slope approach to calculating passive modulus, the coefficient of determination was calculated for raw data included in the short slope, the long slope, and the entire curve (both short and long slopes) for each fiber. The R^2 values were not obviously different when calculated for the short slope (0.97 ± 0.00), long slope (0.97 ± 0.01), or the entire curve (0.95 ± 0.00). However, the use of the dual slope approach allowed for consideration of the sarcomere length-dependence of any significant effects observed (Noonan *et al.*, 2020*b*). Specifically, the short slope covered the sarcomere length (SL) range = 2.4 ± 0.03 µm – 3.0 ± 0.10 µm and the long slope covered the SL range = 3.2 ± 0.13 µm – 3.8 ± 0.18 µm.

Passive Modulus: MHC isoform was determined by comparison of the band pattern of a single fiber to that of a multi-fiber homogenate, termed the "standard" (Figure 11) in a silver-stained acrylamide gel. Because MHC IIA and MHC IIA/X fibers comprised most of the sample and were relatively well represented across biological sex groups and fatigue conditions, statistical analyses were only conducted on these fiber types. Passive modulus was not significantly different between males and females at short ($p=0.604$) nor long ($p=0.609$) fiber lengths, regardless of fatigue condition. The main effect of fatigue on passive modulus was not significant at short lengths (NF: 14.2 ± 5.7 kPa/%Lo, F: 13.8 ± 6.5 kPa/%Lo, $p=0.296$) or long lengths (NF: 30.5 ± 9.7 kPa/%Lo, F: 27.9 ± 13.4 kPa/%Lo, $p=0.051$, Figure 13). Because the

interaction of fatigue and biological sex was significant at both short (p=0.004) and long (p=0.008) lengths, the effect of fatigue on passive modulus was assessed separately in males and females. Subsequent analyses revealed that fatigue-induced reductions in passive modulus were driven by males at short (NF: 14.6 ± 4.1 kPa/%Lo, F:11.6 ± 5.4 kPa/%Lo, p=0.002) and long (NF: 33.1±6.5 kPa/%Lo, F: 26.2 ± 8.8 kPa/%Lo, p<0.001) lengths, whereas modulus in single fibers from females was not significantly different with fatigue at short lengths (NF: 13.7 ± 7.0 kPa/%Lo, F: 15.5 ± 6.9 kPa/%Lo, p=0.226) or long lengths (NF: 27.8 ± 11.7 kPa/%Lo, F: 29.2 ± 15.9 kPa/%Lo, p=0.651, Figure 14C & D). Although males consistently demonstrated reduced passive cellular modulus in fatigued versus non-fatigued fibers at short (Figure 14E) and long (Figure 14F) lengths, the response in females varied considerably by individual, especially at long lengths. A separate set of fibers from two of the young males were treated with BDM and subjected to passive stiffness measures. In these samples, the effect of fatigue on cellular passive modulus was maintained at both short (p=0.027) and long (p=0.009) lengths (Figure 15), consistent with observations in the rest of the fibers from the male cohort. In short, BDM did not influence fatigue-induced reductions in cellular passive modulus. Considering cellular active contractile mechanics (Supplementary Figure 1), there was no main effect of biological sex (p=0.138) or fatigue (p=0.879) on active isometric tension in this sample of MHC IIA and MHC IIA/X fibers.

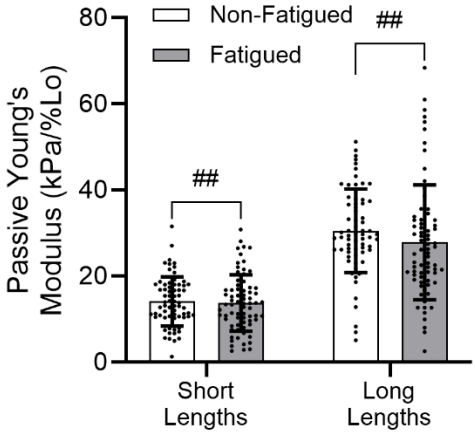

Figure 13. There was no main effect of fatiguing exercise on passive modulus at short (p=0.296) or long (p=0.051) lengths. However, passive modulus was significantly affected by a fatigue by biological sex interaction at short (p=0.004) and long (p=0.008) lengths. Data are shown as mean ± SD. ## Indicates significant interaction between fatigue and biological sex (p<0.01).

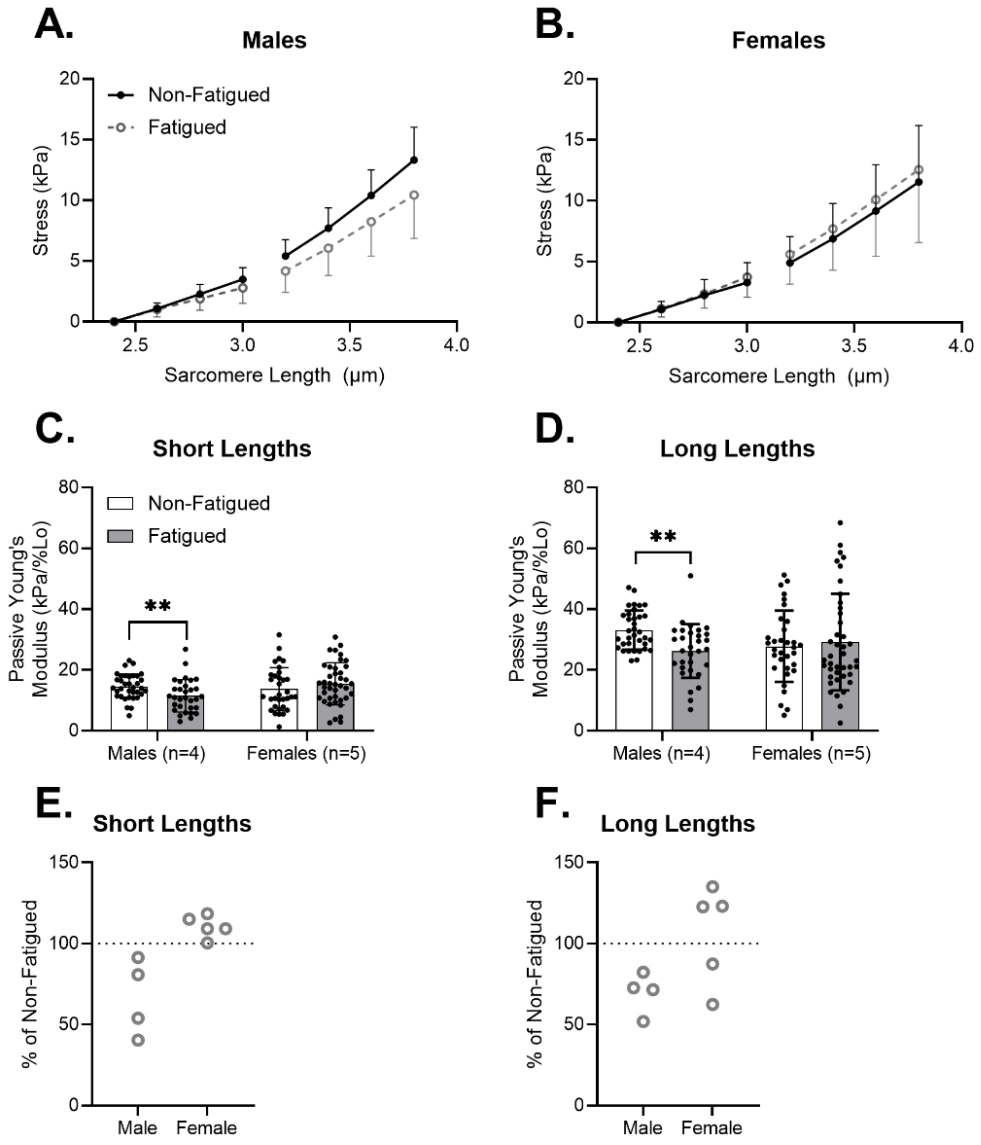

Figure 14. While there was an evident shift in slope of the stress-strain curve between non-fatigued and fatigued fibers at short and long lengths in the male group **(A)**, there was no such shift in the female group **(B)**. Statistical analysis confirmed that fatigue significantly reduced passive modulus in the single fibers of males at short **(C)** and long **(D)** fiber lengths but did not alter mean modulus in the fibers of females. Passive modulus of fatigued fibers was consistently lower compared to non-fatigued fibers in all four male participants at short **(E)** and long **(F)** lengths. However, females exhibited little to no change in passive modulus at short lengths, and variable responses at long lengths. Each individual point in figures 4E and 4F represents the mean of fatigued fibers relative to the mean of non-fatigued fibers, per individual participant. Data in A-D are shown as mean ± SD. ** indicates a significant fatigue effect ($p<0.01$).

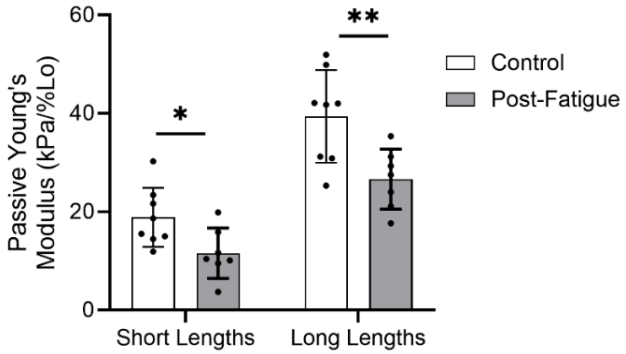

Figure 15. In a subset of fibers that were treated with BDM, passive modulus was significantly reduced in the F versus NF sample at both short and long fiber lengths, suggesting that fatigue-based differences in passive modulus persisted regardless of whether myosin was involved. Data are shown as mean ± SD. ** ($p<0.01$) and * ($p<0.05$) indicate significant differences by fatigue.

Passive Stress: Passive stress was analyzed at each step of the passive stretch protocol. When all MHC IIA and IIA/X fibers were considered, there was no main effect of biological sex nor fatigue condition on passive stress at any SL. However, the interaction of fatigue and biological sex was significant at longer SLs ($p<0.01$ at SL 3.0-3.8 µm, Figure 16A). This interaction effect prompted further study of the effect of fatigue on passive stress in fibers from males and females, separately. As a result, it became clear that fatigue significantly reduces passive stress in fibers from males at most SLs ($p=0.014$ at SL 2.8 µm, $p=0.002$ at SL 3.0 µm, $p=0.001$ at SL 3.2 µm, $p<0.001$ at SL 3.4-3.8 µm, Figure 16B). In contrast, passive stress was not significantly different between non-fatigued and fatigued fibers from females at any SL (Figure 16C).

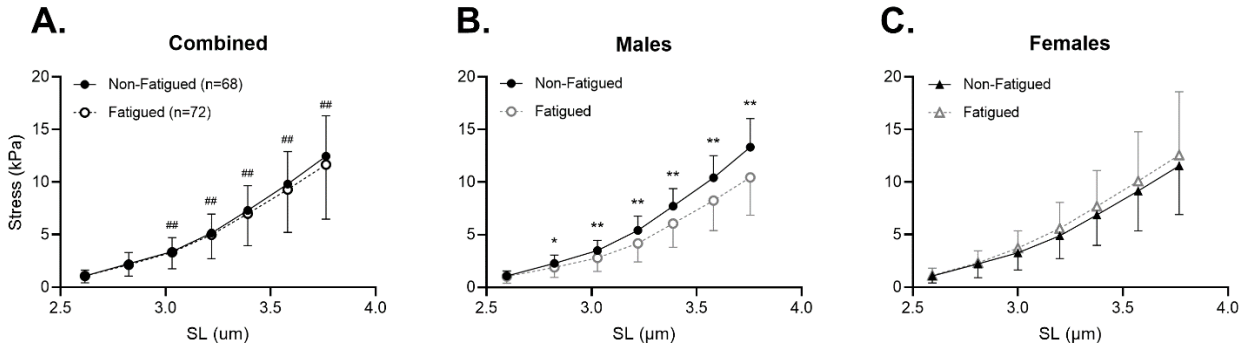

Figure 16. (A) In the combined dataset, there was a significant interaction effect of biological sex * fatigue on passive stress at SL 3.0-3.8 µm. Separate analyses of the effect of fatigue on passive stress in males versus females revealed that fatigue significantly reduced passive stress in males **(B)** but not females **(C)**, consistent with what was observed in the passive modulus data. Data are shown as mean ± SD. Symbols indicate significant effect of ## fatigue by biological sex interaction ($p<0.01$) and * fatigue (single $p<0.05$, double $p<0.01$) indicate significant differences by fatigue.

Titin Phosphorylation: Mass spectrometry results (Figure 17) reveal increased phosphorylation of four titin serines: S12827 (FDR=0.0486), S12900 (FDR=0.0142), S12902 (FDR=0.0367), and S12918 (FDR=0.00195), and decreased phosphorylation at S28585 (FDR=0.0367). The Uniprot entry for human titin (entry Q8WZ42, The UniProt Consortium, 2023) suggests that S12827 is within immunoglobulin (Ig) domain 85 and S12900, S12902, and S12918 are located in between Ig domains 85 and 86. Uniprot also suggests that S28525 is located within Ig domain 132. A previous review summarizing Uniprot data (Hamdani *et al.*, 2017) suggests that in human cardiac titin, S12827, S12900, S12902, and S12918 are located within the elastic I-band of titin and S28585 is located within the inelastic A band, yet it is unclear how similar serine locations are within titin substructures of cardiac versus skeletal titin isoforms.

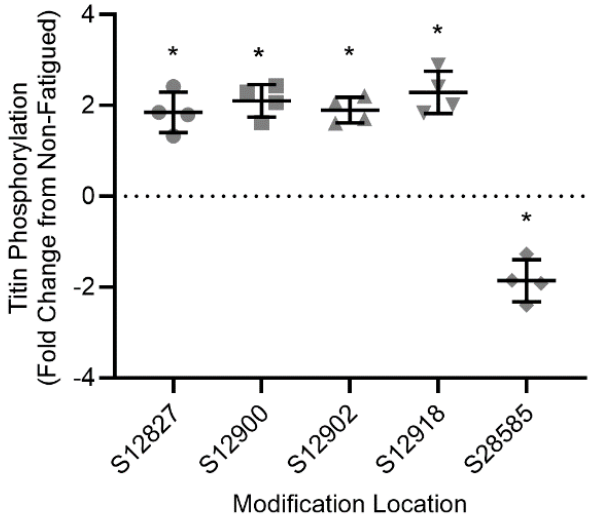

Figure 17. Mass spectrometry analysis demonstrated increased phosphorylation at 4 serine residues, S12827, S12900, S12902, and S12918 and decreased phosphorylation at serine residue S28525of the F versus NF sample. At each serine location, every point in the figure represents data form one participant (2 males, 2 females). Bars represent mean ± SD. * Indicates significantly different from NF (FDR<0.05).

Electron Microscopy: Electron microscopy images do not demonstrate ultrastructural changes following fatiguing exercise (Supplementary Figure *2*). In contrast with published reports of contraction induced damage (Fridén et al., 1983; Fridén, 1984; Roth et al., 1999),

which feature disordered sarcomeres and lack of registration between adjacent Z-lines, the sarcomeres visualized in this study were similar between fatigued and non-fatigued samples.

In-vitro AP and PKA treatments: Fibers included in AP treatments were collected from a subset of participants included in other analyses including 1 older male, 1 older female, and 1 younger male. Because there was no significant main effect of age on passive modulus at short (Older: 17.14 ± 8.08 kPa/%Lo, Young: 10.93 ± 4.78 kPa/%Lo, p=0.194) or long (Older: 21.43 ± 9.67 kPa/%Lo, Young: 16.98 ± 10.77 kPa/%Lo, p=0.140), samples were combined for subsequent analyses. Importantly, statistical analysis conducted without fibers from the young male (Supplementary Figure 4) did not have a different outcome than what is presented below. Single fiber CSA was not significantly different between fatigue conditions (p=0.919) or AP treatment groups (p=0.335, Table 4). Similarly, fiber length was not different between fatigue conditions (p=0.318) or AP treatment groups (p=0.717). Due to the imbalanced representation of MHC isoforms, fiber-type was not considered in subsequent analyses and all fibers were included. Active tension generation was not affected by age (p=0.343) or fatigue condition (p=0.104) but was significantly reduced by AP treatment (p=0.003, Supplementary Figure 3).

Table 4. Descriptive statistics of the fibers included in AP assays.

					MHC				
		N	**CSA (mm^2)**	**Length (mm)**	**I (N)**	**I/IIA (N)**	**IIA (N)**	**IIX (N)**	**IIA/X (N)**
Non-Fatigued	Sham	15	0.0044 ± 0.0020	1.5 ± 0.4	4	2	5	1	3
	AP	16	0.0051 ± 0.0016	1.5 ± 0.2	3	4	2	0	7
Fatigued	Sham	20	0.0051 ± 0.0017	1.6 ± 0.4	6	0	7	2	5
	AP	29	0.0049 ± 0.0015	1.6 ± 0.3	12	0	9	1	6

Data are shown as mean ± SD.

The purpose of this assay was to test the effect of AP treatment on passive stress and Young's Modulus within each fatigue condition. There was no significant effect of AP treatment on passive stress at any SL in non-fatigued fibers (Figure 18A); however, passive stress was significantly reduced by AP treatment at SL=3.6 μm (Sham: 10.16 ± 4.68 kPa, AP: 8.01 ± 3.13 kPa, p=0.031) and 3.8 μm (Sham: 12.08 ± 5.54 kPa, AP: 9.62 ± 3.73 kPa, p=0.033) in fatigued

fibers (Figure 18B). Furthermore, AP treatment did not have a significant effect on passive modulus, in either fatigue condition, at short lengths (Figure 18C), but did significantly reduce passive modulus in fatigued fibers at long lengths (Sham: 23.69 ± 11.12 kPa/%Lo, AP: 18.66 ± 8.55 kPa/%Lo, p=0.032, Figure 18D).

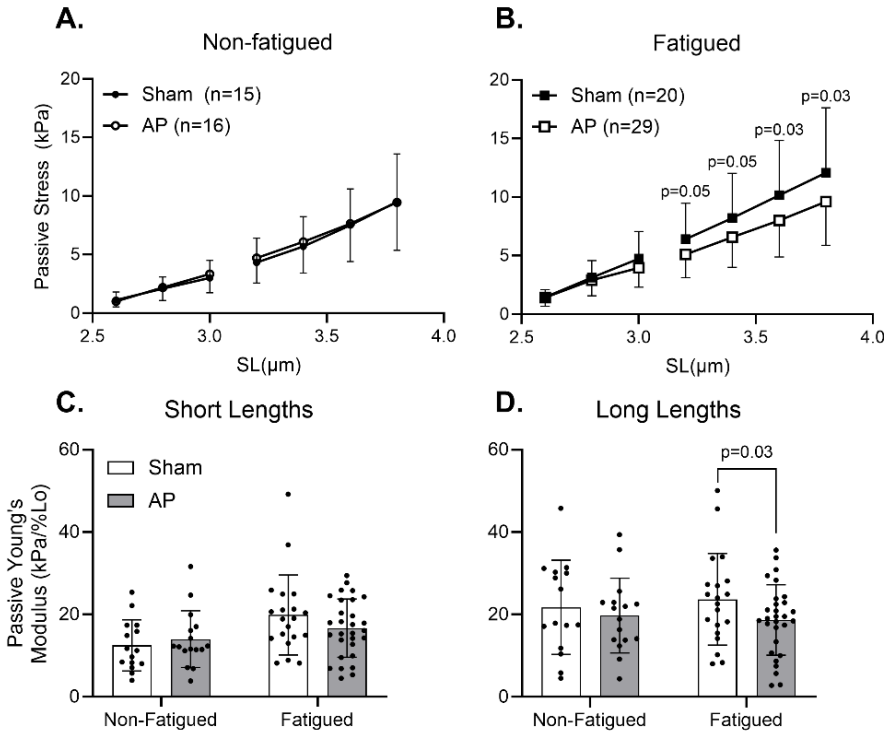

Figure 18. Passive stress was not different by treatment at any strain in non-fatigued fibers **(A)** but was different at longer lengths in fatigued fibers such that AP treatment reduced passive stress **(B)**. When comparing passive modulus values, AP treatment had no significant effect at short lengths **(C)** but did significantly reduce passive modulus of fatigued fibers at long lengths **(D)**. Included fibers were from one young male, one older male, and one older female. Means were compared separately in non-fatigued and fatigued fibers using a mixed model ANOVA with participant as a random effect and treatment as a fixed effect.

Fibers included in PKA treatments were collected from 2 younger females and 1 older female. Age was found to be a significant modifier of passive modulus at short (Older: 18.28 ± 6.01 kPa/%Lo, Young: 13.07 ± 7.72 kPa/%Lo, p<0.01) but not long (Older: 31.46 ± 8.90 kPa/%Lo, Young: 22.87 ± 9.41 kPa/%Lo, p=0.189) lengths. However, analysis of the effects of

fatigue and PKA treatment on cellular passive modulus in older and younger adults, separately (Supplementary Figure 6), did not produce a different outcome than analysis of the collective group. Therefore, the analysis presented here will consider all participants, regardless of age.

Table 5. Descriptive statistics of the fibers included in PKA assays.

					MHC				
		N	**CSA (mm^2)**	**Length (mm)**	**I (N)**	**I/IIA (N)**	**IIA (N)**	**IIX (N)**	**IIA/X (N)**
Non-Fatigued	Sham	12	0.0050 ± 0.0016	1.5 ± 0.5	10	0	2	0	0
	PKA	18	0.0046 ± 0.0021	1.2 ± 0.5	7	0	8	1	2
Fatigued	Sham	18	0.0064 ± 0.0039	1.2 ± 0.3	4	2	8	1	5
	PKA	23	0.0054 ± 0.0028	1.2 ± 0.4	4	2	15	1	1

Data are shown as mean ± SD.

There was no significant difference in single fiber CSA between fatigue conditions (p=0.098) or PKA treatment groups (p=0.299, Table 5). Similarly, there was no difference in single fiber length between fatigue conditions (p=0.105) or PKA treatment groups (p=0.181). Given the relatively imbalanced representation of fiber-types across fatigue and treatment groups, fiber types were considered collectively in subsequent analyses. Active isometric tension generation was significantly increased by PKA treatment (p=0.005, Supplementary Figure 5).

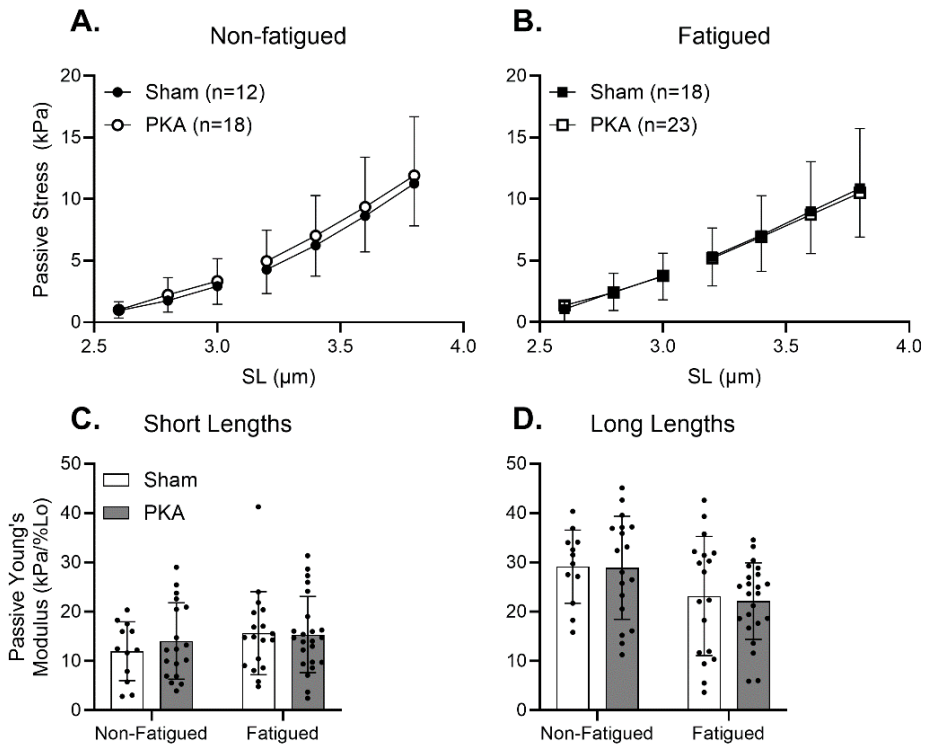

Figure 19. PKA treatment did not affect passive stress values at any length in non-fatigued **(A)** or fatigued **(B)** fibers. Furthermore, PKA treatment did not have a significant effect on passive modulus at short **(C)** or long **(D)** lengths. Included fibers were from one young female and two older females. Means were compared separately in non-fatigued and fatigued fibers using a mixed model ANOVA with participant as a random effect and treatment as a fixed effect.

The purpose of this assay was to see if treatment of single fibers with PKA, previously demonstrated to phosphorylate skeletal titin (Yamasaki *et al.*, 2002; Krüger & Linke, 2006*a*; Wang *et al.*, 2023), would reduce the passive modulus of non-fatigued fibers. Passive stress was not significantly different between sham and PKA treated fibers in the non-fatigued (Figure 19A) or fatigued (Figure 19B) condition. Furthermore, passive modulus was not significantly different by between sham and PKA-treated fibers, in either fatigue condition, at short (Figure 19C) or long (Figure 19D) lengths.

3D. Discussion

Fatiguing exercise reduces cellular passive modulus. The present results demonstrate reduced passive modulus following fatiguing exercise in permeabilized single muscle fibers from young, untrained adults. Importantly, these observations were made in the absence of an obvious exercise-induced damage to the sarcomere ultrastructure (Supplementary Figure *2*). The

observation of comparable active isometric tension in NF and F skeletal muscle fibers (Supplementary Figure *1*) further suggests that fiber integrity was not impaired in our fatigued sample. In these experiments, the use of chemical skinning on dissected single fibers, which permeabilizes the sarcolemma and removes ECM, supports the idea that reductions in cellular passive stress and modulus reflect changes to intracellular proteins, rather than to ECM mechanical properties. Specifically, proteins capable of contributing to altered cellular passive modulus include contractile proteins actin and myosin and viscoelastic protein titin.

In a relaxing solution (pCa 8.0), the contribution of residual crossbridge formation to cellular passive modulus is possible. This idea was initially presented by D.K. Hill (Hill, 1968) and supported by later work demonstrating that a small population of actomyosin interactions contributed to force production in relaxed frog skeletal muscle (Campbell & Lakie, 1998). If a proportion of crossbridges do remain intact in relaxed muscle fibers, fatigue induced PTMs to myosin, presumably still present at the time of passive mechanics measurement, may contribute to changes in passive modulus via altered contribution of residual crossbridge formation. This possibility of residual crossbridge formation was considered in the present study. However, measurement of passive modulus in relaxing solution with 40 mM 2,3-butanedione monoxime (BDM), a myosin inhibitor, did not impact the observation of reduced modulus in fatigued versus non-fatigued fibers (Figure 15), suggesting that residual crossbridge formation was not a primary contributor to fatigue-induced reduction of passive modulus. Instead, the reduced cellular passive modulus observed in this sample was more likely the result of a non-contractile intracellular mechanism.

At the cellular level, passive modulus is primarily determined by the sarcomere protein titin (Lim et al., 2019; Ottenheijm et al., 2012), making it a primary target for study in this research area. Titin-based stiffness can be modified by calcium (Nishikawa, 2020), heat shock proteins (HSPs, Kötter et al., 2014), oxidation (Alegre-Cebollada et al., 2014; Watanabe et al., 2020), and phosphorylation (Hamdani et al., 2017), all of which are upregulated during fatiguing exercise. Therefore, fatiguing exercise may modify titin-based stiffness through PTM of titin elastic domains. For example, exercise increases calcium cycling, prompting calcium-mediated binding of titin to the thin filament (Dutta *et al.*, 2018) which shortens and stiffens the titin-based spring in skeletal muscle (Joumaa *et al.*, 2008). Additionally, reduced muscle pH during exercise

promotes aggregation of titin Ig domains, which increases titin-based stiffness (Kötter *et al.*, 2014). However, previous work in human muscle fibers has demonstrated that HSPs, including HSP 27, can also bind to titin Ig domains, thereby stabilizing unfolded Ig domains and preventing aggregation (Kötter *et al.*, 2014). In this way, HSPs may prevent acidification-induced increase of titin-based stiffness during exercise (Kötter *et al.*, 2014). Exercise also induces oxidative stress, which results in numerous downstream mediators of titin-based stiffness (Beckendorf & Linke, 2015) including S-Glutathionylation, which has been shown to reduce stiffness of muscle cells (Alegre-Cebollada *et al.*, 2014; Watanabe *et al.*, 2020). In the present study, the storage solutions included Dithiothreitol (DTT), an antioxidant, making it unlikely that titin oxidation contributed to the observed changes in cellular passive modulus. Finally, exercise-induced β-adrenergic signaling, coupled with increased concentration of inorganic phosphate, may have contributed to an overall increase in titin phosphorylation (Krüger & Linke, 2006*b*; Hamdani *et al.*, 2017) during fatiguing exercise. Preclinical studies have demonstrated that binding of inorganic phosphate to titin can alter titin-based stiffness, though the nature of mechanical change is dependent on the location of phosphate binding (Müller *et al.*, 2014). In the present study, five significant phosphorylation changes (4 increases, 1 decrease) were identified in the fatigued sample of human skeletal muscle. Therefore, phosphorylation is a possible contributor to the mechanical changes observed following fatiguing exercise.

Fatiguing exercise modifies titin phosphorylation in human skeletal muscle. Mass spectrometry analyses (Figure 17) suggest that the fatiguing exercise utilized in this study altered titin phosphorylation in human vastus lateralis muscle, and these phosphorylation events may have occurred in the elastic regions of titin. The notion that titin phosphorylation is one of the many PTMs with the capacity to alter titin-based stiffness is not new (Hamdani *et al.*, 2017). In fact, it has been previously proposed that phosphorylation of titin Ig domains may reduce the ability of Ig domains to refold (Hamdani *et al.*, 2017) which, given the importance of titin Ig refolding to elastic energy production (Rivas-Pardo *et al.*, 2016), likely reduces titin-based stiffness. This proposed mechanism is similar to another mechanism described previously (Alegre-Cebollada *et al.*, 2014; Watanabe *et al.*, 2020), in which titin oxidation via S-glutathione inhibited titin Ig domain refolding and ultimately decreased the stiffness of human cardiomyocytes. Evidence of modified titin-based stiffness following increased or decreased titin

phosphorylation is present in preclinical skeletal (Müller *et al.*, 2014), preclinical cardiac (Fukuda *et al.*, 2005), and human cardiac (Krüger *et al.*, 2009) muscle research, and the specific stiffness response is highly dependent on the location of the phosphorylation event. In the present study, five serine residues presumably located within the elastic regions of titin (The UniProt Consortium, 2023) exhibited increased or decreased phosphorylation in fatigued versus non-fatigued skeletal muscle, presenting the possibility that altered titin phosphorylation contributed to the changes observed in cellular passive modulus.

In the present study, passive modulus was measured in a subset of single fibers treated with BDM to isolate the specific effects of titin on passive modulus. Furthermore, fatigue-induced reductions in passive modulus were greatest at the longest lengths observed (SL 3.2 ± 0.13µm – 3.8 ± 0.18µm), where the overlap of thick and thin filaments is minimal and passive modulus in permeabilized skeletal muscle cells is primarily titin-based. Finally, support for the notion of this phenomenon being titin driven is provided by the observation of reduced stress decay index (SDI), an index of viscosity (Lim *et al.*, 2019), in the fatigued versus non-fatigued skeletal muscle fibers of males but not females when examined in a larger sample of younger adults, including the present cohort of participants (Appendix B: Supplementary Document, Figure 6). Fatigue-induced reductions in SDI of fibers from males appears to be driven by reductions in peak stress and magnitude of stress decay (Appendix B: Supplementary Document, Figure 7), and persisted in the presence of BDM (Appendix B: Supplementary Document, Figure 8). Considering titin's viscoelastic properties and predominant influence on mechanical properties of permeabilized muscle fibers, especially at long lengths, these observations in cellular SDI are interpreted as further support for the notion that fatiguing exercise alters titin mechanics. Nonetheless, it must be acknowledged that fatiguing exercise has the potential to modify sarcomere proteins other than titin. Although titin is the foremost candidate as a contributor to acute changes in passive mechanical properties, future studies must keep in mind that contributions of other proteins in-vivo (e.g. myosin, actin, desmin) are possible.

The effect of fatiguing exercise on passive modulus is sex specific. The present results suggest that fatiguing exercise reduces skeletal muscle cellular passive modulus in a way that is specific to biological sex (Figure 4A and B). Specifically, cellular passive modulus was significantly reduced at short (Figure 4C) and long (Figure 4D) lengths in skeletal muscle cells

from young, untrained males but not females. The lack of significance in the female cohort may be partially explained by the greater variety in response of passive modulus to fatiguing exercise in females compared to males, especially at longer lengths (Figure 4F). This variation in response might stem from the effects of sex hormones such as estrogen on skeletal muscle. Given the presence of estrogen receptors within skeletal muscle and the effects of estrogen on skeletal muscle strength (Collins *et al.*, 2019), mitochondrial function (Pellegrino *et al.*, 2022; Yoh *et al.*, 2023), and regenerative capacity (Kitajima & Ono, 2016; Pellegrino *et al.*, 2022), estrogen has a clear effect on skeletal muscle cellular function through modification of intracellular proteins. In fact, estradiol has been shown to directly affect regulatory light chain function in skeletal muscle (Lai *et al.*, 2016), prompting the possibility that estrogen might also affect the function of other intracellular proteins, such as titin. In preclinical work using rat cardiac muscle, changes in circulating estrogen prompted shifts in titin isoform distribution in a way that altered cardiac stiffness (Bupha-Intr *et al.*, 2011). This result suggests an influential role of estrogen on the regulation of titin-based stiffness. However, whether estrogen directly impacts titin-based stiffness in human skeletal muscle remains to be seen. Previous work has demonstrated a negative correlation between circulating estrogen and musculotendinous stiffness (Bell *et al.*, 2012). Nonetheless, the effect of the menstrual cycle on whole-muscle stiffness remains unclear, with some evidence of stiffness variation throughout the menstrual cycle (Ham *et al.*, 2020) and other evidence of no change (Bell *et al.*, 2011). In males, previous work found no relationship between circulating estrogen and musculotendinous stiffness (Bell *et al.*, 2012). Although the present study design attempted to control for fluctuations in circulating estrogen throughout the menstrual cycle by collecting biopsies at the same time point (pre-follicular phase) or in individuals using hormonal contraception, inter-individual differences in total circulating estrogen may still have been present in our female participants, perhaps contributing to the diversity in response of passive modulus to fatiguing exercise across female participants (Figure 4E and F). For this reason, future studies of cellular passive modulus in females should consider measuring circulating estrogen at the time of biopsy collection.

Without having blood measures of circulating sex hormones, one can only speculate regarding the cause of reduced passive stress and Young's Modulus in exclusively male participants. There is no difference in fatigue ratio or time to fatigue between male and female

participants (Table 2), so there is no support for the notion that males fatigued to a different degree compared to females. Within the framework of the working hypothesis that titin is a driver of acute changes to cellular passive mechanics, is possible that the profile of sex hormones common in biological males may have impacted signaling pathways that affect titin. For example, circulating testosterone is known to interact with G-protein coupled receptors or sex hormone binding globulin protein (SHBG) in skeletal muscle, which in turn activate downstream pathways including PKA signaling (Dubois *et al.*, 2012). As a result, it is possible that sex-based differences in exercise-induced titin phosphorylation may exist. Although this is not evident in the present LC-MS data for titin phosphorylation changes due to fatiguing exercise (Figure 17), it is important to note that those data are from a separate set of individuals from those included in the cellular mechanics analyses. Whether exercise-induced changes to titin phosphorylation differ between males and females in the cohort used for mechanics studies remains to be seen.

HSP, another proposed mechanism of altered cellular mechanics following fatiguing exercise, may also contribute to sex-based differences in the response of cellular mechanics to fatiguing exercise. Specifically, there is evidence that skeletal muscle expresses higher levels of HSC 70, HSP 25, and αβ crystallin in males compared to females (Romani & Russ, 2013). Furthermore, male rats were shown to express higher quantities of HSP 70 following exercise than females (either ovariectomized and placebo treated, or ovariectomized and estrogen treated), suggesting that estrogen blunts the expression of HSP following a single 60 min bout of running (Paroo *et al.*, 2002). It appears that the time course for observed increase in HSP expression following exercise (measured 24 hrs. after) is too long to explain the sex-based disparity observed in our results. However, it is possible that the increased population of HSPs (including αβ crystallin) present in male skeletal muscle allowed for greater interaction of HSPs with titin to prevent acidification induced aggregation of titin Ig domains (Kötter *et al.*, 2014). For this reason, future studies may consider comparing HSP content (HSP 27 or αβ crystallin, based on Kötter *et al.*, 2014) in skeletal muscle samples from males versus females.

AP/PKA Treatment of Single Fibers. The link between titin phosphorylation and cellular passive mechanics warrants further investigation as a potential mechanism underlying reduced musculoskeletal stiffness following fatiguing exercise. Therefore, in-vitro AP/PKA treatments of single skeletal muscle fibers tested the hypothesis that modification of titin phosphorylation

status would lead to changes in cellular measures of passive stress and modulus. It was previously speculated (Hamdani *et al.*, 2017) that phosphorylation of titin would reduce cellular passive stress and modulus in non-fatigued fibers. Conversely, we hypothesized that titin de-phosphorylation would increase passive stress and modulus of fatigued fibers. The decision to attempt to de-phosphorylate skeletal titin via in-vitro AP treatment was supported by reports of AP use in previous studies (Franssen *et al.*, 2017; Krysiak *et al.*, 2018) to successfully de-phosphorylate cardiac titin. In the present results, treatment of single fibers with AP caused a significant reduction in passive stress (SL = 3.6-3.8 µm, Figure 18B) and Young's Modulus at long lengths (Figure 18D) in fatigued fibers only. This outcome contrasted with our initial hypothesis. Importantly, measurements following AP or sham treatment were not performed in the presence of BDM, a myosin inhibitor. AP has been reported to de-phosphorylate other sarcomere proteins such as myosin regulatory light chain (González *et al.*, 2002) and myosin binding protein C (Kooij *et al.*, 2013), which may have contributed to the reductions in active isometric tension observed here (Supplementary Figure 3). However, the contribution of these proteins to passive stress and modulus measures is small at sarcomere lengths greater than 3.0 µm, where titin is considered the primary source of passive stiffness in skinned myocytes. Coincidentally, these longer lengths (SL = 3.6-3.8 µm) are where the significant effect of AP treatment was observed. As a result, the change in passive stress and modulus observed here is presumed to be titin derived.

Unfortunately, titin phosphorylation was not measured in these treated and untreated samples. As a result, it is impossible to directly attribute the observed mechanical changes to altered titin phosphorylation following AP treatment. Nonetheless, the observation of altered passive stress and modulus at SL where minimal thick/thin filament overlap occurs provides some support for the notion that titin-based measures of stiffness were altered following AP treatment. Although our hypothesis was not supported by the results of AP assays, this outcome does motivate further efforts to more directly link changes to titin phosphorylation to modified skeletal muscle stiffness. Future efforts should confirm titin dephosphorylation following AP treatment and should perform cellular passive mechanics measurements in the presence of BDM or blebbistatin.

The decision to use PKA was motivated by the recognition of PKA as a major signaling molecule in contracting skeletal muscle, and therefore a likely modifier of titin phosphorylation status during fatiguing exercise. This decision was further supported by previous work demonstrating that PKA phosphorylates the skeletal isoform of titin (Krüger & Linke, 2006*a*; Wang *et al.*, 2023). In the present study, neither passive stress nor passive modulus, measured in the presence of BDM to inhibit any crossbridge formation, were significantly affected by PKA treatment. There are considerations to be made in light of this result. First, it is possible that PKA did in fact phosphorylate titin, a possibility that cannot be appropriately addressed given that titin phosphorylation was not successfully measured following PKA treatment, but that the phosphorylation event did not result in altered titin-based measures of stiffness. For example, it is possible that PKA phosphorylated titin at a non-extensible region of the protein, such as the A-band. In fact, our own LC-MS data, interpreted with the help of The UniProt Consortium, 2023, suggest that serine 28585 is located within the inelastic A-band and is phosphorylated during exercise. The titin A-band has a presumed role in mechano-sensing (Granzier *et al.*, 2014) and is known to interact with other sarcomere proteins including myosin and MyBP-C (Linke & Hamdani, 2014), but is not considered a primary contributor to cellular passive extensibility as it is estimated to be ~40 fold less extensible than the elastic I-band region (Granzier *et al.*, 2014).

It is also possible that PKA did cause phosphorylation within the extensible region of the protein, but that this did not result in altered titin-based stiffness. This idea is supported by previous work (Müller *et al.*, 2014) demonstrating that the effect of titin phosphorylation on titin-based stiffness is highly dependent on the serine location of the phosphorylation event. Finally, it is possible that PKA did not, in fact, phosphorylate skeletal muscle titin in our hands. Although we have extensively used PKA to phosphorylate other sarcomere proteins such as MyBP-C (Privett *et al.*, 2021), and the significant increase in active tension generation (Supplementary Figure 5) suggests that PKA incubations altered the function of sarcomere contractile and/or regulatory proteins, it is possible that these incubation conditions were not successful to phosphorylate titin, or that PKA was not the best choice of kinase for titin phosphorylation.

Other groups suggest that PKC may be used to phosphorylate skeletal titin (Hidalgo Carlos *et al.*, 2009), presenting a possible direction for future studies investigating the effect of titin phosphorylation on passive mechanical measures in single skeletal muscle fibers. Finally, it

must also be acknowledged that the PKA assays were performed in females, a group which was later found to lack the response of passive mechanics to fatiguing exercise (Figure 14C-F). It is possible that any potential effect of PKA treatment on cellular passive mechanics was missed due to the lack of a difference in titin phosphorylation between fatigued and non-fatigued samples from these individuals. This cannot be confirmed given the present dataset; however, future studies using this assay should seek to test for an effect of PKA treatment on cellular passive mechanics in young males.

Altogether, the results of the present AP (Figure 18) and PKA (Figure 19) treatments did not support the hypothesis that increased titin phosphorylation results in reduced cellular passive measures of stiffness. The reduced passive stress and modulus observed in fatigued fibers at longer lengths following AP treatment does provide a compelling potential link between titin de-phosphorylation and altered cellular mechanics; however, confirmation of titin phosphorylation would be required to pursue this idea. Importantly, these results must be considered within the context of the many possible PTMs occurring to titin during in-vivo fatiguing exercise (Figure 3). It is unlikely that any one PTM explains the observed changes in cellular passive stress and modulus (Figure 14). Rather, it is plausible that a multitude of PTMs, occurring at specific locations throughout the titin protein, contribute to the observed sex-specific modification of cellular passive mechanics following fatiguing exercise. Moving forward, studies of the mechanism underlying cellular changes to cellular passive mechanics should consider alternative mechanisms of titin phosphorylation (i.e. PKC) as well as other PTMs such as HSP 27 (Liu & Steinacker, 2001; Kötter *et al.*, 2014).

Limitations.

In this study, the uneven distribution of fiber-types limited our ability to test for a mediating effect of MHC on the response of cellular passive modulus to fatiguing exercise. Previous work (Miller *et al.*, 2015) has suggested that cellular passive elastic modulus differs among fiber-types, highlighting the need to consider fiber-type in future studies of passive modulus. Importantly, the conclusions regarding the overall effect of fatigue on cellular passive mechanics were not impacted by inclusion of all fiber-types (I, IIA, IIX, I/IIA, IIA/X) in the preliminary statistical analyses (data not shown). It must also be acknowledged that although the location and exact sequence of titin serines are based on the highly annotated entry for human

titin: Q8WZ42 (The UniProt Consortium, 2023), the precise phosphorylation locations detected in our mass spectrometry analyses, and where they fall along the titin protein, may not yet be fully understood. Therefore, our ability to speculate regarding potential functional implications of phosphorylation/de-phosphorylation at each titin serine is necessarily limited.

There were limitations to the AP/PKA treatments that impacted interpretation of the results from these assays. First, the limited sample size was further complicated by the fact that included participants represented a variety of age/biological sex backgrounds. As shown in supplementary figures (Supplementary Figure *4*, Supplementary Figure *6*), neither age nor biological sex impacted the results presented in this aim. However, the lack of a uniform participant background complicates interpretation. Future investigations regarding the effect of titin phosphorylation should seek to test this mechanism in young males, for which a strong effect of fatiguing exercise on cellular passive stress and modulus (Figure 14 and Appendix B: Supplementary Document) has been established. Secondly, measurement of cellular passive mechanics was not conducted in the presence of BDM, so it is possible that AP treatment of other sarcomere proteins such as regulatory light chain (González *et al.*, 2002) or myosin binding protein C (Kooij *et al.*, 2013) may have impacted the results presented here, especially at shorter lengths (SL = 2.6-3.0 μm). Although this did not likely impact the interpretation of findings at longer SL, any additional studies in this area should conduct cellular passive measures in the presence of BDM. Finally, I was unable to confirm titin de-phosphorylation or phosphorylation following AP or PKA treatment, respectively. Despite years of effort and the recruitment of advice from other labs who have been successful in measuring titin phosphorylation using gel electrophoresis (Fukuda *et al.*, 2005; Hidalgo *et al.*, 2014; Granzier *et al.*, 2014), I was unable to reliably quantify titin phosphorylation using the methods described earlier in this chapter. Future studies can confirm the effect of AP/PKA treatment on titin phosphorylation using LC-MS. Alternatively, use of acrylamide gradient gels (Fukuda *et al.*, 2005) may prove to be a more successful approach to quantifying titin abundance and phosphorylation.

3E. Conclusions

We present novel evidence of reduced cellular passive Young's Modulus following a single bout of fatiguing exercise. This observation parallels previous reports of reduced whole-muscle stiffness following fatiguing exercise (Andonian *et al.*, 2016; Siracusa *et al.*, 2019;

Chalchat *et al.*, 2020), supporting the notion that intracellular mechanisms contribute to acute reduction of whole-muscle stiffness. Furthermore, LC-MS data suggest that titin phosphorylation is altered at 5 serine residues during fatiguing exercise, which previous research (Müller *et al.*, 2014) suggests may contribute to altered titin-based stiffness. Given that prior evidence of fatigue-induced muscle compliance were only recorded in males (Siracusa *et al.*, 2019; Chalchat *et al.*, 2020), it is perhaps not surprising that we only observed the effect at the cellular level in male participants. Perhaps more interesting, the clear link between muscle fatigue and injury risk (Mair *et al.*, 1996) may also be related to sex-based differences in the dynamic response of muscle fiber compliance to fatigue. Nevertheless, our study was somewhat limited in that female participants were measured at a time of presumably limited circulating estradiol.

Future studies of cellular passive modulus in females should consider whether circulating estrogen concentrations alter the response of cellular passive modulus to fatiguing exercise, as this might contribute to the increased incidence of soft-tissue injury in female athletes compared to their male counterparts (Arendt *et al.*, 1999; Deitch *et al.*, 2006; Matzkin & Garvey, 2019) or falls risk and resulting injury in older females (Stevens, 2005; Franse *et al.*, 2017). Last, it remains to be seen whether the observations of altered passive modulus at the cellular level translate to the tissue level of skeletal muscle, an important step to understanding the interplay between intracellular and extracellular contributors to skeletal muscle stiffness and how they might be acutely altered by fatiguing exercise. Ultimately, the study of mechanisms underlying fatigue-induced reductions in skeletal muscle passive stiffness will contribute to efforts aimed at reducing fatigue-induced injury risk in athletes and falls risk in older adults.

4. Aim2: To determine whether cellular observations of fatigue-induced alterations to passive mechanics translate to the tissue level.

4A. Introduction

Preliminary work for Aim 1 demonstrates increased titin phosphorylation coincident with reduced passive stiffness in fatigued single fibers, where titin largely determines passive stiffness. Motivated by initial reports of reduced skeletal muscle stiffness in whole muscle following exercise to fatigue, Aim 2 assessed whether observations made at the cellular level would translate to the tissue level. Unlike cellular mechanics, skeletal muscle mechanics at the tissue and whole-muscle scales are impacted by the inclusion of extracellular collagen-based structures (Meyer & Lieber, 2011; Ward *et al.*, 2020). Therefore, the effect of fatiguing exercise on samples of skeletal muscle including ECM is physiologically relevant. To this end, passive stiffness was compared in bundles of fibers with intact ECM from fatigued versus non-fatigued samples to test the hypothesis that i) passive stress and Young's Modulus would be lower in fatigued versus non-fatigued fiber bundles. Next, the comparison of collagen-fibril orientation in non-fatigued versus fatigued samples was proposed. However, technical limitations precluded this measure, and bundle mechanics data did not present compelling evidence to expect that collagen fibers in ECM were re-aligned during our fatiguing exercise protocol. Instead, ECM morphology was compared in skeletal muscle from males and females to test the hypothesis that ii) sex-based differences in collagen I quantity contributed to differences in bundle passive mechanics. Finally, the role of titin in mediating tissue-level stiffness (Brynnel *et al.*, 2018) was assessed by experimentally eliminating titin-based stiffness in fiber bundles (Ottenheijm *et al.*, 2012; Brynnel *et al.*, 2018) to test the hypothesis that iii) titin contributes to fatigue-induced changes in bundle passive stress and modulus. Ultimately, the goals of this aim were to assess the scalability of cellular passive mechanics measures and to determine how acute changes to cellular level passive mechanics impact measures at the tissue level.

4B. Methods

Study Design, Population, Fatiguing Protocol, Muscle Biopsy Procedure, and Tissue Processing: These details were as described in chapter 3.

Mechanical sample preparation: On the day of experimentation, one bundle was placed in dissection solution. For bundle experiments, groups of 12-14 fibers with intact ECM were dissected from the sample. These smaller bundles were not permeabilized a second time. All prepared bundles were kept in dissecting solution on ice until experimentation.

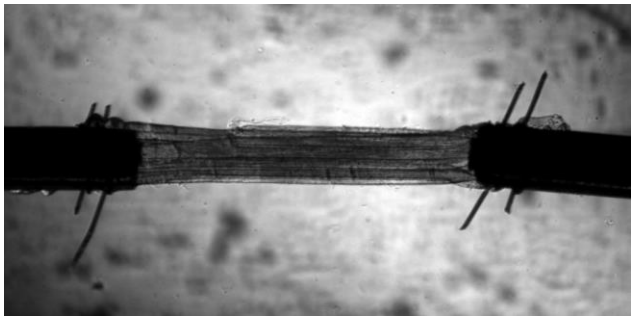

Figure 20. An image of a bundle of fibers with intact ECM mounted between a force transducer (left) and length motor (right).

Single fiber morphology and contractile measures: Prepared bundles were mounted in relaxing solution between a force transducer and a length motor (Aurora Scientific, Inc., Aurora, ON, Canada; Figure 20). Bundles were attached by direct suturing of the bundle to the rods attached to the force transducer and length motor. Bundle length, d_{top}, and d_{side} were measured as described in chapter 3.

Passive stretch protocol: Initial SL was set to 2.4 µm before the bundle was subjected to the same passive stretch protocol as described in chapter 3. All tested bundles were placed in a high-salt sample buffer (5% beta-mercaptoethanol), briefly centrifuged and heated, and stored at -80°C until later assessment of myosin heavy chain (MHC) isoform distribution.

In-vitro titin treatments: KI/KCl - These treatments were performed on fiber bundles to assess titin's contribution to tissue-level passive stiffness as described previously (Ottenheijm *et al.*, 2012; Brynnel *et al.*, 2018). Mounted bundles were subjected to an initial passive-stretch (as described above), followed by incubation in relaxing solution spiked with 0.6M KCl for 30 minutes at 15°C followed by relaxing solution containing 1.0M KI 30 minutes at 15°C. These incubations extract the thick and thin sarcomere filaments, respectively (Ottenheijm *et al.*, 2012). After incubation, bundles were passively stretched to measure post-incubation passive stiffness. Following these experiments, bundles were collected and stored in sample buffer.

Collagen I immunohistochemistry (IHC): Originally, Aim 2 had proposed quantifying ECM collagen fibril orientation using second harmonic generation (SHG) microscopy or

picrosirius red staining. However, SHG microscopy was not readily available, picrosirius red staining was not compatible with our storage method for IHC (fresh frozen, not fixed), and the lack of a clear effect of fatigue on bundle passive mechanics measurements, suggested that quantification of collagen content, rather than collagen fibril orientation, is a more appropriate approach to understanding the passive mechanics measures. Therefore, IHC was performed to quantify the amount of collagen I in skeletal muscle samples from two individuals for which bundle passive mechanics measurements were collected.

At the time of biopsy, bundles of skeletal muscle fibers (~100 fibers) from the vastus lateralis were blotted and embedded in O.C.T. (Tissue-Tek®, Sakura Finetek, USA) before being frozen in isopentane precooled with liquid N2 and subsequently stored at -80°C. On the day of cryo-sectioning, samples were acclimated for 1hr at -20°C before cryo-sectioning at a thickness of 8μm on a Leica Cryostat (Leica CM 1850UV) and placed on glass slides. Samples were dried overnight in a covered opaque box. The next day, samples were washed twice for 10min in a PBS/1% BSA solution, followed by incubation in primary antibodies for type I collagen (C2456, 1:100, Millipore Sigma, St. Louis, MO) and MHC I (BA-D5 MIgG2b, 1:100, DSHB, Iowa City, IA) overnight. Then, samples were washed twice for 5min each and incubated in secondary antibodies for type I collagen (Goat anti-mouse IgG1 AlexaFluor 488, 1:500, Invitrogen, Waltham, MA) and MHC I (Goat anti-mouse IgG2b AlexaFluor 647, 1:500, Invitrogen, Waltham, MA) for 1hr. Samples were then washed twice for 5min each before and after washing with methanol for 10min. Lastly, one drop of SlowFade™ Diamond Antifade Mountant with DAPI (Invitrogen, Waltham, MA) was applied directly on the sample, followed by two drops of permount mounting medium (Electron Microscopy Sciences, Hatfield, PA) on the glass slide and cover slip placed on top. Samples were imaged on a Leica fluorescence microscope (Leica DM4000B) and Leica camera (Leica DFC 360FX) at 10x magnification. Image settings include 400ms exposure and 1.0 gain for collagen, 200ms exposure and 1.0 gain for MHC I, 50ms exposure and 1.0 gain for DAPI.

Analysis was performed in FIJI software. First, a ROI was drawn around the sample, with exclusion of oblong/longitudinal fibers, folds or rips, and incomplete fibers (on the edge of the sample). Next, the signal threshold was set to visualize as much collagen as possible without

creating background signal. This allowed for quantification of the collagen I signal as % Area of the ROI.

Outcome Measures: Passive stress at each SL was calculated as $\frac{F}{CSA}$, where "F" indicates the measured force value at the end of stress relaxation (Figure 1) and "CSA" indicates fiber cross sectional area assuming elliptical shape. CSA =$\pi * (\frac{dtop}{2} * \frac{dside}{2})$, where "$d_{top}$" is the average of three top diameter measures, and "d_{side}" is the average of three side diameter measures. Strain was calculated as $\frac{\Delta L}{Lo}$, where "L_0" indicates initial length. Passive Young's Modulus was calculated as the slope of the stress-strain relationship to account for potential differences in bundle size. Given the linearity of the stress-strain curve of the bundles, one value for Passive Young's Modulus was calculated as the slope of the entire stress-strain curve (rather than the "short length" and "long length" values used for single fibers). Collagen I area was quantified as the % of total ROI.

Statistical Analyses: Statistical testing was conducted using SPSS software package (SPSS, IBM Corp., Armonk, NY, USA). To test for significant differences in the passive stress or Young's Modulus of bundle samples, a linear mixed model was generated with biological sex and fatigue as fixed effects and participant as a random effect. Follow-up analyses tested for an effect of fatigue, with participants as a random effect, on passive stress and modulus of bundle samples from males and females, separately. To test for fatigue-based differences in bundle passive stress and modulus before and/or after KI/KCl treatment, means for the 4 fatigue/treatment groups (non-fatigued pre-KI/KCl, non-fatigued post- KI/KCl, fatigued pre-KI/KCl, fatigued post- KI/KCl) were compared in a two-way analysis of variance with least significance difference (LSD) post-hoc testing. The limited number of samples for which collagen I area was quantified did not warrant statistical analysis; however, this information was useful when interpreting the bundle passive mechanics data.

4C. Results

Descriptive Measures: Within the young cohort, bundle data were collected from two resistance trained (RT) individuals (1 female) and two untrained (UT) individuals (1 female). Training status did not have a significant effect on passive Young's Modulus in this sample (RT:

25.76 ± 12.63 kPa/%Lo, UT: 18.55 ± 11.67 kPa/%Lo; p=0.428). As a result, samples from trained and untrained individuals were combined for subsequent analyses. In total, 84 bundles were assessed. In the total dataset, bundle CSA was not different between males and females (0.148 ± 0.109 vs. 0.063 ± 0.019 mm^2, respectively, p=0.365) or fatigue conditions (non-fatigued: 0.083 ± 0.063, fatigued: 0.097 ± 0.085 mm^2, p=0.154). Bundle length was not different between males and females (2.02 ± 0.43 vs. 2.35 ± 0.38 mm, respectively, p=0.230) or non-fatigued and fatigued samples (2.26 ± 0.44 vs. 2.23 ± 0.40 mm, respectively, p=0.430).

Bundles included in this assay exhibited a wide range of CSAs (0.0166 - 0.4008 mm^2). Bundle CSA has the potential to impact the passive stress and modulus measures made in this study (Malakoutian *et al.*, 2021). Therefore, analyses for this aim were conducted on bundles with CSA +/- 2SD from the mean within each participant (Table 6). The samples eliminated based on CSA beyond 2 SD from the mean can be seen in Supplementary Figure 8. For reference, the same analyses were also conducted on the entire sample of bundles (Supplementary Figure 7). Additionally, outliers identified by passive modulus values greater than 2 SD from the mean, within each participant, were excluded. The statistical results were not different between these two approaches.

Table 6. Descriptive statistics of the bundles included in Aim 2.

		N	CSA (mm^2)	Length (mm)
Male	Non-fatigued	9	0.096 ± 0.043	1.9 ± 0.3
	Fatigued	8	0.087 ± 0.040	2.0 ± 0.4
Female	Non-fatigued	32	0.062 ± 0.016	2.4 ± 0.4
	Fatigued	24	0.066 ± 0.022	2.4 ± 0.3

Data are shown as mean ± SD.

Passive Stress: Passive stress was analyzed at each step of the passive stretch protocol (Figure 21A). There was a main effect of biological sex on bundle passive stress at short lengths (p<0.001 at SL = 2.6 - 2.8 µm; p=0.015 at SL = 3.0 µm), but not at longer SLs. Passive stress was significantly different between non-fatigued and fatigued bundles in samples from females, but not males, at SL = 3.8 µm (NF: 12.58 ± 5.18, F: 15.48 ± 5.97 kPa, p = 0.032).

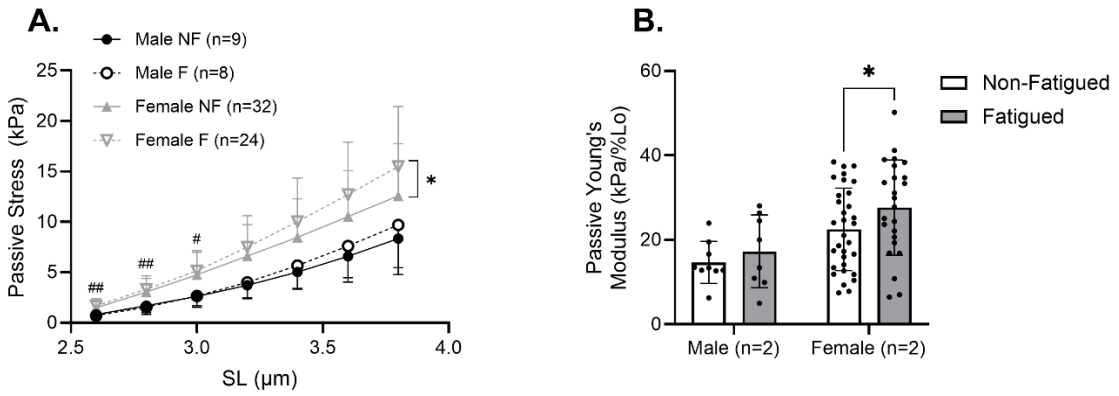

Figure 21. (A) In this subset, passive stress was significantly lower in samples from males versus females at SL=2.6 – 3.0 µm, but not at any other SL. Passive stress was significantly different between non-fatigued and fatigued samples in females at SL=3.8 µm. **(B)** Passive modulus was significantly higher in fatigued versus non-fatigued bundles of females but not males. Data are shown as mean ± SD. Symbols indicate significant effect of #biological sex or *fatigue, single ($p<0.05$) and double ($p<0.001$).

Passive Modulus: Passive Young's Modulus was quantified as the slope of the stress-strain curve for each bundle studied. When the younger cohort was studied as a whole, there was no significant difference between modulus values of males and females (15.88 ± 6.83 vs. 24.72 ± 10.64 kPa/%Lo, respectively, $p = 0.125$) or of non-fatigued and fatigued samples (20.77 ± 9.44 vs. 25.07 ± 11.49 kPa/%Lo, respectively, $p = 0.111$). However, given the imbalanced sample sizes in males versus females (17 vs. 56 bundles, respectively), a subsequent analysis tested the effect of fatigue condition on bundle passive modulus in males and females separately. This analysis revealed a modest but significant increase in passive modulus of the fatigued versus non-fatigued bundles (27.67 ± 11.28 vs. 22.51 ± 9.73 kPa/%Lo, $p=0.033$) in the female cohort but not the male cohort (17.28 ± 8.62 vs. 14.63 ± 4.98 kPa/%Lo, $p=0.442$, Figure 21B).

Collagen content: Collagen area was quantified for one young female and one young male for which bundle mechanics data were collected. The sample from the young female contained more collagen than that of the male (10.35% area versus 6.45% area, respectively).

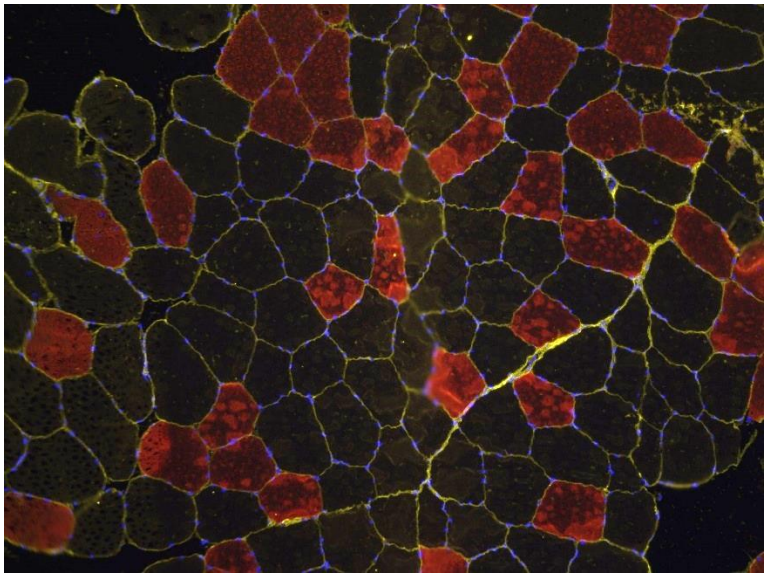

Figure 22. Representative IHC image of skeletal muscle sample from one younger male. Samples were stained with antibodies for MHC I (red), nuclei (blue), and collagen I (yellow). Image brightened in Word, for clarity.

KI/KCl Experiments: Altogether, KI/KCl experiments were performed in fatigued and non-fatigued bundles collected from one young female (11 NF, 6F), one young male (9NF, 6F), and one older male (5NF,7F). Given the effects of bundle CSA on passive mechanics measures (Malakoutian *et al.*, 2021), samples with bundle CSA values greater than 2 SD from the mean, within each participant, were excluded from analysis. Additionally, outliers identified by passive modulus values greater than 2 SD from the mean, within each participant, were excluded. Samples considered outliers are illustrated in Supplementary Figure 9.

Passive stress (Figure 23A) was significantly lower in bundles from pre-treatment, non-fatigued versus fatigued samples longer lengths ($p=0.027$ at SL 3.2 µm; $p=0.006$ at SL 3.4 µm; $p= 0.005$ at SL 3.6 µm; $p=0.014$ at SL 3.8 µm). KI/KCl treatment significantly reduced passive stress in bundles from both fatigued and non-fatigued samples, at all SLs ($p<0.01$ for all). Finally, the potential for inter-participant variability to impact analyses was considered by including "participant" in a univariate ANOVA alongside condition (non-fatigued/fatigued, treated/untreated). Passive stress was significantly impacted by the main effect of participant at most lengths (Supplementary Figure 10). As a result, data from each participant were considered, separately, in later analyses (Figure 24).

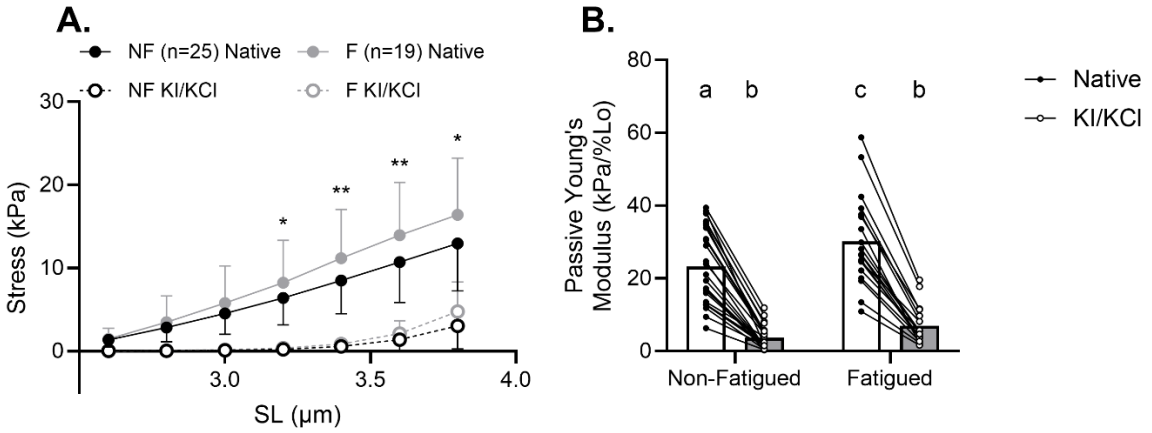

Figure 23. (A) Stress-SL data demonstrate the dramatic reduction in passive stress of non-fatigued (NF) and fatigued (F) samples following KI/KCl treatment. Symbols represents *significant difference between native NF and F samples (single, $p<0.05$; double, $p<0.01$). **(B)** The difference in passive modulus between NF and F samples in the native condition was eliminated after treatment with KI/KCl. Different letters indicate a significant difference ($p<0.05$). All data are shown as mean ± SD.

When quantified as passive Young's Modulus (Figure 23B), values were significantly higher in untreated ("native") fatigued versus non-fatigued bundles (30.14 ± 12.36 vs. 23.26 ± 10.44 kPa/%Lo, respectively, $p=0.025$) but not between treated ("KI/KCl") fatigued and non-fatigued bundles ($p=0.325$). Passive modulus was significantly reduced following KI/KCl treatment in both non-fatigued (23.26 ± 10.44 vs. 3.73 ± 3.07 kPa/%Lo, $p<0.01$) and fatigued (30.14 ± 12.36 vs. 6.96 ± 5.11 kPa/%Lo, $p<0.01$) bundles. The significant main effect of "participant" on passive modulus (older male: 22.27 ± 16.22 kPa/%Lo; young male: 11.45 ± 10.36 kPa/%Lo; young female: 14.75 ± 13.15 kPa/%Lo, $p<0.001$) warranted consideration of passive modulus data in each participant, separately (Figure 24). Doing so revealed that all samples responded to the KI/KCl treatment similarly, but that the fatigue-based difference evident in the native bundles of the combined cohort was driven by the samples from the young female (Figure 24A), whereas there was no fatigue-based difference in the native bundles from the young male (Figure 24B) or older male (Figure 24C).

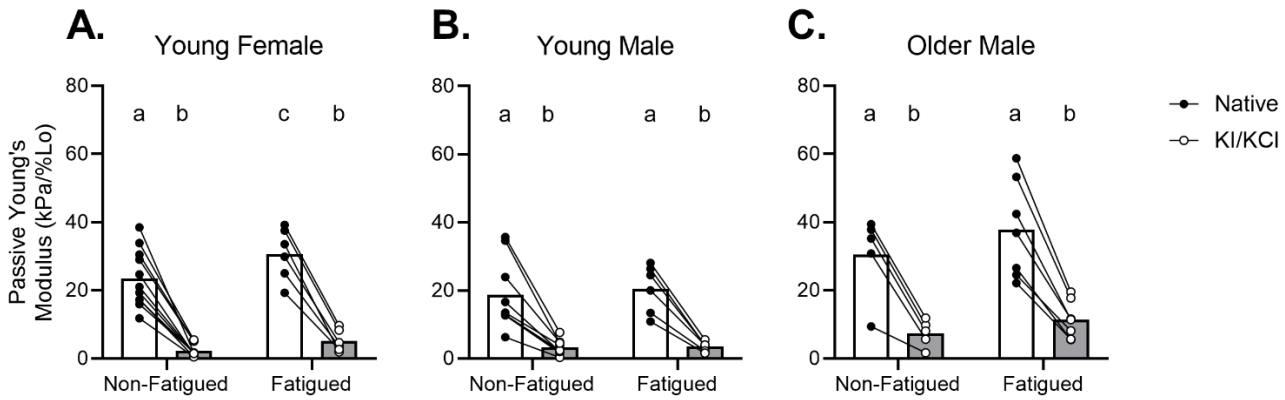

Figure 24. When viewing the passive modulus data for each individual separately, it becomes evident that the KI/KCl treatment affected all samples in a similar way. Separating the participants in this way suggests that the difference between fatigued and non-fatigued native samples in the combined group (Figure 21) may be driven by the samples from the young female **(A)**, rather than the young male **(B)** or older male **(C)**.

4D. Discussion

In this sample of skeletal muscle fiber bundles, passive stress and modulus trended higher in females versus males. In the females, passive modulus, but not stress, was found to be significantly higher in bundles from fatigued versus non-fatigued skeletal muscle (Figure 21). Although previous work has studied the effect of biological sex on skeletal muscle mechanical properties at the cellular (Privett *et al.*, 2024*a*) and musculotendinous (Kubo *et al.*, 2003; Mongold *et al.*, 2022) scales, there has not been a previous study of sex-based differences of muscle mechanical properties at the level of the fiber bundle. In fact, much of the work studying mechanical properties of fibers bundles was performed in the animal model (Meyer & Lieber, 2011; Noonan *et al.*, 2020*a*; Ward *et al.*, 2020) and the potential influence of biological sex was either not considered or not mentioned. Therefore, much of the effort that went into Aim 2 was aimed at improving our approach to collecting passive mechanics measures at the fiber bundle level and identifying potential influences on bundle-level measures. In the end, the high variability in this dataset prompts the discussion of the considerations to be made when conducting these bundle passive mechanics measures.

Throughout these studies, it became clear that the size of fiber bundles, determined by the individual preparing the sample, impacts the passive stress/modulus measures of the sample.

Specifically, larger bundles tend to have lower passive modulus, likely due to the inclusion of relatively less ECM (Malakoutian *et al.*, 2021). ECM is stiffer compared to single fibers, which explains the non-linear increase of passive mechanical properties from single fiber to fascicle and whole-muscle scales of organization (Ward *et al.*, 2020). However, at the level of the fiber bundle, samples are prepared by mechanical removal of fibers and their surrounding ECM from the outer boundaries of the desired sample. As a result, it is possible that a greater proportion of ECM is being mechanically removed during the preparation of a larger versus smaller bundle. In the present sample, bundles from male participants tended to be larger than those from females (Table 6), which may have contributed to the trend towards lower passive stress and modulus measures in bundles from males versus females (Figure 21). What's more, permeabilized fibers within these prepared bundles are known to swell in dissecting and relaxing solution (Godt & Maughan, 1977), which may cause error during bundle measurement. This error was likely perpetuated in subsequent calculations of passive stress and Young's Modulus, causing lower-than-actual values to be presented for stress and modulus.

Variability in fiber size in this subset of females and males (0.0054 ± 0.0019 vs. 0.0065 ± 0.0032 mm^2, respectively, $p=0.575$) may have further impacted bundle passive mechanics. Previous work (Noonan *et al.*, 2020*c*) suggested that smaller fibers tend to be stiffer compared to larger fibers due to the greater proportion of the stiffer basement membrane compared to the relatively less stiff internal area of the fiber. Coupled with the notion that smaller fibers within a bundle increase the relative proportion of CSA that is occupied by ECM (Malakoutian *et al.*, 2021), it is possible that differences in fiber size and bundle size may have contributed to unequal

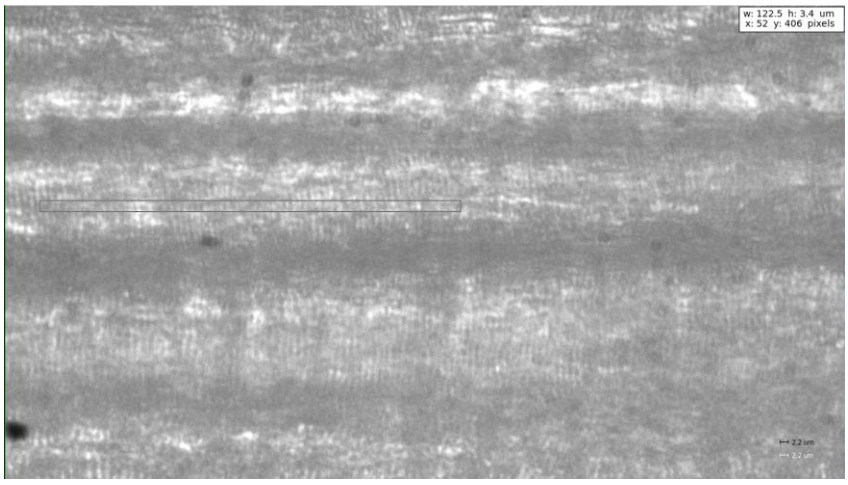

Figure 25. An image of the high magnification view (40x) of a mounted bundle. Note the ROI used (rectangle left of center of the bundle image) to measure SL, and the scale bars (indicating 2.2 µm) in the bottom right of the image.

inclusion of ECM across samples and subsequent variability in bundle passive stress and modulus measures. However, an estimate of the number of fibers included per bundle (average bundle size ÷ average fiber size, calculated separately for males and females) suggests some consistency across biological sexes: an estimated 13.6 fibers/bundle in males and 11.7 fibers/bundle in females. I was unable to quantify the relative CSA occupied by collagen I, a primary component of ECM, in the same bundles that were included in the present mechanical assays. However, quantification of collagen I in samples different from those used in passive mechanics assays (Figure 22 and associated results) suggest modestly greater amounts of collagen I in skeletal muscle samples from females compared to males. If this small sample is representative of the samples tested in the mechanical analyses, it is possible that the inclusion of more collagen I in the ECM of bundles from young females contributed to the trends towards higher passive stress and modulus observed compared to males.

It is also important to consider that, although SL was tracked throughout the passive stretch protocol and the starting point for all bundle stretches was at SL=2.4 μm, it is possible that some inconsistency in stress-sarcomere relationships may have contributed to the variability in the present dataset. For example, although care was taken to set the starting SL in a way that best represents the SL of all fibers in view, the field of view at 40x is limited with respect to the entire bundle (Figure 25). As a result, it is possible that sarcomeres in another part of the bundle may be at a different length. This SL heterogeneity has been reported elsewhere (Hegarty & Hooper, 1971; Willems & Huijing, 1994) and may have been exacerbated as the passive stretch protocol proceeded, creating variability in where along the stress-SL relationship these measures were taken. Although the relative change in sample length was consistent in each step (7% L_o), for each sample, variability in SL would have affected the relative contribution of intracellular proteins and ECM to passive stress at each length.

Despite the high degree of variability in bundle-level passive modulus data, a statistically significant difference was observed between the fatigued and non-fatigued bundles in the female subset (Figure 21B). In these two females, fiber-level data also demonstrated increased passive modulus in fatigued versus non-fatigued samples from these two individuals (Supplementary Figure 15). These results suggest that the impact of fatiguing exercise on cellular passive modulus can translate up to samples of muscle including ECM, partially supporting the initial

hypothesis. Furthermore, when intracellular contributions to bundle passive modulus were eliminated via KI/KCl treatment, designed to depolymerize the sarcomere thick and thin filaments to abolish titin-based stiffness (Granzier & Irving, 1995; Ottenheijm *et al.*, 2012), any fatigue-based difference in bundle passive modulus disappeared (Figure 23, Figure 24). These results suggest that fatigue-induced differences in bundle passive modulus are at least partially due to altered titin-based mechanics, in support of hypothesis iii for this aim.

Although the present dataset for the female participants was relatively well populated, that of the males was comparatively sparce, limiting interpretations that could be drawn. This was partially due to the necessarily limited sample collected during human muscle biopsy studies. In response to these limitations, future efforts in the MCBL will be aimed at adding participants and samples to this dataset, with intention to balance the number of samples between males and females. As suggested earlier in this discussion, it will be crucial that individuals responsible for preparing the samples continue to control the size of the bundles collected for each participant. Furthermore, consideration of the relative size of the fibers should be considered when deciding on a target bundle size.

4E. Conclusion

The overall hypothesis of this dissertation was that the viscoelastic protein titin mediates skeletal muscle passive mechanics. Aim 2 was designed to test the hypothesis that titin-based stiffness also influences bundle-level passive mechanics, motivated by previous work suggesting that titin-based stiffness impacts whole-muscle mechanics (Brynnel *et al.*, 2018). The present results provide some support for the notion that fatiguing exercise can impact passive modulus of bundles, in part due to altered titin-based stiffness. However, this work also highlighted that this scale of sample (bundles of 12-14 fibers with surrounding ECM) is accompanied by a high degree of difficulty and variability that limits the interpretation of results. Additionally, the comparable values in passive modulus between fibers (Figure 16) and bundles (Figure 23) suggest that the inclusion of ECM in samples of this size might not be sufficient to get a clear idea of how altered cellular passive mechanics impact muscle with intact extracellular, collagen-based structures. Perhaps measurements at the bundle level are not necessary to characterize chronic or acute mediators of skeletal muscle mechanics. The work presented in this document has demonstrated that cellular measures provide a robust approach to measuring the effect of

acute (fatigue, Aim 1) and chronic (training, Appendix B: Supplementary Document) mediators of skeletal muscle function. For tissue-level assessment, passive measures in skeletal muscle fascicles have been previously used to characterize the non-linear scaling of mechanical properties from cellular through whole-muscle levels (Ward *et al.*, 2020). Although these types of measures cannot be performed using human biopsy samples, future efforts to test whether fatigue-induced changes to cellular passive measures translate to the tissue-level may consider doing so in a rodent model. This approach would reduce the burden of sample preparation, reduce variability in sample sizes, and test the scalability of the fatigue-induced cellular phenotype in the presence of a physiologically relevant non-linear increase in skeletal muscle passive mechanics.

5. Aim3: To explore whether age modifies the effect of fatigue on skeletal muscle cellular passive modulus and titin PTM.

5A. Introduction

Given the myriad age-related changes to the neuromuscular system, age likely mediates the effect of acute fatigue on skeletal muscle mechanical properties. Specifically, age-related reductions in post-synaptic excitability (Suetta *et al.*, 2009) may reduce beta-adrenergic signaling (Ford *et al.*, 1995; Ryall *et al.*, 2007) and the subsequent accumulation of inorganic phosphate and muscle acidosis (Lanza *et al.*, 2007) or calcium cycling (Suetta *et al.*, 2009) during exercise in older adults. Collectively, these effects may reduce PTM of sarcomere proteins such as titin during exercise, which could differentially modify the effect of fatiguing exercise on cellular passive mechanics of older versus younger skeletal muscle. What's more, age-related changes to titin phosphorylation (Salcan *et al.*, 2020) and/or content may also impact muscle stiffness and the mechanical response to fatigue in older adults. Therefore, Aim 3 sought to explore the relationship between acute fatigue and skeletal muscle compliance in older adults. It was initially proposed that these studies would only be conducted in older versus younger females; therefore, there were no hypotheses related to a mediating effect of biological sex on age-related changes to skeletal muscle mechanical properties. However, the opportunity to include older males facilitated the exploratory study of biological sex effects on the mechanical properties of skeletal muscle cells and bundles in older adults. Age-related attenuation of skeletal muscle excitation-contraction coupling and beta-adrenergic signaling, coupled with reported increases in muscle fiber stiffness with age (Lim *et al.*, 2019; Noonan *et al.*, 2020*b*), supported the hypothesis that i) non-fatigued fibers would be stiffer and fatigue would induce less compliance in fibers from older versus younger adults. Secondly, bundle passive stiffness was measured in fatigue and non-fatigued samples from older and younger participants to assess whether age-related observations in single fibers translate to tissue level. We hypothesized that ii) passive stress and modulus would be higher and fatigue would induce less compliance in bundles from older versus younger adults. These studies are clinically relevant, as older adults more frequently reach the limits of their physical ability and fatigue has been linked to increased falls risk in older adults (Morrison *et al.*, 2016).

Although reports of preferential loss of titin in disuse (Udaka *et al.*, 2007) and age-related alterations to skeletal muscle phosphoproteome (Gannon *et al.*, 2008) supported the assessment of titin abundance and phosphorylation status in older participants, these measures have not yet been collected.

5B. Methods

Population: Eight older (aged 65-80) and 9 younger (18-35 years) males and females opted to participate in this study. Potential volunteers were excluded if they had orthopedic limitations (severe osteoarthritis, prior joint replacement, etc.) or participated in regular, rigorous exercise (resistance training, competitive athletics). Included participants reported no endocrine disease (hypo/hyperthyroidism, Addison ’s Disease or Cushing’s syndrome, etc.), uncontrolled hypertension (>140/90 mmHg), neuromuscular disorder, significant heart, liver, kidney or respiratory disease, and/or diabetes. Participants were non-tobacco-smokers and had no current alcohol disorder. Finally, participants taking medications known to affect muscle stiffness or beta-adrenergic signaling of neuromuscular activation (including but not limited to beta blockers, calcium channel blockers, and muscle relaxers) or anabolic steroids were not included. Female participants were either post-menopausal (older cohort) or were tested in the pre-follicular phase of the menstrual cycle (n=4), within 5 days of menses onset.

Fatiguing Protocol, Muscle Biopsy Procedure, and Tissue Processing: These details were as described in Chapter 3. Time elapsed before acquisition of a biopsy sample was collected for 7/8 older adults and 6/9 younger adults. Average time elapsed = 12 ± 3 minutes in older adults and 10 ± 5 minutes in younger adults.

Mechanical sample preparation: For fiber experiments, one bundle was placed in dissection solution spiked with 1% Triton X-100 to fully de-membranate the sample (“skinning” or “permeabilizing”) before dissection. Next, the sample was moved to plain dissecting solution and single fibers were extracted from the bundle as shown (Figure 8). Dissected single fibers were skinned a second time before use in experiments. Separately, samples used in bundle experiments were not subjected to any form of permeabilizing (e.g. not treated with 1% Triton X-100) beyond the exposure to 50% glycerol in storage solution. For bundle experiments, groups

of 7-12 fibers with intact ECM were dissected from the sample. All prepared fibers and bundles were kept in dissecting solution on ice until experimentation.

Single fiber and bundle morphology and contractile measures: Prepared fibers and bundles were mounted in relaxing solution between a force transducer and a length motor (Aurora Scientific, Inc., Aurora, ON, Canada; Figure 9). Single fibers were mounted using the Moss clamp technique (Moss, 1979). Bundles were measured by direct suturing of the bundle to the rods attached to the force transducer and length motor. Methods to measure fiber or bundle dimensions were detailed previously. Diameter measures were used in calculation of stress (force per unit area, kPa), and length measures were used to calculate strain. Prior to passive measures, active tension was measured in single fibers at SL 2.65 μm by moving the fiber to pre-activating solution followed by activating solution. Bundles were not activated prior to passive measures.

Passive stretch protocol: Passive stretch measures were performed in relaxing solution. Both single fibers and fiber bundles including ECM were assessed using the same passive stretch protocol described in Chapter 3. Following passive measures, all tested fibers and bundles were placed in a high-salt sample buffer (5% beta-mercaptoethanol), briefly centrifuged and heated, and stored at -80°C until later assessment of myosin heavy chain (MHC) isoform.

Collagen I immunohistochemistry (IHC): IHC was performed, using methods identical to those described for Aim 2, to quantify the amount of collagen I in skeletal muscle samples from the individuals for which bundle passive mechanics measurements were collected. Samples for younger and older adults were stained concurrently.

Outcome Measures: At the whole-muscle level, relative peak torque and power were calculated by dividing absolute values for torque (N) and power (W) by the participant body weight (kg). Passive stress at each SL was calculated as $\frac{F}{CSA}$, where "F" indicates the measured force value at the end of stress relaxation (Figure 1) and "CSA" indicates fiber or bundle cross sectional area assuming elliptical shape. CSA $=\pi * (\frac{dtop}{2} * \frac{dside}{2})$, where "$d_{top}$" is the average of three top diameter measures, and "d_{side}" is the average of three side diameter measures. Strain was calculated as $\frac{\Delta L}{Lo}$, where "L_0" indicates initial length. Passive stiffness was quantified as Young's Modulus to account for potential differences in fiber size across samples. Passive

Young's Modulus was calculated as the slope of the stress-strain relationship at shorter fiber lengths (strain = 1.0-1.24 %Lo) and at longer fiber lengths (strain = 1.32-1.56 %Lo). Separate slopes were calculated for shorter and longer fiber lengths to consider the length dependence of cellular passive modulus measures (Noonan *et al.*, 2020*b*). Bundle passive Young's Modulus was calculated as the slope of the stress-strain relationship to account for potential differences in bundle size. Within the range of lengths assessed, the stress-strain curves of bundles were more linear compared to those observed in single fibers; therefore, the primary reason for considering short and long lengths independently was obviated. As a result, a single value for Passive Young's Modulus was calculated as the slope of the entire stress-strain curve. Collagen I area was quantified as the % of total ROI.

Statistical Analysis: Statistical testing was conducted using SPSS software package (SPSS, IBM Corp., Armonk, NY, USA), unless otherwise specified. Anthropometric measures and activity data were compared between older and younger males and females using a two-way ANOVA. To evaluate differences in single fiber passive stress and passive modulus (short and long lengths), separate linear mixed models were run with fatigue, age, biological sex, and interaction terms as fixed effects and participant ID as a random effect to account for fiber variation within individuals, as described previously (Callahan et al., 2015a). Subsequent analyses to investigate interactions between age and fatigue or biological sex and fatigue used separate linear mixed models in older and younger males and females, each including fatigue as a fixed effect and participant ID as a random effect. To determine whether maximally activated tension, single fiber CSA, or fiber length differed by age, biological sex or fatigue, a linear mixed effects model was run with age, sex, fatigue, and interaction terms as main effects and participant ID as a random effect. To test for significant differences in the passive Young's Modulus of bundle samples, a linear mixed model was generated with age, biological sex, and fatigue as fixed effects and participant as a random effect. Follow-up analyses tested for an effect of age, with participant as a random effect, on passive modulus of bundle samples from males and females, separately.

5C. Results

Participant anthropometrics and activity: 9 young (5 females) and 8 older (4 females) adults were included in the analyses for this study. Older participants were aged 74 ± 3 years and

younger participants were aged 21 ± 3 years. The younger cohort was comprised of the untrained young adults analyzed in Aim 1. In the present sample of 17 participants, BMI was not significantly different between males and females (p=0.717) or between older and younger adults (p=0.533, Table 7). Height was significantly higher in males versus females (186.9 ± 19.8 vs. 162.9 ± 6.9, respectively, p=0.007), but was not different between older and younger participants (p=0.734). Weight was significantly higher in males versus females (80.8 ±11.5 vs. 60.5 ± 9.6, respectively, p=0.001), but was not different between older and younger adults (p=0.546). Although activity data were collected for all younger participants, activity data were collected for 2/4 older males and 3/4 older females due to equipment failure. The average number of steps completed per day was significantly higher in the older (12674 ± 5032 steps/day) versus younger (7201 ± 1794 steps/day, p=0.011). Time spent in moderate activity (75-125 steps/minute) was significantly higher in older (101.5 ± 40.0) versus younger (54.0 ± 16.0 min/day, p=0.010) adults. There were no significant differences in minutes spent in light (< 75 steps/minute, p=0.272) or vigorous (>125 steps/minute, p=0.086) activity between older and younger adults. There was no main effect of biological sex on step count (p=0.360), time spent in light activity (p=0.385), time spent in moderate activity (p=0.610), or time spent in vigorous activity (p=0.597).

Table 7. Anthropometric and activity data of older and younger participants.

Age		N	BMI (kg/m^2)	Height (cm)[#]	Weight (kg) [#]	Step Count (steps/day) [A]	Light Activity (min./day)	Moderate Activity (min./day) [A]	Vigorous Activity (min./day)
Young	**Male**	4	24.4 ± 1.2	185.3 ± 13.0	84.0 ± 10.1	7108 ± 1525	37.6 ± 6.7	50.8 ± 15	1.1 ± 1.2
	Female	5	20.9 ± 0.6	162.1 ± 6.1	55.0 ± 3.2	7274 ± 2162	26.6 ± 9.1	56.5 ± 18.2	0.5 ± 0.6
Older	**Male**	4	23.0 ± 8.0	188.6 ± 27.2	77.5 ± 13.3	14936 ± 8625	36.3 ± 3.9	114.9 ± 70.7	5.0 ± 5.7
	Female	4	25.0 ± 3.3	164.0 ± 8.6	67.4 ± 10.9	11165 ± 2214	38.8 ± 10.0	92.6 ± 20.1	3.6 ± 5.9

Symbols indicate significant difference between biological sex[#] or age [A] groups ($p<0.05$). Data are shown as mean ± SD.

Fatiguing exercise and whole-muscle contractile performance: Average time to fatigue was not significantly different between older and younger adults (p=0.306) or males and females (p=0.244, Table 8). Similarly, fatigue ratio was not significantly different across age (p=0.857)

or biological sex groups (p=0.346). Relative peak power was significantly higher in males versus females (5.37 ± 1.47 vs. 3.63 ± 1.92 W/kg, respectively, p=0.029) and higher in younger versus older adults (5.27 ±2.22 vs. 3.52 ± 0.84 W/kg, respectively, p=0.026), yet the interaction effect of age by biological sex on absolute peak power was not significant (p=0.730). Relative peak torque was significantly higher in males versus females (2.79 ± 0.64 vs. 2.25 ± 0.43 N/kg, respectively, p=0.001) and younger versus older adults (2.90 ± 0.48 vs. 2.06 ± 0.33 N/kg, respectively, p<0.001). The interaction effect of age by biological sex on relative peak torque was not significant (p=0.109). Statistical differences between age and biological sex groups were not different when absolute values for peak power and peak torque were considered (Supplementary Table 4).

Table 8. Fatigue data and whole-muscle performance of older versus younger adults.

Age		Time to Fatigue (sec)	Fatigue Ratio	Relative Peak Power (W/kg) $^{\#A}$	Relative Peak Torque (N/kg) $^{\#A}$
Young	**Female**	68±9	0.34±0.10	5.43±0.32	2.54±0.12
	Male	75±29	0.41±0.16	6.43±1.42	3.34±0.34
Older	**Female**	71±14	0.36±0.05	2.74±0.13	1.88±0.39
	Male	125±101	0.40±0.11	4.03±0.70	2.24±0.15

Symbols indicate significant difference between biological sex$^{\#}$ or age ^{A} groups (p<0.05). Data are shown as mean ± SD.

Single fiber characteristics: Fiber CSA was significantly different between males (0.0067 ± 0.0020 mm^2) and females (0.0044 ± 0.0015 mm^2, p<0.01), but was not different between older (0.0054 ± 0.0022 mm^2) and younger (0.0055 ± 0.0019 mm^2, p=0.857) adults (Table 9). Given the diversity in fiber-type distributions among the participant groups, it was decided to limit statistical analyses to MHC IIA and IIA/X fibers (n=257). Importantly, passive modulus was not different between MHC IIA and MHC IIA/X fibers at short or long lengths, in any participant group (Supplementary Table 1). Active tension in this sample was not significantly different between non-fatigued and fatigued samples (p=0.080), males and females (p=0.410) or older and younger adults (p=0.569, Supplementary Figure 11).

Table 9: Descriptive statistics of the single fibers included in the study of effects of aging and fatigue on cellular passive mechanics.

		n	CSA (mm^2) #	Length (mm)	Fiber type distribution (n)			
					I	IIA	IIX	IIA/X
Young	**Female**	107	0.0046 ± 0.0014	1.5 ± 0.4	23	50	2	24
	Male	92	0.0066 ± 0.0019	1.7 ± 0.4	3	44	21	22
Older	**Female**	154	0.0043 ± 0.0016	1.5 ± 0.4	55	51	7	26
	Male	92	0.0068 ± 0.0021	1.7 ± 0.5	60	29	2	11

Data are shown as mean ± SD. Percents are not reported for MHC I/IIA or I/IIA/IIX because they collectively made up only 6.2% of the overall dataset. Symbols indicate main effects of #biological sex ($p<0.05$).

Passive Stress: Passive stress was analyzed at each SL (Supplementary Table 5) studied throughout the passive stretch protocol. When all MHC IIA and MHC IIA/X fibers were considered, the interaction of fatigue and biological sex was significant at all SLs ($p<0.01$ at SL 2.6-3.8 µm, Figure 26A). Additionally, the interaction of fatigue and age was significant at one SL ($p=0.042$ at SL 3.0 µm). When all non-fatigued fibers were considered, there was a main effect of aging on passive stress at one SL ($p=0.045$ at SL 3.0 µm, Figure 26B). The main effect of biological sex on passive stress was not significant in non-fatigued fibers at any SL. The interaction effect of biological sex and fatigue in the combined dataset prompted further study of the effect of fatigue on passive stress in fibers from males and females, separately. As a result, it became clear that fatigue significantly reduces passive stress in fibers from males at all SLs ($p<0.01$ at SL 2.6-3.8 µm, Figure 27A). In contrast, passive stress was not significantly different between non-fatigued and fatigued fibers from females at any SL (Figure 27B). For those interested, the effect of fatiguing exercise on passive stress in each participant group (older and younger, male and female) can be seen in Supplementary Figure 12.

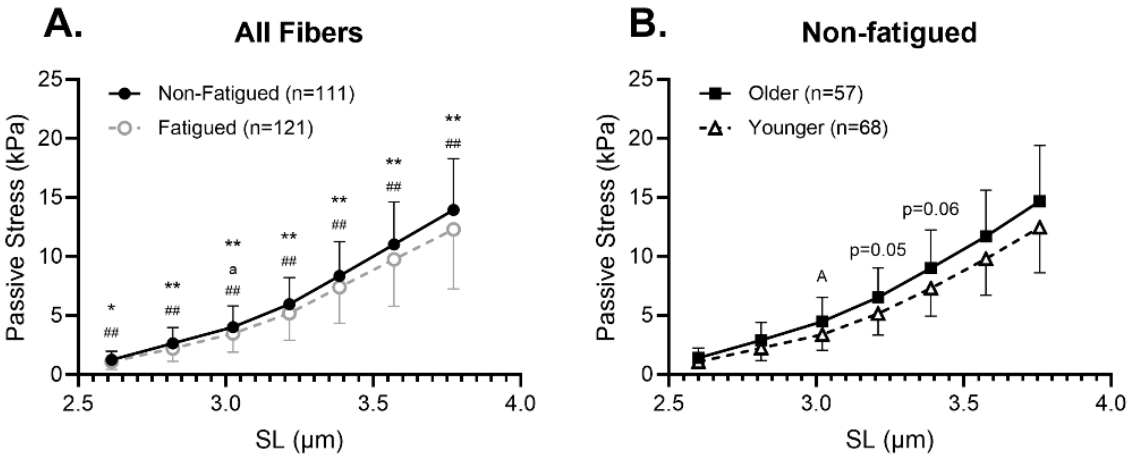

Figure 26. (A) When all MHC IIA and MHC IIA/X fibers were considered, passive stress was significantly reduced by fatigue at all SLs. What's more, interactions between age*fatigue and biological sex*fatigue impacted passive stress in a SL-dependent manner. **(B)** When only non-fatigued MHC IIA and MHC IIA/X fibers were considered, passive stress was significantly higher in older versus younger samples at SL=3.0 μm. Data are shown as mean ± SD. Symbols indicate a significant effect of * fatigue, [a] fatigue*age interaction, [#] fatigue*biological sex interaction, [A] age. Single ($p<0.05$), double ($p<0.01$).

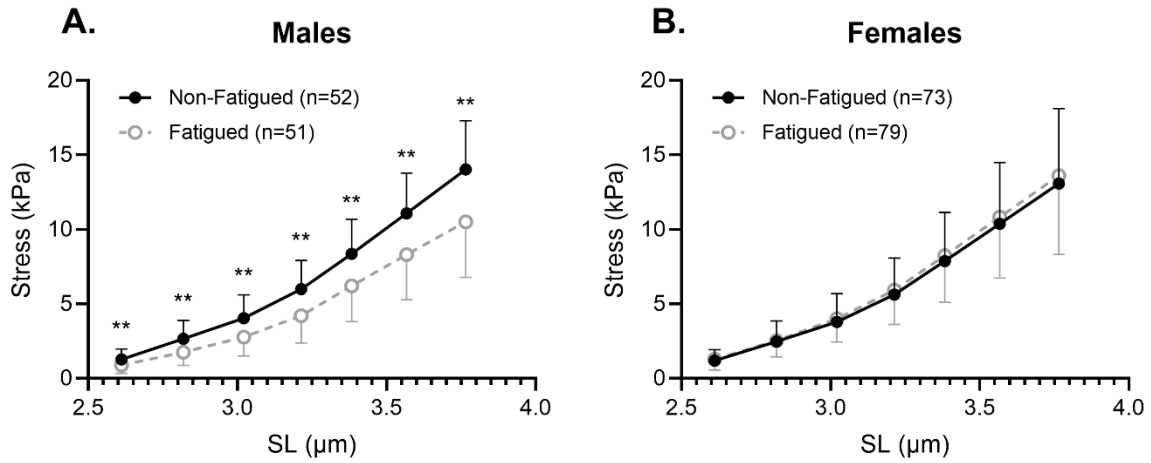

Figure 27. Cellular passive stress was significantly lower in fatigued versus non-fatigued fibers of males **(A)** but not in fibers of females **(B)**. Data are shown as mean ± SD. Symbols indicate a significant main effect of fatigue *($p<0.05$) or **($p<0.01$).

Passive Modulus: Passive modulus was not significantly different between males and females at short ($p=0.603$) or long ($p=0.646$) fiber lengths, regardless of fatigue condition. There was also no main effect of age on passive modulus at short ($p=0.091$) or long ($p=0.232$) lengths

when all MHC IIA and MHC IIA/X (non-fatigued and fatigued) fibers were considered. There was a significant main effect of fatigue on passive modulus was at short lengths (NF: 16.2 ± 7.5 kPa/%Lo, F: 14.3 ± 6.6 kPa/%Lo, p<0.001) and long lengths (NF: 32.0 ± 10.5 kPa/%Lo, F: 29.4 ± 12.5 kPa/%Lo, p=0.012, Figure 28A). The interaction of fatigue and biological sex was significant at both short (p<0.001) and long (p=0.003) lengths, and the interaction of age and fatigue was significant at short lengths (p=0.023). When only non-fatigued fibers were considered (Figure 28B), passive modulus was significantly higher in fibers from older adults versus younger adults at short lengths (18.7 ± 8.6 kPa/%Lo vs. 14.1 ± 5.7 kPa/%Lo, p=0.042) but not long lengths (p=0.163). Subsequent analyses revealed that fatigue-induced reductions in passive modulus were driven by males at short (NF: 16.8 ± 6.6 kPa/%Lo, F:11.1 ± 5.4 kPa/%Lo, p<0.001) and long (NF: 33.5±6.8 kPa/%Lo, F: 25.7 ± 9.5 kPa/%Lo, p<0.001) lengths, whereas modulus in single fibers from females was not significantly different with fatigue at short lengths (NF: 15.8 ± 8.1 kPa/%Lo, F: 16.4 ± 6.5 kPa/%Lo, p=0.754) or long lengths (NF: 31.0 ± 12.4 kPa/%Lo, F: 32.0 ± 13.7 kPa/%Lo, p=0.764, Figure 29). The effect of fatigue on passive modulus within each age- and biological sex-group can be seen in Supplementary Figure 13.

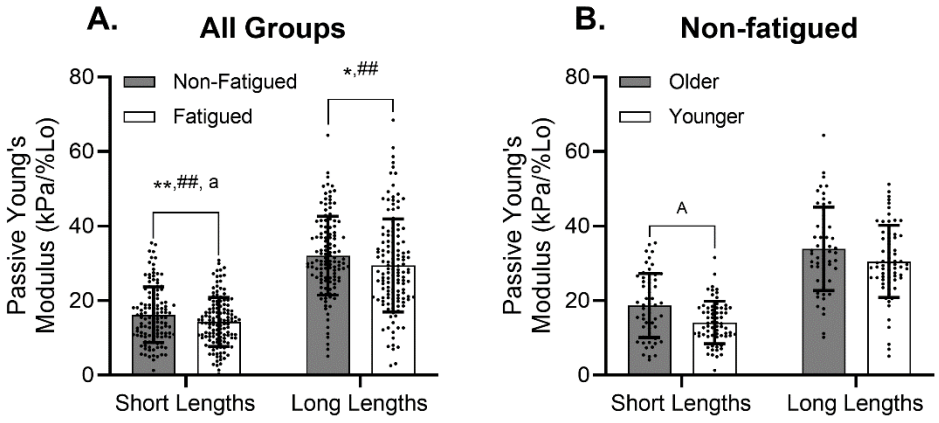

Figure 28. **(A)** When all MHC IIA and IIA/X fibers are considered, cellular passive modulus is significantly reduced by fatigue at short and long lengths. Furthermore, cellular passive modulus is affected by a fatigue by biological sex interaction at short and long lengths and by a fatigue by age interaction at short lengths. **(B)** When only non-fatigued fibers are considered, cellular passive modulus is significantly higher in fibers from older versus younger participants at short, but not long, lengths. Data are shown as mean ± SD. Symbols indicate significant effects of *fatigue, # biological sex by fatigue interaction, [a] aging by fatigue interaction, [A] main effect of age. Single (p<0.05), double (p<0.01).

While there was no main effect of fatiguing exercise on cellular passive modulus in female participants, inter-individual differences in cellular response were noted within the group. This observation prompted the qualitative look at changes to mean cellular passive modulus in fatigued versus non-fatigued samples, for each participant. This figure (Figure 30) suggests that both young and older female participants do exhibit some change in cellular passive modulus as a result of the fatiguing exercise, yet the diversity within the female cohort precludes any statistically significant change in the group mean.

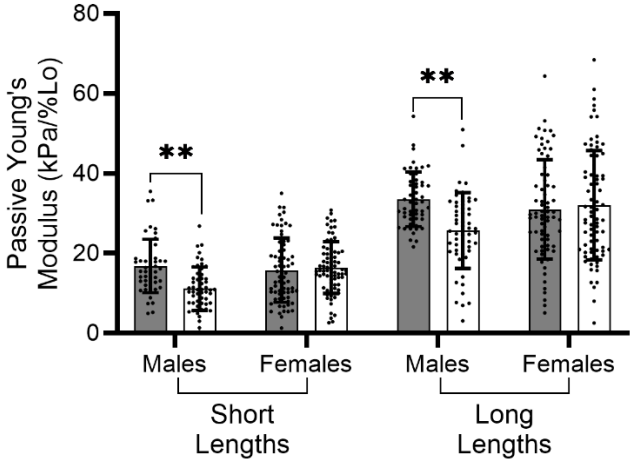

Figure 29. Cellular passive modulus is significantly reduced by fatigue at short and long lengths in fibers from males but not females. Data are shown as mean ± SD. Symbols indicate significant effects of fatigue, *($p<0.05$) or **($p<0.001$).

Bundle sample characteristics. Passive stress and Young's Modulus were measured in bundles from a subset of the participants included in cellular assays: 2 older males, 3 older females, 2 younger males, and 2 younger females. In line with the finding that bundle size can impact measures of passive stiffness (Malakoutian *et al.*, 2021), bundles with CSA measures that fell outside of 2 SD from the mean were excluded from analysis (Supplementary Figure 8). In total, 141 bundles were included in the analyses for Aim 3 (Table 10). Bundle CSA was not different by age ($p=0.793$), biological sex ($p=0.172$), or fatigue ($p=0.264$). Similarly, bundle length was not different by age ($p=0.134$) or fatigue ($p=0.699$), though samples were longer in females versus males (2.46 ± 0.42 versus 2.02 ± 0.38 mm, respectively, $p=0.015$). However, SL was set to 2.4 µm in all bundles prior to initiation of the passive stretch protocol used to measure passive stress and modulus, so it is unlikely that the observed gender-based difference in sample length impacted the present results.

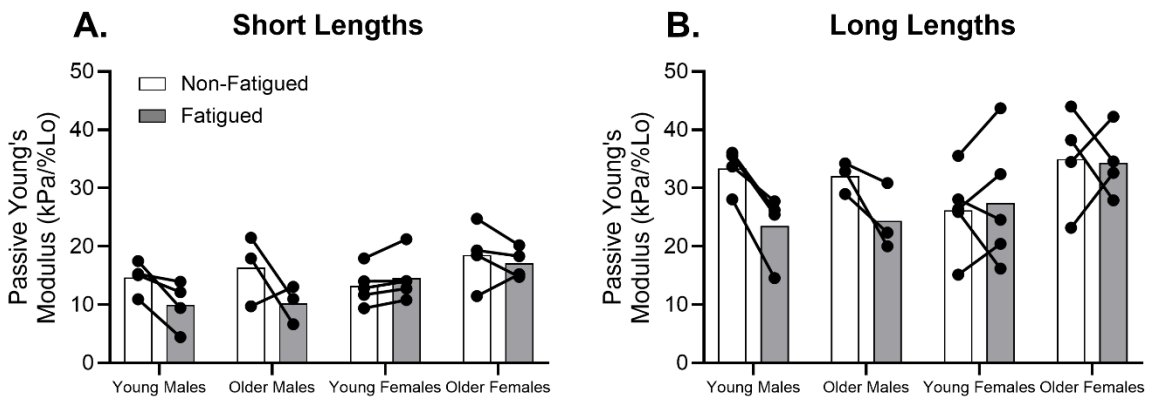

Figure 30. A qualitative look at the variability in change of mean passive modulus on a per-individual basis. At short **(A)** and long **(B)** lengths, it appears that while male participants demonstrate consistent changes to passive modulus resulting from fatigue, females exhibit diversity in the response of passive modulus to fatiguing exercise.

Bundle Passive Mechanics. When all bundles were considered, there were no main effects of fatigue or age on passive stress at any SL. Passive stress was significantly higher in fibers from females versus males at SL 2.8 µm ($p=0.023$). What's more, the interaction between biological sex and age was significant at some SLs ($p=0.008$ at SL 2.6 µm, $p<0.001$ at SL 2.8 µm, $p=0.015$ at SL 3.0 µm, $p=0.039$ at SL 3.2 µm). For this reason, the main effect of age was tested within each biological sex. Although a lack of significant main effect or interaction effect of fatigue on bundle passive stress precluded its inclusion in subsequent statistical analyses, stress data for non-fatigued and fatigued bundles are plotted separately in Figure 31 for reference. In males, passive stress was higher in bundles from older versus younger participants at short lengths ($p=0.023$ at SL 2.6 µm, $p=0.031$ at SL 2.8 µm, Figure 31A). In females, passive stress was higher in bundles from younger versus older participants at short lengths ($p<0.001$ at SL 2.8 µm, $p=0.034$ at SL 3.0 µm, $p=0.034$ at SL 3.2 µm, Figure 31B).

Table 10. Descriptive statistics of the bundles included in Aim 3.

		N	CSA (mm^2)	Length (mm)[#]
Male	Older	17	0.080 ± 0.036	2.1 ± 0.4
	Younger	17	0.092 ± 0.041	1.9 ± 0.3
Female	Older	51	0.079 ± 0.028	2.6 ± 0.4
	Younger	56	0.064 ± 0.019	2.4 ± 0.4

Data are shown as mean ± SD. [#]Indicates a significant effect of biological sex ($p<0.05$).

When all bundles were considered collectively, there were no significant main effects of fatigue (p=0.102), biological sex (p=0.661), or age (p=0.618) on bundle passive modulus. Given the relatively low numbers of participants within each group, the effect of fatigue on bundle passive modulus was explored in each participant group separately (Figure 32). No significant effect of fatigue was found on bundle passive modulus in older males (p=0.399), older females (p=0.752), or younger males (p=0.442). However, bundle passive modulus was significantly higher in the fatigued versus non-fatigued bundles of young females (27.67±11.28 vs. 22.51±9.73 kPa/%Lo, respectively, p=0.033).

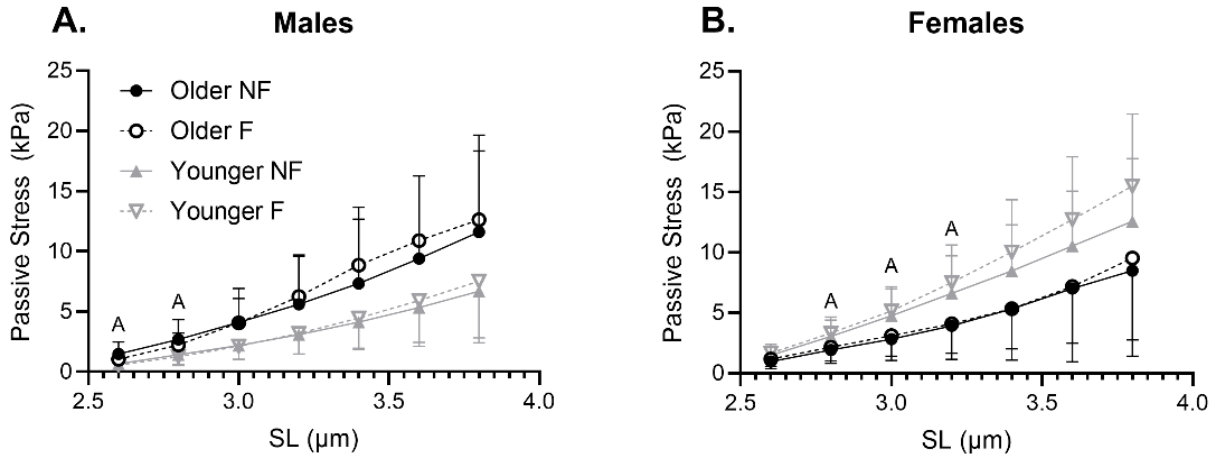

Figure 31. Comparison of bundle passive stress in older versus younger participants. **(A)** In males, bundle passive stress was significantly higher in older versus younger samples at SL 2.6-2.8 μm, but not at any other SL. Fatigue did not significantly affect bundle passive stress at any length, in either older or younger males. **(B)** In females, passive stress was significantly higher in bundles from younger versus older participants at SL 2.8-3.2 μm, but not at any other SL. Fatigue did not significantly alter bundle passive stress at any length, in either age group. Data are shown as mean ± SD. [A] Indicates a significant main effect of aging ($p<0.05$).

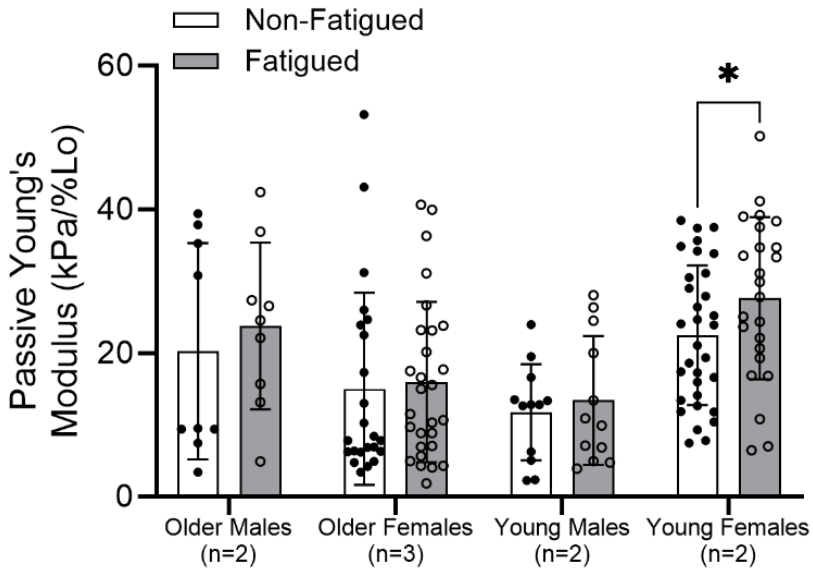

Figure 32. Comparison of bundle passive modulus across age and biological sex groups. Bundle passive modulus was significantly reduced by fatiguing exercise in young females, but not in any other participant group. Data are shown as mean ± SD. * Indicates a significant effect of fatigue ($p<0.05$).

Collagen content: Collagen area was quantified for 3 females (1 young) and two males (1 young) for which bundle mechanics data were collected. A sample image is shown in Figure 33. The collagen I content in the sample from the young male (6.45%) trended lower than that of samples from the young female (10.35%), older male (11.09%) or older female (11.40%).

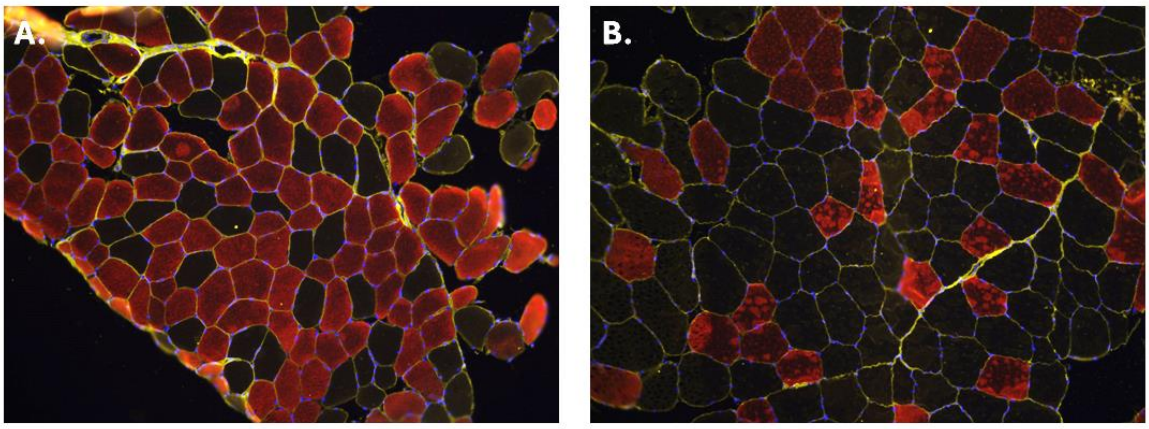

Figure 33. Representative IHC image staining for MHC I (red), nuclei (blue) and collagen I (yellow) in skeletal muscle from one older male **(A)** and one younger male **(B).** Image was brightened in Word, for clarity.

5D. Discussion

Study Sample. In this sample of older and younger adults, anthropometric measures were not different across age groups but were different between males and females. Interestingly, the older cohort appeared to be more active, completing more steps per day and more minutes of moderate physical activity per day, on average (Table 7). As a result, it is possible that the unintentional, age-related difference in habitual activity in this study sample may have impacted our ability to test for an effect of aging on cellular and bundle-level passive mechanical measures. This idea is supported by our work in trained versus untrained younger adults (Appendix B: Supplementary Document) demonstrating that chronic training not only alters cellular passive stress and modulus, but also mediates the effect of fatiguing exercise on these cellular passive measures. Although there is a distinction between intentional resistance training, as was the case in the comparison of trained versus untrained young adults, and differences in habitual step count and minutes of moderate activity, there is a clear influence of chronic activity level on these cellular measures that must be considered. Nonetheless, the whole-muscle performance data from the present sample of older and younger adults suggest that inherent contractile function is lower in older versus younger adults (Table 8), confirming an aged phenotype of the skeletal muscle sampled for these studies consistent with previous reports (Suetta *et al.*, 2019).

At the cellular level, there was no difference in fiber CSA (Table 9) between older and younger participants, which agrees with some (Lim *et al.*, 2019; Noonan *et al.*, 2020*b*) but not all (Lexell & Taylor, 1991) previous reports. It is possible that the lack of a fiber size difference in this sample was in part due to the high activity level of the included participants. Separately, there was a noticeable difference in fiber type distribution between older and younger adults. While older adults collectively contributed a greater percentage of MHC I fibers (~47%), consistent with previous reports whole-muscle fiber-type distribution (Lexell *et al.*, 1988), samples from younger adults only contributed ~13% MHC I fibers overall to these passive mechanics analyses. Interestingly, quantification of MHC isoform using SDS-PAGE on muscle homogenate samples from each participant revealed that MHC I comprised a larger percentage of the harvested skeletal muscle sample in younger adults than is represented in the fibers presented in Table 9. Specifically, muscle homogenates assessed via SDS-PAGE included ~20% MHC I isoform in young males and ~40% MHC I isoform in young females (Supplementary

Figure 14). This contradiction between the representation of MHC I isoform in the mechanics data (lower %) versus the MHC homogenate samples run out on a gel (higher %) suggests that there was a selection bias present during dissection of single fibers for mechanical analysis. We have explored this possibility before and hypothesized that MHC I fibers tend to recoil within the bundle of fibers once the sample is untied from the glass rod on which it is stored. As a result, we have since developed a method to estimate fiber-type during dissection (Privett *et al.*, 2024*b*), and began using this approach during data collection. Nonetheless, the effects of earlier fiber-type selection bias are present in the current dataset, and unfortunately preclude analysis of MHC isoform on passive stress and modulus. Importantly, when analyses included all fiber-types (data not shown), the effect of fatigue on passive stress and modulus was consistent with the results presented in this document.

Cellular Mechanics. In the collective sample of MHC IIA and MHC IIA/X fibers presented here, passive stress (Figure 26A) and Young's Modulus (Figure 28A) were both found to be reduced by fatiguing exercise in a biological-sex-dependent manner, consistent with the results of Aim 1. Subsequent analyses revealed that, as was observed in Aim 1, the effect of fatigue on passive stress (Figure 27) and modulus (Figure 29) was significant in males but not in females. These results do not support the initial hypothesis for Aim 3, considering that age did not mediate the effect of fatigue on cellular passive mechanics. Although titin phosphorylation was not quantified in our older adults, a limitation of the current dataset, the observed reductions in passive stress and passive modulus are presumed to be due to altered titin-based stiffness resulting from titin phosphorylation. While the present dataset is not positioned to comment on any direct evidence of altered titin-based stiffness, the observation of larger fatigue-induced differences in passive stress at longer SLs (~3.4-3.8 μm), where overlap between thick and thin filaments is minimal, supports the notion that titin is at least partially responsible for the observed reductions in passive stress.

We hypothesized that muscle fibers from older adults would exhibit higher passive stress and modulus compared to fibers from younger adults. In reality, aging was only demonstrated to increase passive stress at SL=3.0 μm (Figure 26B) and increase passive modulus at short lengths (Figure 28B), providing some support for this hypothesis. This was surprising, considering previous work (Noonan *et al.*, 2020*b*) reporting that fibers from older adults generated increased

passive stress at SL=2.1-3.55 μm in a pooled sample of MHC I and MHC II (subtype not specified) fibers. Similarly, another study (Lim *et al.*, 2019) reported increased passive force at SL=3.0-4.2 μm in MHC I and MHC II (subtype not specified) fibers from older versus younger participants. Importantly, the analysis presented in Aim 3 only included MHC IIA and IIA/X fibers, which may contribute to the disparity in results. In the previous two studies (Lim *et al.*, 2019; Noonan *et al.*, 2020*b*), the use of isolated, permeabilized single fibers suggests an intracellular protein contributed to the observed age effect - although the ECM is a common target for age-related changes (Wood *et al.*, 2014), it is not present in permeabilized single fibers. Titin may contribute to age-related changes to cellular mechanics. First, there is evidence that aging is associated with changes to baseline titin phosphorylation (Salcan *et al.*, 2020), which may impact titin-based stiffness (Fukuda *et al.*, 2005; Müller *et al.*, 2014; Hamdani *et al.*, 2017), a predominant determinant of cellular measures of stiffness. Furthermore, titin phosphorylation status can mediate titin degradation in skeletal muscle (Wang *et al.*, 2018, 2023), presenting the possibility that age-related changes to titin phosphorylation may also affect titin quantity in skeletal muscle. Finally, one may speculate that aging is associated with a shift toward a shorter, therefore stiffer (Frontera & Ochala, 2015), titin isoform, though this has not yet been studied.

The evidence of a main effect of age on cellular passive stress and Young's modulus was sparse in the present dataset, partially supporting the initial hypothesis for Aim 3. Physical activity has been demonstrated to ameliorate age-related changes to skeletal muscle function (D'Antona *et al.*, 2007; Aagaard *et al.*, 2010; Johansson *et al.*, 2021). Therefore, the extraordinary physical activity levels of the older participants in this study may have attenuated the expected age-related changes to skeletal muscle and limited our ability to test the effect of aging per se on cellular passive mechanics. Our study of the effect of resistance training, another chronic mediator of skeletal muscle function, on cellular passive mechanics (Appendix B: Supplementary Document) highlights the impact of physical activity on baseline cellular mechanics and the mediating effect of fatiguing exercise. Although it is unknown how physical activity may have influenced our ability to observe age-related differences in cellular stress/modulus and the response to fatiguing exercise, the collection of studies in this document supports the idea that chronic modifiers of muscle stiffness have the potential to impact measures at the cellular level.

We originally hypothesized that aging would mitigate the effect of fatiguing exercise on cellular passive stress and Young's Modulus. This hypothesis was based on the notion that age-related changes to inorganic phosphate accumulation and pH changes (Lanza *et al.*, 2007), calcium cycling (Suetta *et al.*, 2009), and beta-adrenergic signaling (Ryall *et al.*, 2007) during exercise might alter regulation of titin PTM and subsequent titin-based stiffness. The present results do not provide strong support for this idea because the interaction between biological sex and fatigue was found to have a much stronger impact on cellular passive mechanics. As discussed for Aim 1, it is speculated that biological sex exerts a mediating influence on cellular passive mechanics via circulating sex hormones. Specifically, circulating estrogen is speculated to contribute to the observed variability in cellular passive modulus following fatiguing exercise (Figure 30) as discussed in Aim 1. It is also possible that circulating levels of testosterone can impact passive stress and modulus measures via the interaction of testosterone with G-protein coupled receptors or sex hormone binding globulin protein (SHBG) in skeletal muscle and activation of downstream PKA-mediated pathways (Dubois *et al.*, 2012) creating the possibility that titin might be phosphorylated. Finally, it may be that greater amounts of in HSPs in the skeletal muscle of males (Romani & Russ, 2013) enabled a more robust interaction of HSP with titin (Kötter *et al.*, 2014). Given the clear impact of biological sex in younger (Aim 1), older (Aim 3), and resistance trained (Appendix B: Supplementary Document) individuals, measures of circulating sex hormones should be collected at the time of biopsy in future studies.

Bundle Mechanics. We hypothesized that non-fatigued fiber bundles would exhibit higher passive stress and modulus in samples from older versus younger participants, based on reports of increased collagen content and cross-linking in advanced age (Wood *et al.*, 2014; Pavan *et al.*, 2020). In the present results, passive stress was different between older and younger samples in a sex-dependent and length-dependent manner (Figure 31), however, there was no main effect of age on passive modulus values (Figure 32). The divergent effect of age on passive stress in males and females was unexpected. At this scale of sample (12-14 fibers with surrounding ECM), the impact of cellular mechanical properties on bundle level measures is likely larger than observed in vivo (discussed in Aim 2). Furthermore, the comparison of passive modulus data across the fiber and bundle scales, within each participant group (Supplementary Figure 15), suggests that age-, sex-, and fatigue-related the trends in bundles data arise from the passive properties of the

constituent fibers. IHC with staining for collagen I confirms that fibers likely comprise the majority of bundle CSA at this scale. Furthermore, these IHC data suggest that bundles from the young males contain the least collagen I in the ECM, which may have contributed to the low passive modulus observed in this group compared to other participants (Figure 32). However, IHC with collagen I stain would need to be performed on a larger sample size to appropriately support or refute this claim.

We also initially hypothesized that fatiguing exercise would reduce passive stress and modulus at the bundle level in older and younger adults. However, the results do not provide support for this hypothesis. While passive modulus was significantly higher in bundles from the fatigued versus the non-fatigued limb in samples from young females (Figure 32, also discussed in Aim 2), a significant effect of fatigue was not observed on passive modulus in any other participant group. The lack of significant difference in the present data set may be at least in part due to the high variability across samples within each participant group. The possible sources of this variability, and proposed methods to address them, were discussed in Aim 2. Finally, it is possible that the high activity level present in this cohort of older adults mediated any age-related changes in skeletal muscle structural (ECM) or proteomic (titin) changes that might have been expected to manifest at the bundle level. Moving forward, care could be taken to improve the comparative activity levels between age groups to better position this study to detect any age-related changes in bundle-level passive mechanics.

5E. Conclusion.

These results demonstrate an effect of fatiguing exercise on cellular passive stress and Young's Modulus in skeletal muscle samples from older and younger males, but not females. Although the group means were not significant between non-fatigued and fatigued fibers of females, examination of the cellular data on a per-individual basis highlight the fact that females exhibit a more diverse response of cellular mechanics to fatiguing exercise. At the bundle level, no significant effect of fatiguing exercise was observed in passive stress or Young's Modulus. What's more, the evident differences in bundle mechanics appeared to derive from the inherent characteristics of the constituent fibers, rather than from an ECM-based mechanism. As a result, measurement of passive mechanics at this scale of bundle (12-14 fibers/bundle) may not be necessary to characterize chronic (age) and acute (fatigue) mediators of skeletal muscle stiffness.

Rather, careful interpretation of the more reliable cellular data coupled with study of larger bundles (~100 fibers) or corresponding whole muscle performance (Biodex) or structural (ultrasound) data may provide a more complete understanding of the mechanisms of age- and fatigue-related changes to skeletal muscle measures of stiffness.

6. Final Discussion and Conclusions

These studies examined the effect of fatiguing exercise on intracellular mediators of skeletal muscle passive mechanics, and how these intracellular mechanisms contribute to tissue-level measures, in younger and older males and females. The primary finding was that fatiguing exercise reduced cellular measures of passive stress and Young's Modulus in skeletal muscle fibers from young (Aim 1) and older (Aim 3) males. In permeabilized skeletal muscle cells, primary contributors to muscle stiffness include the motor proteins, actin and myosin, and the viscoelastic protein titin. The persistence of altered passive mechanics at long sarcomere lengths, where actin and myosin are not optimally interacting, in the presence of BDM, a myosin inhibitor, supports the notion that actin and myosin interactions are not the primary mechanism of this fatigue-induced alteration. Rather, titin is a likely contributor. Coincidentally, phosphoproteomic analysis revealed that titin phosphorylation was altered by fatiguing exercise, supporting the hypothesis that exercise modifies titin phosphorylation, which has the potential to alter titin-based stiffness. However, in-vitro assays to experimentally dephosphorylate or phosphorylate titin did not replicate the effect of fatiguing exercise on cellular passive stress or modulus. Though, AP treatment did significantly reduce cellular passive stress and modulus at long SL (3.6-3.8 μm), where titin is assumed to be the predominant course of passive stress. This intriguing mechanical result motivates further study to determine whether titin phosphorylation status impacts cellular passive mechanics in human skeletal muscle. Future studies may consider testing an effect of fatiguing exercise on myofibril passive mechanics to isolate the influence of sarcomere proteins. Additionally, in-vitro treatments to test other proposed titin PTMs, such as HSP 27, and further analysis of titin proteomics in more diverse samples of participants may improve our understanding of how exercise impacts titin structure and function.

The results presented provide strong evidence that the effect of fatiguing exercise on cellular passive stress and modulus is highly dependent on biological sex. Whereas younger and older males demonstrated consistent reductions in passive mechanics in fatigued versus non-fatigued fibers, females did not exhibit a consistent response. In fact, the lack of a significant effect of fatigue on cellular passive mechanics in females appears to be the result of variability in response to the fatiguing exercise: some females exhibited higher cellular passive modulus in fatigued versus non-fatigued fibers, other females exhibited lower modulus. This variability may

have been caused by inter-individual differences in circulating estrogen amongst female participants. Therefore, future efforts in this research will include the collection of blood samples at the time of biopsy to quantify intramuscular (biopsy) and circulating (blood sample) sex hormone concentrations.

Current literature suggests a role of estrogen in regulating sarcomere protein function (Lai *et al.*, 2016) and titin isoform distribution (Bupha-Intr *et al.*, 2011), presenting the potential for titin function to be mediated by estrogen concentration. Estrogen may also influence skeletal muscle mitochondrial function (Pellegrino *et al.*, 2022; Yoh *et al.*, 2023), thereby altering the concentration of heat shock proteins (Liu & Steinacker, 2001) and oxidative molecules such as glutathione (Marí *et al.*, 2009), both of which are potential regulators of titin structure and function, in the sarcoplasm. Given the robust effect of fatigue on cellular passive mechanics in male participants, testosterone concentration should also be considered. Testosterone interacts with G-protein coupled receptors and SHBG in skeletal muscle, both of which activate PKA-mediated pathways (Dubois *et al.*, 2012), which may increase the potential for titin phosphorylation. Males have also been shown to have greater intramuscular stores of HSPs (Romani & Russ, 2013), potentially facilitating a stronger interaction of HSPs with titin (Kötter *et al.*, 2014) in males versus females. Collectively, the literature supports the notion that sex hormones have the potential to impact a titin-based mechanism of acute regulation of cellular passive mechanics.

The hypothesis that sex hormones impact cellular passive mechanics via a titin-based mechanism was generated by the observation that fatiguing exercise impacted cellular passive mechanics in males, but not females. Yet, this idea was not supported by the comparison of passive stress and Young's Modulus in this cohort of older versus younger participants. In females, estrogen levels decline in the years before menopause, after which they remain constantly low (Chidi-Ogbolu & Baar, 2019). In males, testosterone levels begin dropping in the early 4th decade of life and continue to decline at a constant rate thereafter (Allan & McLachlan, 2004). Therefore, it would be expected that any effect of sex hormones on titin mechanics would be evident in the comparison of cellular passive mechanics of older versus younger participants, given the anticipated differences in hormone profiles. However, in the present sample there was no effect of aging on the acute regulation of cellular passive mechanics, suggesting that

additional mechanisms must be considered. I have previously proposed HSP 27 and alphaβ-crystallin as alternative mechanisms of altered cellular passive mechanics following fatiguing exercise in males versus females. Interestingly, the quantity of these small HSPs has been demonstrated to increase with advanced aging in human vastus lateralis muscle (Yamaguchi *et al.*, 2007) and in rat gastrocnemius muscle (Doran *et al.*, 2007). In line with the hypothesis that HSP 27 and alphaβ-crystallin interact with titin (Kötter *et al.*, 2014) to reduce titin-based stiffness in a sex-dependent manner (Romani & Russ, 2013), the age-related increases in small HSP concentration may preserve the acute regulation of cellular passive mechanics in older males, despite concurrent age-related changes to sex hormones (Allan & McLachlan, 2004).

Another consideration to make is the fact that skeletal muscle fiber type composition is correlated to whole-muscle fatiguability (Thorstensson & Karlsson, 1976). The metabolic, calcium handling, and kinetic characteristics of the three human MHC isoforms have been well studied (Casey *et al.*, 1996; Schiaffino & Reggiani, 2011), and it is generally accepted that these inherent traits render MHC II fibers more prone to fatigue than MHC I fibers. Although there were no muscle-level differences in the magnitude of fatigue across any groups ("fatigue ratio", Table 2 and Table 8), participant groups examined in the present studies differed in fiber type distributions (Supplementary Figure 14), presenting the possibility for fiber type-based differences in cellular fatigue to mediate the effect of fatiguing exercise on cellular passive mechanics. This possibility was accounted for by limiting analyses to MHC IIA and IIA/X fibers. We also determined that fatigue-induced changes to cellular passive mechanics are primarily attributable to titin-based mechanism(s), rather than actomyosin interactions. Nonetheless, future efforts should consider the potential role of fiber type differences in the cellular fatiguing process and its potential to impact titin PTMs and subsequent alterations to titin-based passive mechanics.

To test whether the fatiguing exercise impacts tissue mechanics, bundles of 12-14 fibers with intact ECM from young (Aim 2) and older (Aim 3) participants were subjected to the same passive measures that were used at the cellular level. There were no substantial differences in bundle passive modulus between males and females or older and younger adults. Assessment of collagen I content in a subset of participants for which bundle measurements were made complemented the mechanics measurements in that muscle from young males contained the

lowest amount of collagen I and generated the lowest measures of passive stress and modulus. Fatiguing exercise was only shown to impact passive modulus in bundles from young females. In support of the overall hypothesis that fatigue-induced changes to skeletal muscle mechanics are mediated by titin, in-vitro assays to remove titin-based stiffness in bundles were successful in eliminating any pre-existing fatigue-based differences in bundle modulus. Although cellular findings were not replicated at the bundle level, these assays collectively support the notion that intracellular mechanisms including titin influence tissue passive mechanics, though their relative impact remains unclear.

Considering the relative similarity of passive modulus measures between fibers and bundles, the high variability in bundle mechanics data, and the relatively small size of the bundles themselves, measurements at this scale of sample may not be necessary to characterize age- or fatigue-related changes to skeletal muscle mechanics. However, the task of interpreting cellular findings in the context of whole-muscle function requires an understanding of the scalability of cellular mechanisms. Therefore, future efforts should seek to assess how titin-based mechanics influence skeletal muscle at levels of organization including physiologically relevant amounts of ECM, perhaps at the fascicle level in pre-clinical studies.

Finally, it must be acknowledged that the interpretations drawn from these studies regarding relation to in-vivo muscle function are limited by the fact that the mechanical measures presented here were collected in a passive state. Although this work seeks to contribute to the body of research aimed at understanding the etiology of exercise- induced (young athletes) and falls-induced (older adults) injuries, injury to in-vivo skeletal muscle or ACL is more likely to occur during active loading. Titin, the intracellular protein proposed to contribute to changes in skeletal muscle passive mechanical properties, is also believed to play a role in active muscle mechanics (Herzog, 2014; Herzog *et al.*, 2016). Specifically, titin has been implicated in the residual force enhancement (RFE) is observed following active lengthening (i.e. eccentric contraction) at the level of the skeletal muscle sarcomere (Leonard *et al.*, 2010), single fiber (Pinnell *et al.*, 2019), and whole muscle (Power *et al.*, 2012, 2013; Nishikawa, 2016; Chapman *et al.*, 2018; de Campos *et al.*, 2022). Though the cause of RFE is still under investigation, the leading hypothesis, cited in most reports or reviews on the subject, suggests that muscle

activation causes calcium-mediated binding and/or winding of the titin N2A region to actin (Nishikawa, 2016, 2020) that effectively shortens and reduces the extensibility of titin.

We have developed a protocol to measure RFE in single permeabilized muscle fibers (Supplementary Figure 16) and have observed residual tension enhancement (RFE normalized to cellular CSA) in permeabilized single fibers from a subset of the present cohort (Supplementary Figure 17). As a reasonable follow-up to the present studies testing the effect of fatiguing exercise on measures of passive lengthening, future efforts should seek to test the effect of fatiguing exercise on skeletal muscle cellular RFE, especially in males. These follow-up studies would not only include a more physiologically relevant measure of muscle cellular mechanics (active lengthening), but they would also continue to test the hypothesis that titin is a contributor to altered skeletal muscle mechanical properties following fatiguing exercise. What's more, the examination of RFE presents a cellular measure of muscle active mechanics (active lengthening) that is clinically significant considering the high incidence of muscle strain injury in male athletes (Cross *et al.*, 2013; Dalton *et al.*, 2015).

Altogether, these studies support the notion that intracellular mechanisms contribute to acute changes in skeletal muscle passive mechanics in younger and older adults, though their relative impact at the whole-muscle level remains unclear. This collection of studies contributes to the body of work aimed at understanding how skeletal muscle mechanical properties are regulated, which may have implications for reducing injuries in athletes and falls-risk in older adults.

Appendix A: Supplementary Figures

Supplementary Table 1. A table of p-values demonstrating the lack of effect of MHC on passive modulus at short or long lengths, when only MHC IIA and MHC IIA/X fibers are considered. These values were generated using a linear mixed model including passive modulus as a dependent variable (short and long lengths were tested separately), participant as a random effect, and MHC, fatigue condition, and MHC*fatigue condition as fixed effects. SPSS was programmed to produce separate results for each participant group. This lack of fiber-type effect in this subset was used as justification for excluding MHC isoform as a main effect in subsequent analyses of cellular passive mechanics in younger (Aim 1) and older (Aim 3) adults. "Num." = numerator, "Denom." = denominator, "df" = degrees of freedom, "F" = f statistic.

		Short Lengths				**Long Lengths**			
Group	**Source**	Num. df	Denom. df	F	p	Num. df	Denom. df	F	p
Older Male (n=4)	Intercept	1	2.19	20.85	0.04	1	1.88	70.49	0.02
	MHC	1	36.00	0.00	0.96	1	31.30	0.84	0.37
	Condition	1	35.05	4.33	**0.05**	1	21.53	0.99	0.33
	MHC * Condition	1	35.99	0.02	0.88	1	31.39	0.10	0.75
Older Female (n=4)	Intercept	1	3.02	71.81	0.00	1	2.87	90.79	0.00
	MHC	1	66.18	0.00	0.95	1	69.61	1.14	0.29
	Condition	1	70.71	0.16	0.69	1	70.44	0.03	0.85
	MHC * Condition	1	70.43	0.37	0.54	1	70.20	0.16	0.69
Young Male (n=4)	Intercept	1	2.67	94.72	0.00	1	2.59	247.15	0.00
	MHC	1	59.05	3.02	0.09	1	59.13	0.46	0.50
	Condition	1	59.85	11.08	**0.00**	1	60.15	16.17	**0.00**
	MHC * Condition	1	59.90	0.06	0.80	1	60.21	0.11	0.74
Young Female (n=5)	Intercept	1	4.61	64.12	0.00	1	4.46	43.01	0.00
	MHC	1	49.15	2.20	0.14	1	63.51	0.01	0.95
	Condition	1	66.70	1.05	0.31	1	66.44	0.00	0.95
	MHC * Condition	1	68.02	0.18	0.67	1	67.39	1.92	0.17

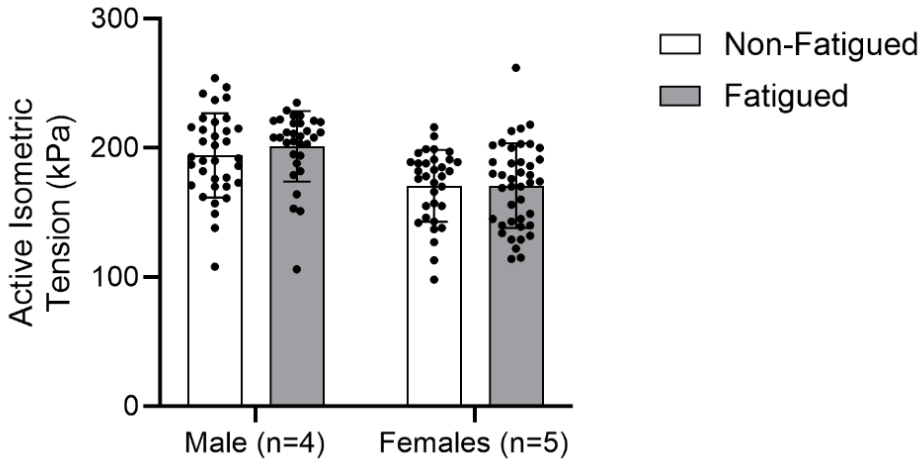

Supplementary Figure 1.Cellular active tension was not significantly different between younger males and females (p=0.138) nor fatigue conditions (p=0.879). Data are shown as mean ± SD.

Supplementary Table 2. Measured SL at each degree of strain in the young cohort. Fiber SL was tracked throughout the passive stretch protocol. There was some variability in SL at each stretched length (note the ranges), especially at longer lengths. However, mean SL was generally consistent between males and females.

Gender	Strain (%Lo)	Min.	Max.	Mean	SD
Male	100	2.24	2.51	2.40	0.03
	108	2.13	2.72	2.60	0.07
	116	2.34	3.15	2.82	0.11
	124	2.86	3.32	3.02	0.10
	132	2.98	3.56	3.21	0.11
	140	2.89	3.78	3.39	0.14
	148	3.28	3.91	3.57	0.13
	156	3.26	4.09	3.76	0.16
Female	100	2.25	2.49	2.40	0.03
	108	2.33	2.75	2.60	0.06
	116	2.56	3.02	2.81	0.08
	124	2.63	3.24	3.00	0.10
	132	2.65	3.63	3.20	0.13
	140	2.97	3.78	3.38	0.13
	148	3.19	4.08	3.57	0.14
	156	3.33	4.10	3.77	0.15

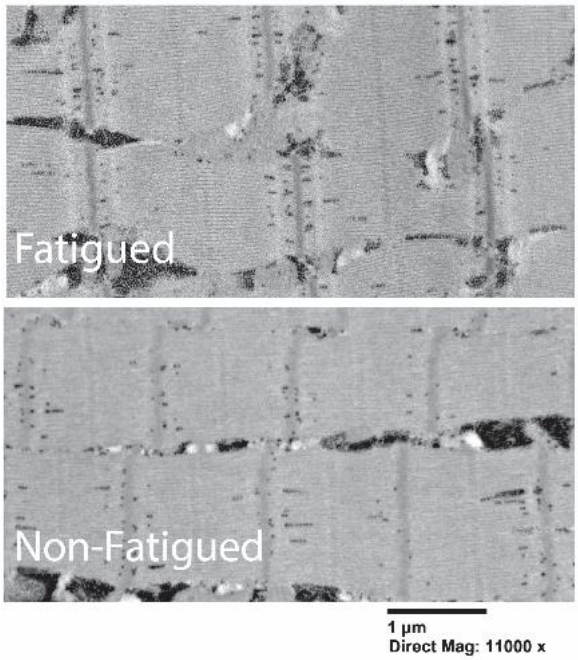

Supplementary Figure 2. Representative electron microscopy images from fatigued and non-fatigued skeletal muscle samples did not show evidence of altered sarcomere ultrastructure resulting from the fatigue protocol used in this study.

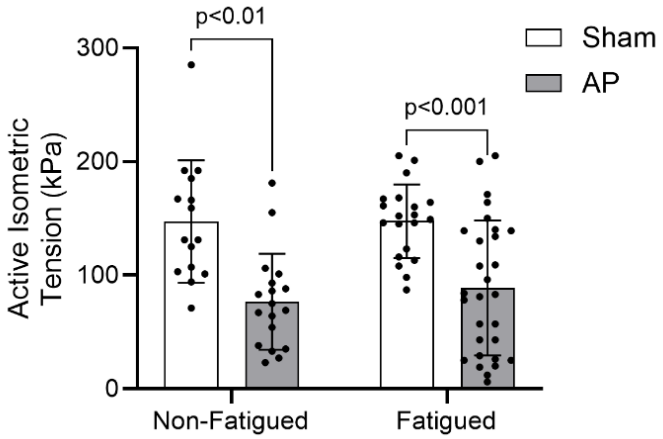

Supplementary Figure 3. There was no significant effect of age (p=0.343) or fatigue (p=0.104) on active tension generation. However, there was a main effect of AP treatment on active tension (p=0.003). This assay was intended to test the effect of AP treatment on cellular mechanics within each fatigue condition, so the effect of AP on active tension generation was tested in non-fatigued and fatigued fibers, separately. AP treatment significantly reduced active tension generation in non-fatigued (p=0.005) and fatigued (p<0.001) fibers.

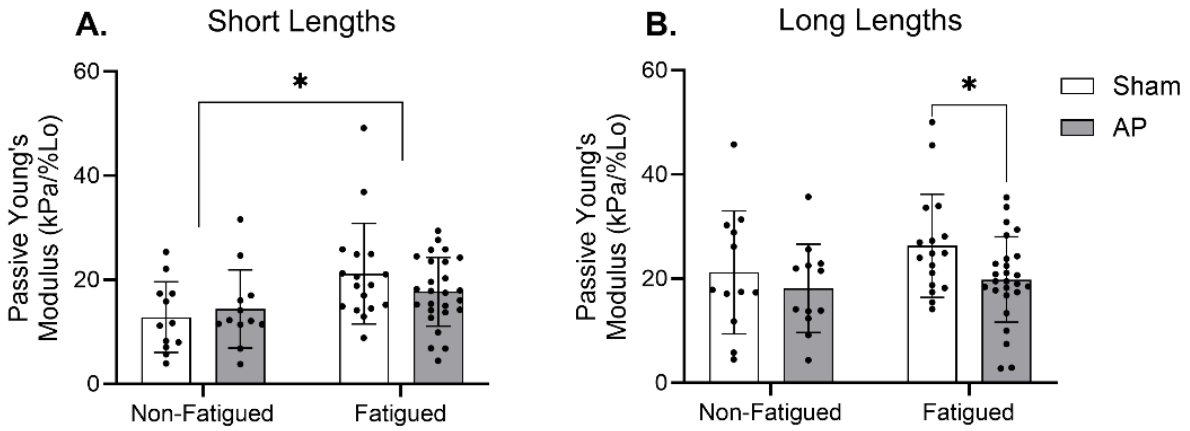

Supplementary Figure 4. The subset of fibers from older adults was better represented (n=67 fibers) compared to that of the younger adults (n=13 fibers). As a result, the effect of AP treatment on passive modulus of non-fatigued and fatigued fibers was tested exclusively in older adults to determine if the outcome was affected by exclusion of fibers from the young male. **(A)** At short lengths, passive modulus was significantly higher in fatigued versus non-fatigued fibers (19.10 ± 8.03 vs. 13.63 ± 7.03 kPa/%Lo, respectively, $p<0.01$) regardless of AP treatment. There was no effect of AP treatment in the non-fatigued ($p=0.592$) or fatigued ($p=0.169$) fibers. **(B)** At long lengths, AP treatment reduced passive modulus of fatigued fibers (sham: 26.31 ± 9.90 kPa/%Lo, AP: 19.85 ± 8.19 kPa/%Lo, $p=0.025$), but not non-fatigued fibers ($p=0.430$). Altogether, the effect of AP treatment on cellular passive modulus was not affected by exclusion of data from the younger adult. Data are shown as mean ± SD. * Indicates significant effect ($p<0.05$).

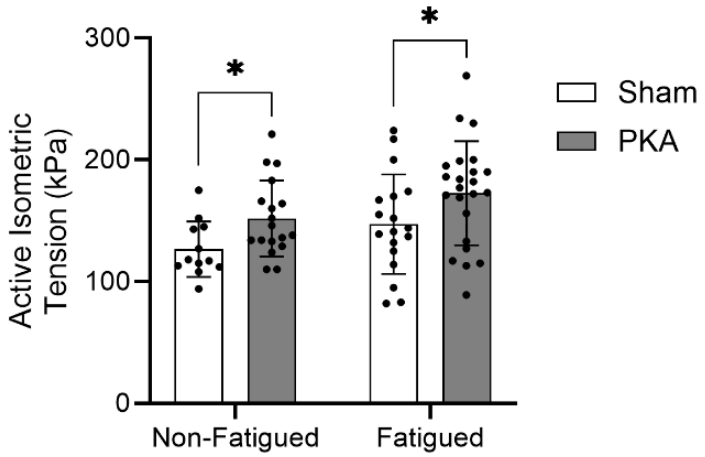

Supplementary Figure 5. There was no main effect of age ($p=0.997$), nor was there an age*PKA interaction ($p=0.572$), on cellular active tension. Active tension was higher in fatigued versus non-fatigued fibers (161.51 ± 43.34 kPa vs. 141.80 ± 30.48 kPa, respectively, $p=0.002$) and higher in PKA treated versus sham fibers (163.56 ± 39.10 vs. 139.00 ± 35.82 kPa, respectively, $p=0.005$). Because the purpose of this assay was to test the effect of PKA on cellular mechanics within each fatigue condition, final analysis revealed that PKA treatment significantly increased active isometric tension in both non-fatigued ($p=0.013$) and fatigued ($p=0.026$) fibers.

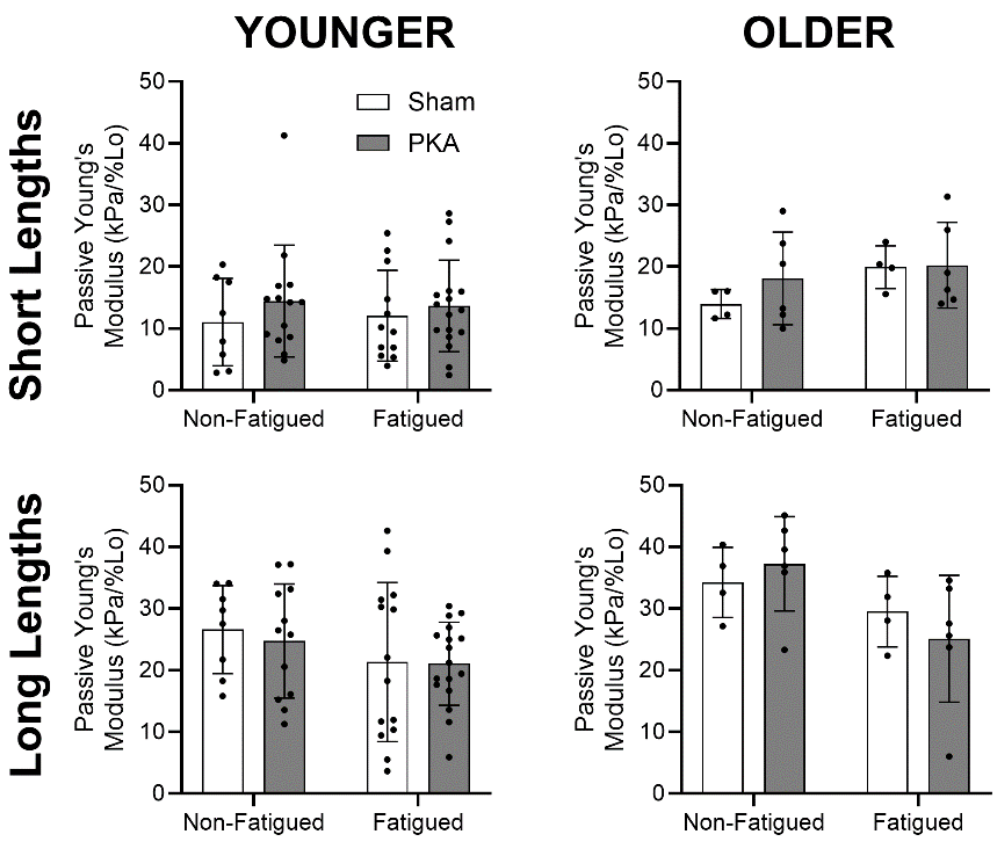

Supplementary Figure 6. PKA treatment did not significantly affect passive modulus at any length, in any age group, in either fatigue condition.

Supplementary Table 3. Descriptive statistics of the entire dataset collected for Aim 2 (including outliers excluded from Aim 2 analysis).

		N	CSA (mm^2)	Length (mm)
Male	Non-fatigued	14	0.133 ± 0.097	2.1 ± 0.4
	Fatigued	12	0.166 ± 0.123	1.9 ± 0.5
Female	Non-fatigued	33	0.061 ± 0.016	2.3 ± 0.4
	Fatigued	25	0.065 ± 0.022	2.4 ± 0.3

Data are shown as mean ± SD.

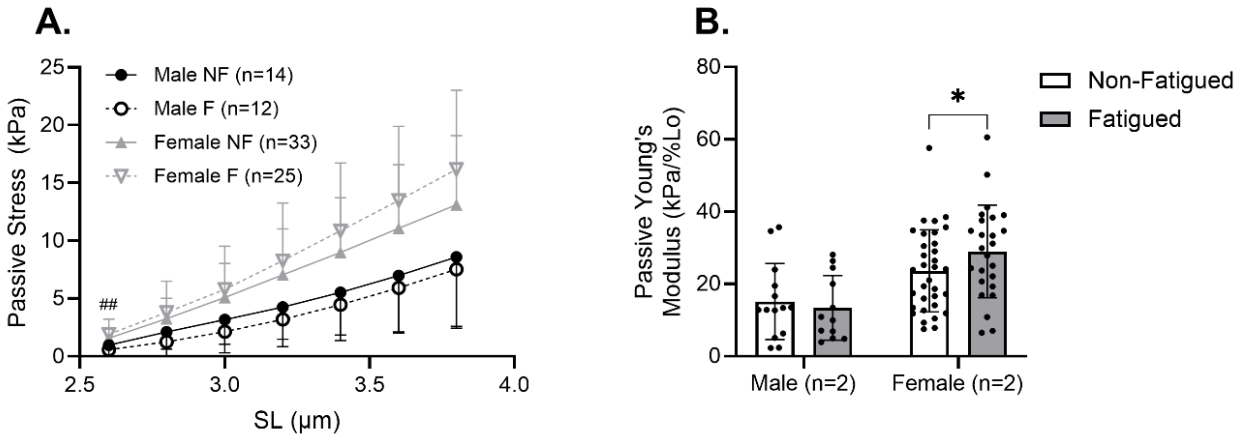

Supplementary Figure 7. Statistical analysis of the entire sample of bundles produced comparable results to those reported in Aim 2. **(A)** Comparison of passive stress between males and females revealed a significant difference at SL=2.6 µm (Males: 0.79 ± 0.75 kPa, Females: 1.72 ± 1.08 kPa, $p<0.01$), but not at any other length. Furthermore, fatiguing exercise did not significantly affect passive stress measures in either group, at any SL. **(B)** Although tissue-level passive modulus was not affected by fatiguing exercise in the male cohort, it was significantly increased by fatiguing exercise in the female cohort ($p=0.036$).

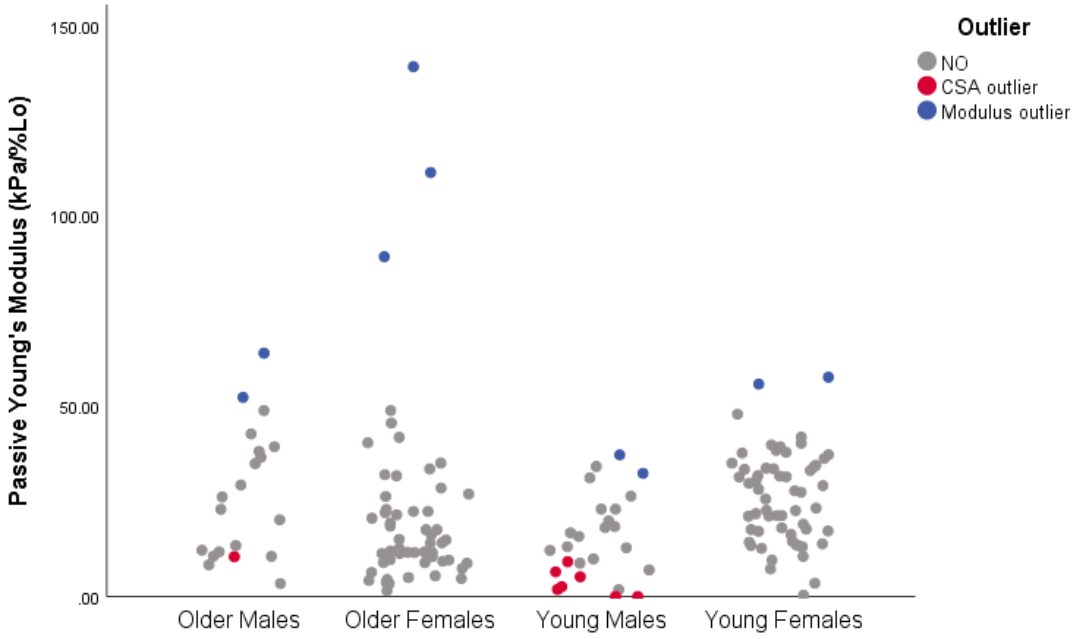

Supplementary Figure 8. Illustration of the samples considered outliers in Aims 2 and 3 (not KI/KCL treated). Samples of bundles with CSA values ± 2 SD from each group mean (indicated in red), and samples with passive modulus values ± 2 SD from each group mean (indicated in blue) were considered outliers.

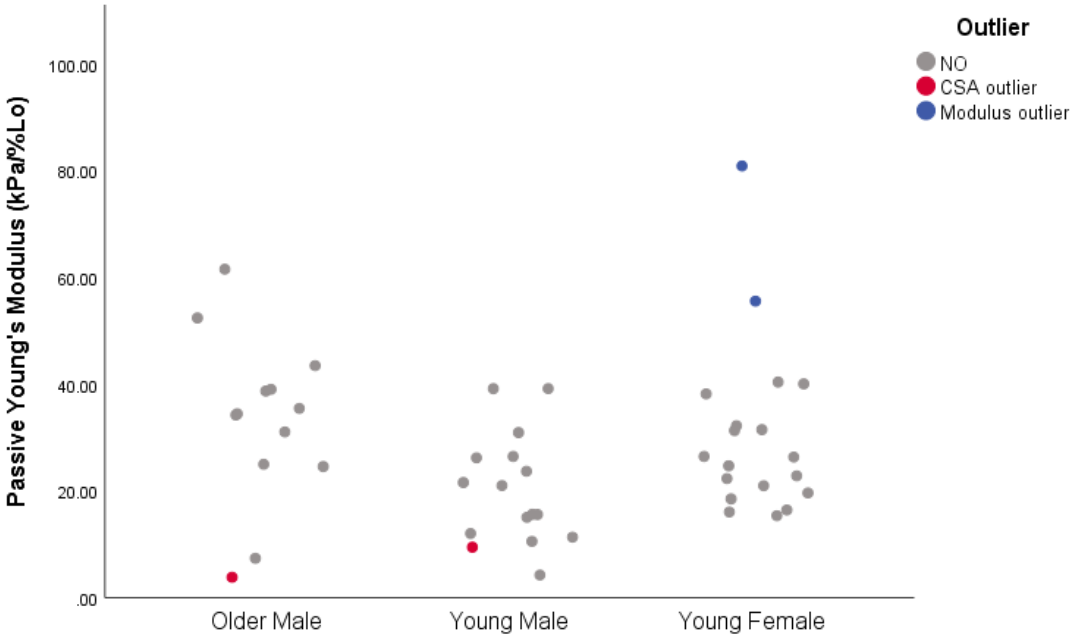

Supplementary Figure 9. Illustration of the samples considered outliers in Aim 2 (KI/KCL treated). Bundles with CSA values ± 2 SD from each group mean (indicated in red), and samples with passive modulus values ± 2 SD from each group mean (indicated in blue) were considered outliers.

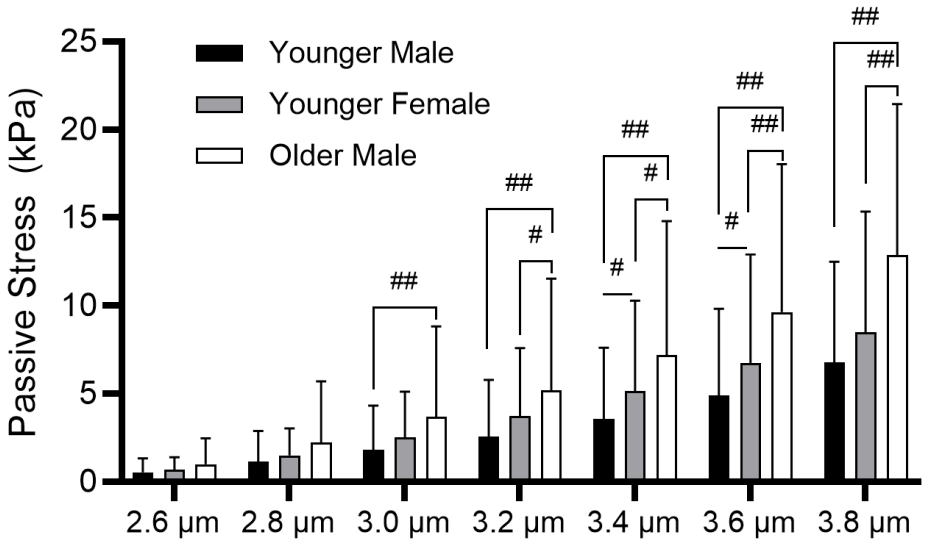

Supplementary Figure 10. Passive stress was significantly different across participants included in the KI/KCl analyses, at most lengths. #Indicates significant main effect of participant (single, $p<0.05$; double, $p<0.01$). Data are shown as mean ± SD.

Supplementary Table 4. Absolute and relative values for whole-muscle performance of older versus younger adults.

Age		Absolute Peak Power (W) [#A]	Relative Peak Power (W/kg) [#A]	Absolute Peak Torque (N) [#A]	Relative Peak Torque (N/kg) [#A]
Young	**Female**	295±33	5.43±0.32	140±8	2.54±0.12
	Male	532±95	6.43±1.42	281±44	3.34±0.34
Older	**Female**	185±36	2.74±0.13	125±17	1.88±0.39
	Male	334±59	4.03±0.7	174±32	2.24±0.15

Symbols indicate significant difference between biological sex[#] or age [A] groups ($p<0.05$). Data are shown as mean ± SD.

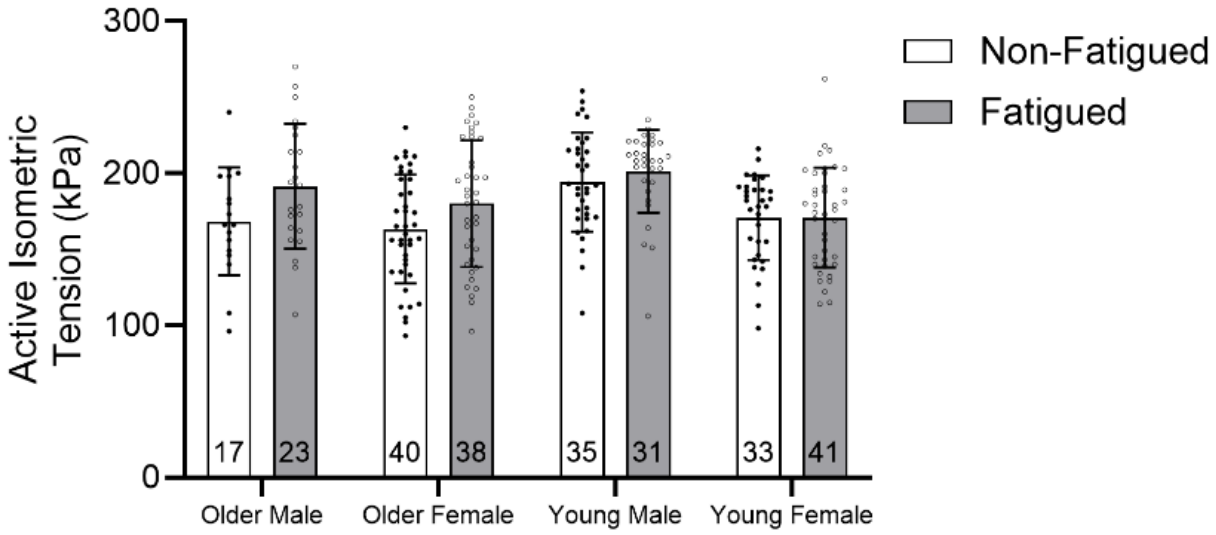

Supplementary Figure 11. In this sample of MHC IIA and IIA/X fibers, active isometric tension was not affected by fatigue (0.080), biological sex (p=0.410), or age (p=0.569). Data are shown as mean ± SD.

Supplementary Table 5. Measured SL at each degree of strain in the older cohort. Fiber SL was tracked throughout the passive stretch protocol. There was some variability in SL at each stretched length. However, mean SL was generally consistent between males and females.

Gender	Strain (%Lo)	Min.	Max.	Mean	SD
Male	100	2.37	2.96	2.43	0.10
	108	2.34	2.73	2.61	0.06
	116	2.71	3.20	2.83	0.09
	124	2.82	3.85	3.04	0.17
	132	2.96	3.39	3.16	0.10
	140	3.01	4.89	3.36	0.29
	148	3.28	3.96	3.53	0.14
	156	3.43	4.97	3.76	0.27
Female	100	2.31	2.44	2.40	0.02
	108	2.42	2.70	2.61	0.04
	116	2.08	2.93	2.80	0.10
	124	2.77	3.14	2.99	0.07
	132	2.75	3.67	3.18	0.11
	140	3.03	3.61	3.36	0.09
	148	3.13	4.12	3.54	0.13
	156	3.23	4.62	3.72	0.19

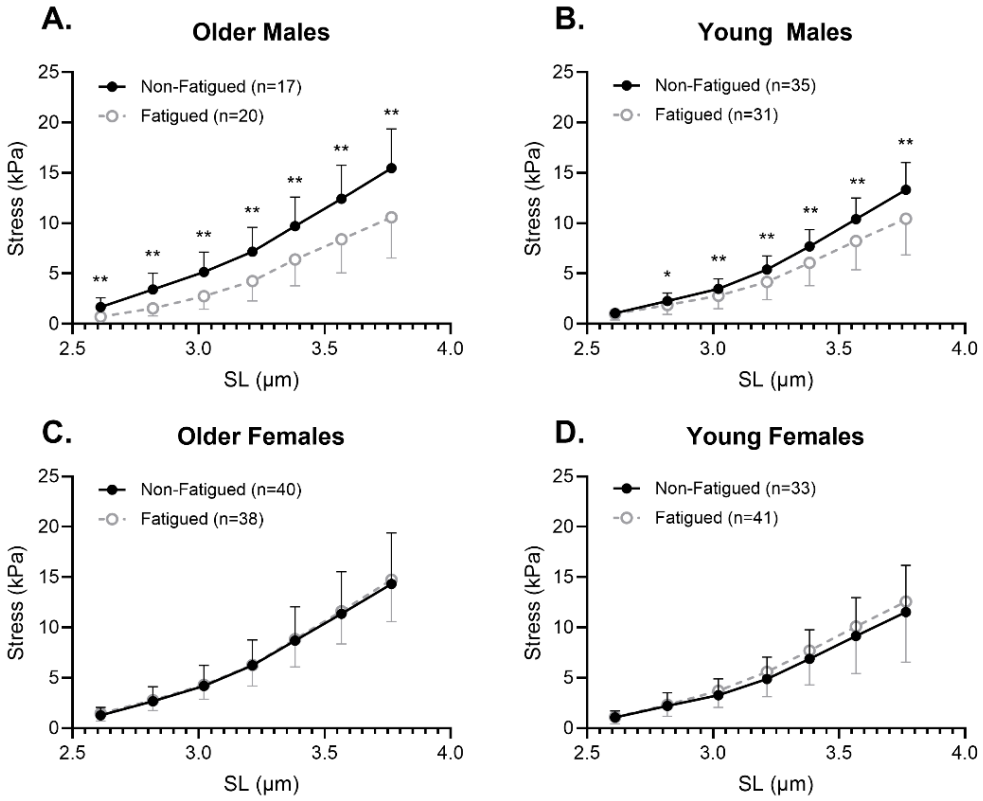

Supplementary Figure 12. Cellular passive stress was significantly lower in fatigued versus non-fatigued fibers of older males **(A)** and younger males **(B)**, but not in fibers of older females **(C)** or younger females **(D)**. Data are shown as mean ± SD. Symbols indicate a significant main effect of fatigue *($p<0.05$) or **($p<0.01$).

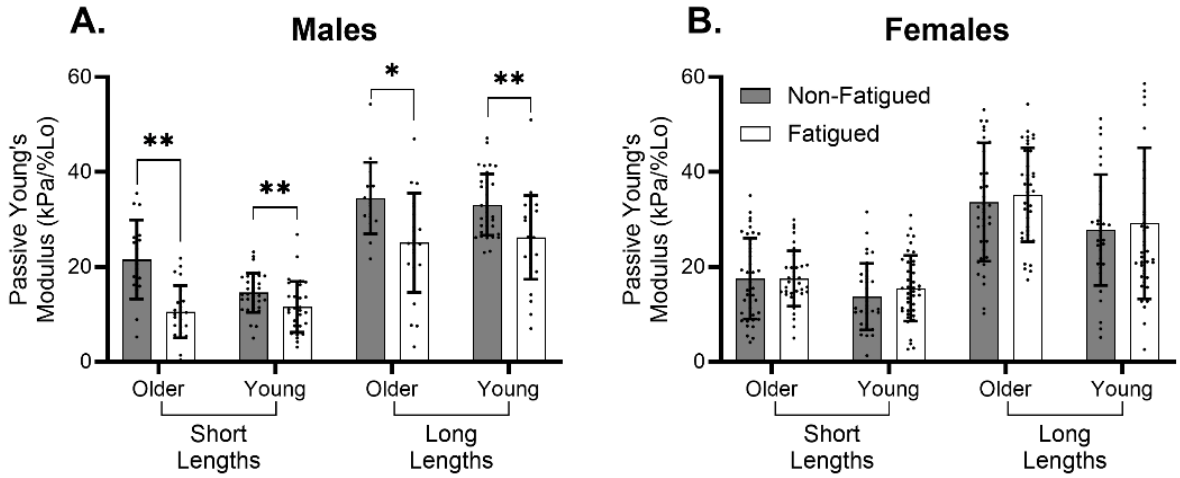

Supplementary Figure 13. When cellular passive modulus data are broken down into age- and biological sex-based groups, it becomes clear that older and younger males exhibited reduced passive modulus in fatigued fibers at short and long lengths **(A)**. On the other hand, passive modulus was not affected by fatigue in older or younger females at any length **(B)**. Data are shown as mean ± SD. Symbols indicate a significant effect of fatigue *($p<0.05$), **($p<0.01$).

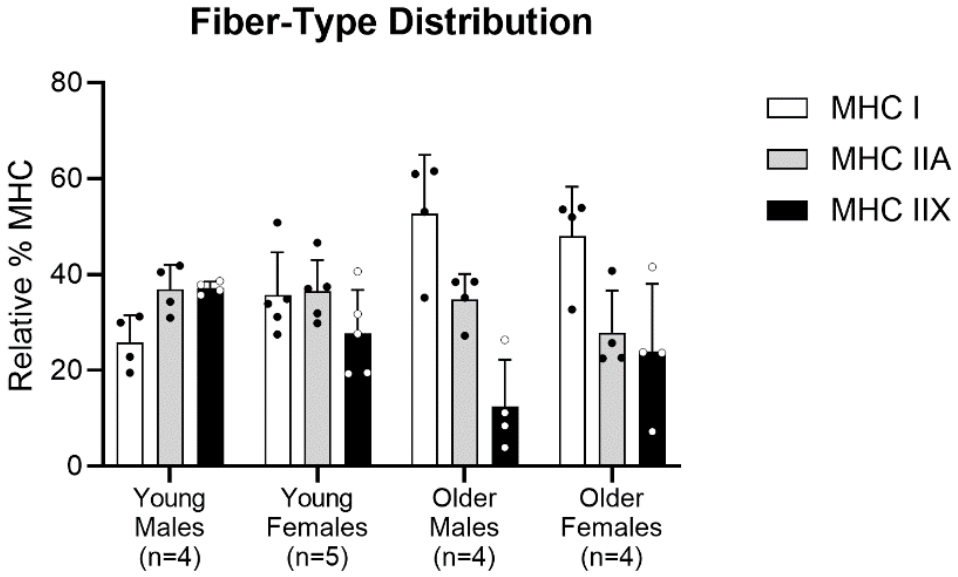

Supplementary Figure 14. MHC standards, made up of a homogenate of all fiber types during muscle dissection on biopsy day, for each participant were run on an SDS-PAGE gel to quantify the relative percent of each MHC isoform included in the sample. Although this form of quantification does not provide information regarding hybrid isoforms, it provides a useful view at the relative percent of MHC I and MHC II isoforms, and how they differ in older versus younger adults, within the same sample from which fibers were later dissected.

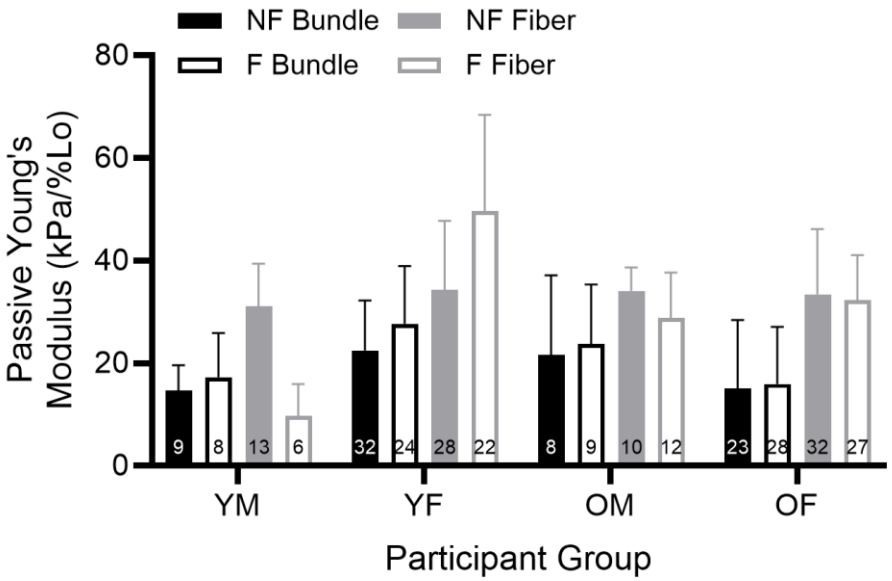

Supplementary Figure 15. A comparison of the passive modulus of bundles and fibers (MHC IIA and IIA/X) from the same subset of individuals as that examined in Aim 3. When graphed together, it becomes clear that passive modulus values for each age/biological sex group are similar at the cellular (modulus at long SL) and bundle (modulus of the entire stress-strain curve) level. Additionally, trends evident in the fiber data tend to be visible in the bundle data. Data are shown as mean ± SD. YM = young males, YF = young females, OM = older males, OF = older females.

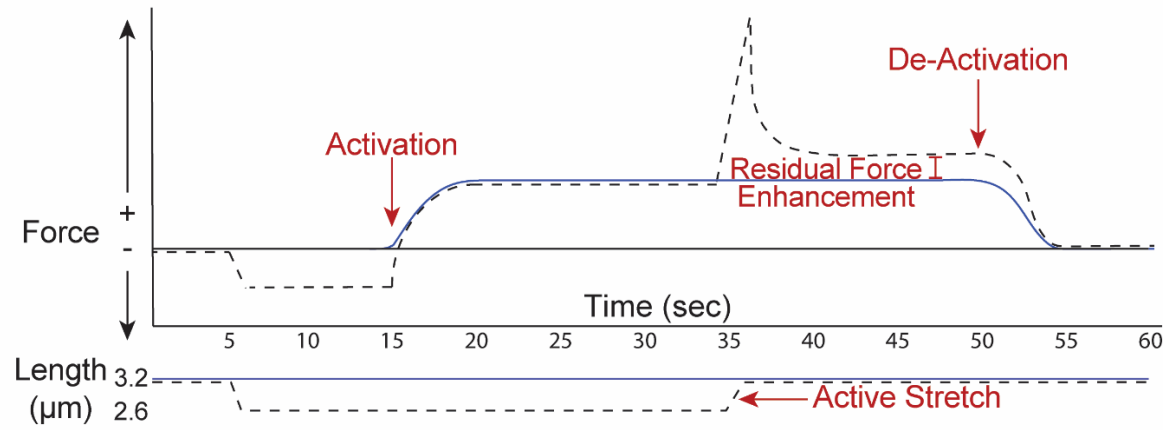

Supplementary Figure 16. To measure RFE, isometric tension at standard reference length (sarcomere length = 3.2 μM, solid blue line) was compared to tension generated at the same length following active stretch (dashed black line). RFE is quantified as the difference between steady state force production in the isometric reference condition versus the active stretch condition. In the active stretch condition, RFE likely reflects the contribution of titin to force generation under active loading.

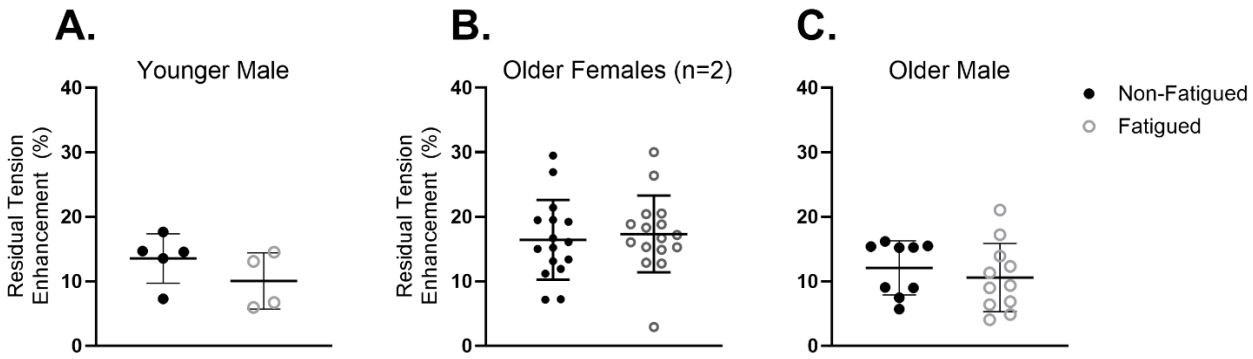

Supplementary Figure 17. Preliminary studies confirm that RFE (quantified on the y-axis as "Residual Tension Enhancement") is observed in skeletal muscle fibers from the cohort included in this dissertation. Although there is not yet a clear effect of fatiguing exercise on measures of RFE in this limited sample, the trend toward reduced tension enhancement in one young male (a member of the cohort for which a robust effect of fatigue on cellular passive stress and Young's Modulus was observed in these dissertation studies) motivates the future study of RFE in fatigued and non-fatigued skeletal muscle samples from males.

Appendix B: Supplementary Document
Planned submission: August 2024

RESEARCH ARTICLE

RUNNING HEAD (60 characters): Mediators of Cellular Viscoelasticity in Human Skeletal Muscle

Chronic and Acute Mediators of Passive Viscoelasticity in Human Skeletal Muscle Fibers

Grace E. Privett, Austin W. Ricci, Karen W. Needham, and Damien M. Callahan
Department of Human Physiology, University of Oregon, Eugene, OR, USA

Correspondence: Damien M. Callahan (damienc@uoregon.edu)

Abstract (250 words)

Cellular viscoelastic modulus in skeletal muscle tissue responds dynamically to chronic stressors, such as age and resistance training. Recent evidence suggests that passive tissue mechanics may also be sensitive to acute stimuli such as mechanical loading and/or acivation-induced muscle fatigue. Many of these insights are derived from experiments that rely on preclinical models of age and acute muscle activation. Therefore, we sought to understand the relative responsiveness of muscle cellular passive mechanics to chronic (resistance training) and acute (muscle fatigue) stressors in healthy young males and females categorized as "resistance trained" or "untrained". We measured cellular passive mechanical measures (stress, Young's Modulus) to the hypothesis that Young's Modulus and stress would be greater in trained than untrained and that acute fatigue would reduce these measures. We further assessed the translation of these findings to composite tissue by repeating these analyses in samples from a sub-set of participants. containing multiple muscle fibers and associated extracellular matrix. We report a main effect of training such that cellular passive mechanical measures were increased in samples from trained versus untrained participants. We likewise report reductions in passive mechanical measures following fatiguing exercise. Surprisingly, both training and acute fatigue only impacted muscle fiber passive measures in males, whereas females showed a more variable response across participants. Together, these data suggest males have more dynamic response in muscle tissue mechanics to acute and chronic stressors, perhaps lending insight into potential mechanisms related to sex-based differences in musculotendinous injury risk.

New and noteworthy (75 words)

We report that passive stress and modulus in single muscle fibers was higher in resistance trained healthy adults and fatiguing exercise reduced passive stress and modulus. In each case, dynamic responsiveness of muscle fibers to chronic and acute stressors was observed consistently in males, whereas responses in females varied considerably. We provide further evidence that cellular mechanisms may contribute to multicellular muscle tissue samples, suggesting these findings have relevance to in vivo tissue mechanics.

Keywords: skeletal muscle, fatigue, training, stress decay, viscoelasticity, passive mechanics, cellular stiffness, titin

Introduction

Skeletal muscle viscoelasticity affects functional mobility through multiple interrelated mechanisms including its influence on joint stability (Blackburn *et al.*, 2011), and the dampening of impact forces (Sarvazyan *et al.*, 2014) during musculoskeletal loading. Viscoelastic behavior of muscle also contributes to the rate and mechanical efficiency of force transfer from muscle to tendon (Wilson & Flanagan, 2008). Prior studies report that whole-muscle stiffness and viscosity are transiently altered by a single bout of fatiguing exercise in the Vastus Lateralis (VL) (Chalchat *et al.*, 2020). This transient change to VL mechanical properties may be maladaptive, considering that muscular fatigue was previously shown to decrease the capacity for skeletal muscle to absorb strain elastic energy before incurring injury (Mair *et al.*, 1996). As such, acute, fatigue-induced changes to skeletal muscle viscoelasticity may contribute to the high prevalence of hamstring injury in male athletes (Watsford *et al.*, 2010; Cross *et al.*, 2013) or knee joint destabilization (Blackburn *et al.*, 2011) and subsequent ACL injury in female athletes (Myer *et al.*, 2008*a*; De Ste Croix *et al.*, 2015). Connective tissue injury risk is higher in female athletes (Deitch *et al.*, 2006), and given the likely relationship between muscle viscoelastic properties and tissue injury risk, it is logically appealing to predict that biological sex, muscle fatigue and injury risk share a complex dynamic contributing to sex-disparity in rates of soft tissue injury.

At the cellular level, we have demonstrated fatigue-induced reductions in passive Young's Modulus, a measure of stiffness accounting for differences in cell ("fiber") size, in VL samples from young, recreationally active adults in a sex-dependent manner (Privett *et al.*, 2024*a*). At the single fiber level, passive modulus is largely attributed to the intracellular protein titin (Ottenheijm *et al.*, 2012; Lim *et al.*, 2019). Titin is a viscoelastic protein that is subject to post-translational modifications (PTM), many of which can alter titin-based stiffness if they occur at an extensible region of the protein (Hamdani *et al.*, 2017). Ample study of PTM-induced changes to titin-based mechanical properties has been conducted in cardiac muscle, which has demonstrated that phosphorylation of cardiac titin regulates cardiomyocyte mechanics in health and disease (Granzier & Irving, 1995; Wu *et al.*, 2000, 2002; Yamasaki *et al.*, 2002; Fukuda *et al.*, 2005; Krüger *et al.*, 2009; LeWinter & Granzier, 2014). Skeletal muscle titin can also be phosphorylated (Müller *et al.*, 2014; Privett *et al.*, 2024*a*), though whether titin phosphorylation alters viscoelasticity in skeletal muscle is not yet clear. Exercise is a multimodal and dynamic physiological stimulus that likely induces multiple PTMs to consider in skeletal muscle. These include phosphorylation (Müller *et al.*, 2014), S-glutathionylation (Alegre-Cebollada *et al.*, 2014; Watanabe *et al.*, 2020) and the binding of small heat shock proteins (HSP, 47), the latter of which has been shown to protect against stress-induced stiffening (Kötter *et al.*, 2014). Evidence supports the notion that titin directly influences whole muscle function (Brynnel *et al.*, 2018), suggesting acute regulation of titin may influence skeletal muscle mechanics (Privett *et al.*, 2024*a*). Therefore, this current study sought to test the role of intracellular contributors to changes in tissue-level mechanical properties by comparing the impact of acute fatigue on viscoelastic properties of single fibers (titin-based) and in bundles of fibers with intact extracellular matrix (ECM) who's modulus is presumably impacted by several factors outside the myofiber.

Although the study of altered VL mechanical properties following fatiguing exercise may have high clinical relevance for athletes, it remains to be seen whether the neuromuscular adaptations to chronic training mediate these

observations. Chronic training has been demonstrated to increase active (Mongold *et al.*, 2022) and resting (Klinge *et al.*, 1997) musculoskeletal stiffness in some, though not all (Blazevich, 2019) studies. Evidence of training-based changes to collagen expression, synthesis, and accumulation in the ECM (Kjær, 2004) suggests that altered stiffness due to training may be the result of modified ECM-based stiffness. Although it is unclear whether chronic training impacts ECM-based measures of stiffness in the literature, jump training in rats has been shown to increase the passive stiffness of extensor digitorum longus (EDL) and rectus femoris (RF) muscles in conjunction with increased collagen concentration (Ducomps *et al.*, 2003). At the cellular level, training was shown to alter the stiffness of permeabilized skeletal muscle fibers in a length-dependent manner (Noonan *et al.*, 2020*a*) suggesting that intracellular mechanisms may contribute to training-based changes in skeletal muscle stiffness. Therefore, the present study compared baseline measures of cellular passive viscoelasticity in VL samples from untrained (UT) and resistance trained (RT) young males and females and expanded upon our previous work (Privett *et al.*, 2024*a*) by assessing whether chronic training mediates the effect of fatiguing exercise on cellular passive mechanics.

Although the majority of previous research focused on measures of elasticity, viscosity is equally important to consider given its role in skeletal muscle extensibility and the absorption and dissipation of external mechanical loads (Sarvazyan *et al.*, 2014). Therefore, this present study sought to extend our previous work by considering the effect of fatigue on the viscoelasticity of human skeletal muscle cells. To do so, stress decay index (SDI) was calculated using the magnitude and rate of stress relaxation at each SL studied.

The purpose of this study was to compare passive viscoelastic properties in VL samples obtained from exercised ("fatigued") and non-exercised ("non-fatigued") limbs of UT and RT young adults. It was hypothesized that passive mechanical measures (stress, Young's Modulus) would be reduced in fatigued versus non-fatigued skeletal muscle fibers from all participants. Based on evidence of training-induced increases in stiffness in the literature (Noonan *et al.*, 2020*a*), it was also hypothesized that the cellular passive mechanical measures would be higher in RT versus UT individuals. To consider the "viscous" element of skeletal muscle viscoelasticity, SDI was compared in fatigued and non-fatigued skeletal muscle cells. Finally, passive modulus was measured in bundles of fibers with intact ECM, termed here as "composite muscle tissue" (CMT) before and after chemical elimination of intracellular contributors to passive modulus to assess the extent to which intracellular mechanisms contribute to observations of altered CMT passive modulus after fatiguing exercise. It was hypothesized that any effect of fatiguing exercise on measures of CMT stiffness would be abolished by elimination of intracellular contributors to passive modulus.

Methods

Population: This protocol was approved by the Institutional Review Board at the University of Oregon. 19 young (aged 21 ± 3 yrs.), RT and UT males and females from the University of Oregon and surrounding community consented to participate in this study. Participants were considered RT if they reported between five and seven sessions, each at least 1-hour in duration, of weight training, with at least three sessions focused on the lower limbs. Participants were considered UT if they reported recreational levels of activity with no participation in structured physical exercise and no resistance training. Initial self-report of physical activity history was confirmed by use of ActivePal accelerometers as described previously (Dowd *et al.*, 2012). To limit the potential for menstrual cycle-

dependent variation in circulating estradiol and associated potential impacts on skeletal muscle mechanical properties, all female volunteers either reported use of hormonal contraceptive or were tested in the pre-follicular phase of the menstrual cycle, (within 5 days of menses onset). Participants reported no orthopedic limitations (severe osteoarthritis, joint replacement, or other orthopedic surgery in the previous six months), endocrine disease (hypo/hyper thyroidism, Addison's Disease or Cushing's syndrome), uncontrolled hypertension (>140/90 mmHg), neuromuscular disorder, significant heart, liver, kidney or respiratory disease, or diabetes. Participants were non-tobacco-smokers and had no current alcohol disorder. Finally, participants taking medications known to affect muscle stiffness or beta-adrenergic signaling of neuromuscular activation (including but not limited to beta blockers, calcium channel blockers, and muscle relaxers) or anabolic steroids were not included.

Study Design: Participants visited the lab on 2 occasions separated by at least 1 week. During the first visit, non-invasive measures of voluntary strength, power, and fatigue of their dominant knee extensors (KE) were collected using a Biodex System 3 dynamometer (Biodex Medical Systems, Shirley, NY) and participants were familiarized with the exercise protocol. During the second visit, volunteers performed maximal voluntary isometric contractions of the KE followed by fatiguing exercise to task failure. Fatiguing exercise was followed by bilateral, percutaneous needle muscle biopsies: one on the exercised limb immediately following exercise ("fatigued") and the second on the contralateral, non-exercised limb ("non-fatigued").

Fatigue Protocol: The fatigue protocol utilized for this study was described in detail previously (Privett *et al.*, 2024*a*). Briefly, Participants were seated on the Biodex dynamometer with hips and knee flexed at 90° (180° = full extension). After completion of three maximum voluntary isometric contractions (MVIC) of the knee extensors of the dominant leg, participants performed repeated, voluntary knee extensions to task failure while the Biodex applied a load set to 30% MVIC maximal torque. Task failure was identified as the inability to perform knee extension through at least 50% range of motion. Fatigue was quantified as the Fatigue Ratio = $\frac{Final\ Power}{Initial\ Power}$, where "initial power" represents the average peak power of the first five knee extensions performed during fatiguing exercise, and "final power" represents the average peak power from the last five knee extensions. Time to fatigue (task failure) was recorded for all participants.

Muscle Biopsy Procedure: Percutaneous needle biopsy of the VL was performed within 9 ± 4 minutes immediately following task failure, under sterile conditions as previously detailed (Tarnopolsky *et al.*, 2011). First, the biopsy site was sterilized and local anesthetic (1 or 2% lidocaine HCL [Hospira Worldwide, Lake Forest, IL, USA]) was administered via injection. Next, a small (~5mm) incision was made in the skin and muscle fascia, allowing for the passage of a Bergstrom biopsy needle (5 mm diameter) to the belly of the VL muscle to acquire sample at a depth of ~2-3 cm. Following acquisition of biopsy sample, the collected muscle was retrieved from the needle using forceps.

Tissue Processing and Dissection: The details of tissue processing for mechanics were detailed elsewhere (Privett *et al.*, 2024*a*). Briefly, sample collected during biopsy was placed in dissecting solution (MDS, 120.782 mM NaMS, 5.00 mM EGTA, 0.118 mM $CaCl_2$, 1.00 mM $MgCl_2$, 5.00 mM ATP-Na_2H_2, 0.25 mM KH_2PO_4, 20.00 mM BES, 1.789mM KOH, 1mM Dithiothreitol (DTT)), parsed into bundles of ~50 fibers, and tied to glass rods before advancement through solutions of increasing glycerol content and storage in 50% glycerol solution (5.00 mM

EGTA, 2.50 mM $MgCl_2$, 2.50 mM ATP-Na_2H_2, 10 mM imidazole, 170.00 mM potassium propionate, 1.00 mM sodium azide, 50% glycerol by volume) at -20°C. Sample allocated for mechanics analyses were used within 4 weeks following biopsy. Preparation for mechanical assays was described previously (Privett *et al.*, 2024*a*). Briefly, fiber bundles and dissected single fibers were chemically skinned (MDS + 1% Triton X-100), transferred to plain MDS, and kept on ice until experimentation. For CMT experiments, fiber bundles were transferred directly from 50% glycerol solution to plain MDS (no further chemical skinning). Then, strips of fibers with surrounding ECM were dissected from the bundle and kept on ice until experimentation.

Single fiber morphology and contractile measures: Prepared fibers were mounted in relaxing solution (67.286 mM NaMS, 5.00 mM EGTA, 0.118 mM $CaCl_2$, 6.867 mM $MgCl_2$, 0.25 mM KH_2PO_4, 20.00 mM BES, 0.262 mM KOH, 1.00 mM DTT, 5.392 mM Mg-ATP, 15.00 mM CP, 300 U/mL CPK) between a force transducer and a length motor (Aurora Scientific, Inc., Aurora, ON, Canada) using the Moss clamp technique (Moss, 1979). Passive tension was measured by zeroing the force transducer while the fiber was slacked, then stretching the fiber to sarcomere length (SL) 2.65 µm. Active tension was measured at SL 2.65 µm by moving the fiber to pre-activating solution (81.181 mM NaMS, 5.00 mM EGTA, 0.012 mM $CaCl_2$, 6.724 mM $MgCl_2$, 5.00 mM KH_2PO_4, 20.00 mM BES, 1.00 mM DTT, 5.397 mM Mg-ATP, 15.00 mM CP, 300 U/mL CPK) followed by activating solution (57.549 mM NaMS, 5.00 mM EGTA, 5.021 mM $CaCl_2$, 6.711 mM $MgCl_2$, 5.00 mM KH_2PO_4, 20.00 mM BES, 9.674 mM KOH, 1.00 mM DTT, 5.437 mM Mg-ATP, 15.00 mM CP, 300 U/mL CPK). Once a steady state tension was recorded, the sample was returned to relaxing solution. All fibers were activated (pCa 4.5) prior to passive stretching to measure active tension and confirm fiber viability.

Passive stretch protocol: Passive stretch measures were performed in relaxing solution (pCa 8.0) using a passive stretch protocol adapted from previous work (Lim *et al.*, 2019). Initial sarcomere length was set to 2.4 µm, followed by 7 incremental stretches to reach a final length of 156% of initial length (SL = 3.5-4.0 µm). Each stretch lengthened the sample 8% of initial length and held this position for 2 minutes of stress-relaxation. Sarcomere length was measured throughout the protocol using an inverted microscope located beneath the single fiber rig. To determine the extent to which actomyosin interactions contributed to measures of passive viscoelasticity, a subset of fibers from two sedentary males was subjected to the passive stretch protocol in relaxing solution with the addition of 40 mM 2,3-butanedione monoxime (BDM), a myosin inhibitor. Following completion of the passive stretch protocol, each fiber was collected and placed in gel loading buffer (2% SDS, 62.5 mM Tris, 10% glycerol, 0.001% bromophenol blue, 5% β-mercaptoethanol, pH 6.8), centrifuged and heated at 65ºC for 2 minutes, then stored at -80°C until later assessment of myosin heavy chain (MHC) isoform.

KI/KCl treatment: To assess titin's contribution to passive modulus in CMT, mounted bundles of ~7-12 fibers with intact ECM were treated with KCl and KI to extract the thick and thin sarcomeric filaments, respectively (Ottenheijm *et al.*, 2012; Brynnel *et al.*, 2018). CMT samples were first subjected to an initial passive-stretch (as described above), after which the sample was incubated in relaxing solution containing 0.6M KCl for 35 minutes at 15°C followed by relaxing solution containing 1.0M KI 35 minutes at 15°C. After incubation, CMT samples were passively stretched a second time to measure post-incubation passive stiffness. Following these experiments, CMT samples were collected and stored in gel loading buffer.

MHC isoform identification: Sodium dodecyl sulfate poly acrylamide gel electrophoresis (SDS-PAGE) was used to determine the MHC isoform of single muscle fibers. Sample from each fiber was loaded into its own well of a 4% stacking / 7% resolving polyacrylamide gel. The gel was run at 70 V for 3.5 hours followed by 200 V for 20 hours at 4°C (Miller *et al.*, 2010). Gels were stained with silver and the resulting MHC isoform (I, IIA, and/or IIX) expression was determined by comparison to a standard made from a multi-fiber homogenate (Figure 2).

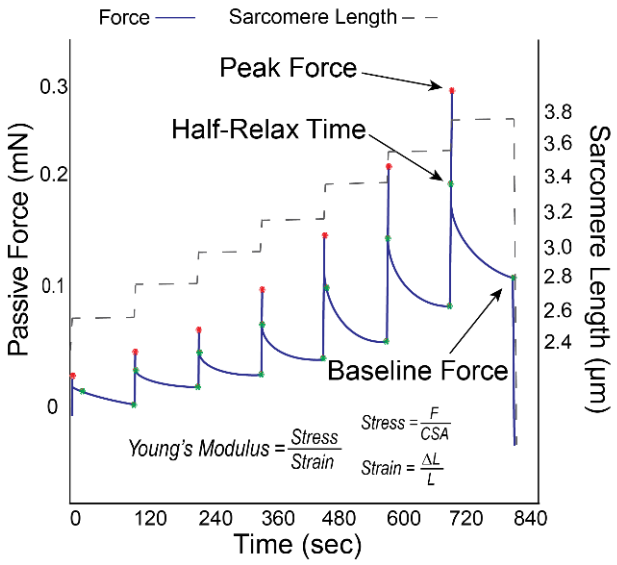

Figure 1: Sample force trace indicating the outcome measures produced by this passive stretch protocol.

Outcome Measures: Maximally activated tension was quantified as the plateau of active force divided by fiber CSA. Passive stress at each sarcomere length (SL) was calculated as $\frac{Baseline\ F}{CSA}$, where "Baseline F" indicates force following stress relaxation (Figure 1) and "CSA" indicates fiber cross sectional area assuming elliptical shape. CSA=$\pi \times (\frac{dtop}{2} \times \frac{dside}{2})$, where "$d_{top}$" is the average of three top diameter measures, and "d_{side}" is the average of three side diameter measures. Strain was calculated as$\frac{\Delta L}{Lo}$, where "L_0" indicates initial length. Using raw stress data, passive Young's Modulus was calculated as the slope of the stress-strain relationship at shorter fiber lengths (strain = 1.0-1.24 %Lo) and at longer fiber lengths (strain = 1.32-1.56 %Lo). For fiber measures of passive modulus, separate slopes were calculated for shorter and longer fiber lengths to consider the length dependence of passive modulus measures. Stress decay index (SDI) was calculated as previously (Lim *et al.*, 2019): $(peak\ stress - stress) \times \frac{T1/2}{log2}$. Peak stress = $\frac{Peak\ force}{CSA}$ and $T_{1/2}$ = half-relax time (Figure 1). For tissue-level measures, passive Young's Modulus was calculated as one slope of the stress-strain curve, given the lack of a clear curvilinear inflection point such as that observed in the stress-strain data of the fibers. Then, the direction and magnitude of change in modulus between non-fatigued and fatigued CMT was calculated for each CMT sample as $\frac{F-NF\mu}{NF\mu}$, where "F" indicates the fatigued value for each individual CMT sample and "NF_{μ}" indicates the group mean of the non-fatigued CMT samples. For KI/KCl passive measures of CMT, passive modulus was calculated as one slope of the stress-strain curve.

Statistical Analyses: Statistical testing was conducted using SPSS software package (SPSS, IBM Corp., Armonk, NY, USA) unless otherwise specified. At each SL, differences in passive stress and SDI were evaluated using separate linear mixed models including fatigue, biological sex, training, and interaction terms and participant ID as a random effect. To evaluate differences in single fiber passive modulus at short and long lengths, a linear mixed model was run with fatigue, biological sex, training and interaction terms as fixed effects and participant ID as a random effect to account for fiber variation within individuals, as described previously (Callahan *et al.*, 2015*a*). To test for differences in maximally activated tension, a mixed effects model was run including sex, training, and fatigue as main effects and participant ID as a random effect. Of note, because MHC IIA fibers were similarly represented across all groups, all statistical analyses for single fiber mechanics included only MHC IIA fibers. While we were not well-positioned to perform statistical assessment for interactions with fiber type and other main effects (sex/fatigue) in our cohort (See Table 2), we considered this to be the most rigorous and conservative approach to test our hypotheses with respect to sex and fatigue, though we acknowledge it limits fiber number somewhat (206 fibers out of 423, total). To test for significant differences in the passive Young's Modulus of CMT samples, a linear mixed model was generated with biological sex and fatigue as fixed effects and participant as a random effect. Follow-up analyses tested for an effect of fatigue, with participants as a random effect, on passive modulus of CMT samples from males and females, separately. To test for fatigue-based differences in CMT passive modulus before and/or after KI/KCl treatment, means for the 4 fatigue/treatment groups (non-fatigued pre-KI/KCl, non-fatigued post- KI/KCl, fatigued pre- KI/KCl, fatigued post- KI/KCl) were compared in a univariate analysis of variance with least significance difference (LSD) post-hoc testing.

Results

Descriptive Measures: There were significant main effects of biological sex on height and weight such that males were taller than females (184.3 ± 8.6 vs. 161.6 ± 4.9 cm, respectively, $p<0.01$) and weighed more than females (81.3 ± 9.3 vs. 57.4 ± 5.2 kg, respectively, $p<0.01$, Table 1). There was no significant main effect of training on height ($p=0.691$) or weight ($p=0.997$). BMI was significantly higher in males versus females (23.9 ± 1.7 versus 22.0 ± 1.8 kg/m^2, respectively, $p=0.023$), but was not different between RT and UT participants ($p=0.463$). Regarding activity levels, RT participants exhibited higher step count (12505 ± 2823 vs. 7201 ± 2162 steps, respectively, $p<0.01$) and minutes in moderate physical activity (101.8 ± 19.3 vs. 54.0 ± 16.0 minutes, respectively, $p<0.01$). There was no effect of biological sex on step count ($p=0.928$) or time spent in moderate physical activity ($p=0.614$). There was no significant main effect of training status or biological sex on minutes in light physical activity ($p=0.090$ and 0.185, respectively) or minutes in vigorous physical activity ($p=0.183$ and $p=0.400$, respectively). In total, data were collected and analyzed for 424 fibers (Table 2). Single fiber CSA was greater in males versus females (0.0074 ± 0.0024 vs. 0.0050 ± 0.0016 mm^2, respectively, $p<0.01$) and greater in RT versus UT participants (0.0065 ± 0.0025 vs. 0.0055 ± 0.0019 mm^2, respectively, $p=0.047$). There was no effect of biological sex ($p=0.344$) or training ($p=0.484$) on fiber length. MHC isoform of individual fibers was determined using SDS-PAGE (Figure 2). Fiber type distribution differed between males and females such that females exhibited a greater

proportion of MHC I fibers than males (28% versus 6%, respectively). In both groups, MHC II (including IIA, IIX, and A/X) fibers comprised the majority of the sample (72% in females, 94% in males). Because MHC IIA fibers were similarly represented across all groups, all statistical analyses for single fiber mechanics included only MHC IIA fibers as mentioned above.

Table 11: Anthropometric and Activity Data of Included Participants.

		n	Height (cm) *	Weight (kg) *	BMI (kg/m^2) *	Step Count (steps/day) #	Light Activity (mins/day)	Moderate Activity (mins/day) #	Vigorous Activity (mins/day)
UT	**Female**	5	162.1 ± 6.1	55.0 ± 3.2	20.9 ± 0.6	7274±2162	27 ± 9	56 ± 18	0.5 ± 0.6
	Male	4	185.3 ± 13.0	84.0 ± 10.1	24.4 ± 1.2	7108±1525	38 ± 7	51 ± 15	1.1 ± 1.2
RT	**Female**	5	160.1 ± 3.9	60.0 ± 6.0	23.1 ± 2.1	12357±2531	40 ± 13	96 ± 16	5.0 ± 6.2
	Male	5	183.6 ± 4.5	79.1 ± 9.2	23.4 ± 2.1	12752±3864	43 ± 12	111 ± 24	1.5 ± 1.3

Symbols indicate a significant main effect of * biological sex or # training between groups ($p<0.05$). Data are shown as mean ± SD.

Table 2: Summary Statistics of Fibers Analyzed.

		n	CSA (mm^2) *,#	Length (mm)	Relative % MHC			
					I	IIA	IIX	IIA/X
UT	**Female**	107	0.0046 ± 0.0014	1.5 ± 0.4	22	47	2	22
	Male	92	0.0066 ± 0.0019	1.7 ± 0.4	3	49	23	24
RT	**Female**	128	0.0053 ± 0.0016	1.6 ± 0.6	34	47	2	12
	Male	97	0.0081 ± 0.0026	1.8 ± 0.5	9	55	2	34

Data are shown as mean ± SD. Percents are not reported for MHC I/IIA or I/IIA/IIX because they collectively made up only 3.1% of the overall dataset. Symbols indicate main effects of *biological sex or # training (all $p<0.05$).

Fatiguing exercise and whole-muscle contractile measures: Due to technical limitations related to data loss during transfer, time to fatigue, and knee extensor power measures are reported for 18/19 and and 16/19 volunteers, respectively. The average time to fatigue was not significantly different by training status ($p=0.453$) or biological sex ($p=0.559$). Similarly, there was no effect of training status ($p=0.415$) or biological sex (0.926) on fatigue ratio ($n=16$, Table 3). Absolute peak power was significantly higher in RT versus UT (608.35 ± 295.87 versus 413.84 ± 143.11 W, respectively, $p=0.017$) and male versus female (683.13 ± 238.86 versus 339.06 ± 70.27 W, respectively, $p<0.001$) participants. Relative peak power was significantly higher in RT versus UT (8.27 ± 2.58 versus 5.93 ± 1.09 W/kg, respectively, $p=0.002$) and male versus female (8.40 ± 2.60 versus 5.81 ± 0.64 W, respectively, $p=0.001$) participants. Absolute peak torque was significantly higher in RT versus UT (279.55 ± 102.78 versus 202.45 ± 79.51 N, respectively, $p=0.004$) and male versus female (327.32 ± 60.12 versus 167.16 ± 50.97 N, respectively, $p<0.001$) participants. Finally, relative peak torque was significantly higher in RT versus UT (3.91 ± 0.96 versus 2.90 ± 0.48 N/kg, respectively, $p=0.001$) and male versus female (4.06 ± 0.80 versus 2.87 ± 0.60 N/kg, respectively, $p<0.001$) participants.

Table 3: Fatigue data and whole-muscle performance

		Time to Fatigue (sec)	Fatigue Ratio	Peak Power (W) *#	Relative Peak Power (W/kg) *#	Peak Torque (N) *#	Relative Peak Torque (N/kg) *#
UT	**Female**	68±8.8	0.34±0.10	295±33	5.43±0.32	140±8	2.54±0.12
	Male	75±29	0.41±0.16	532±95	6.43±1.42	281±44	3.34±0.34
RT	**Female**	99±74	0.36±0.12	383±73	6.19±0.68	195±62	3.20±0.73
	Male	71±14	0.28±0.10	834±252	10.37±1.85	364±44	4.62±0.53

Symbols indicate a significant main effect of *biological sex or #training between groups ($p<0.05$). Data are shown as mean ± SD.

Maximal Isometric Tension: Considering the known impact of MHC isoform on active tension, and the relative balance in proportion of MHC IIA fibers across groups, maximally active isometric tension was analyzed in MHC IIA fibers only. There was no main effect of training ($p=0.219$), biological sex ($p=0.843$), or fatigue condition ($p=0.653$) on maximal isometric tension; however, the interaction between biological sex and fatigue was significant ($p=0.013$) such that maximal tension was reduced modestly (~5%) by fatiguing exercise in males (174.0 ± 37.7 vs. 164.7 ± 46.2 kPa, respectively $p=0.021$) but not females (178.1 ± 36.4 vs. 179.0 ± 37.1 kPa, respectively, $p=0.163$, Figure 3).

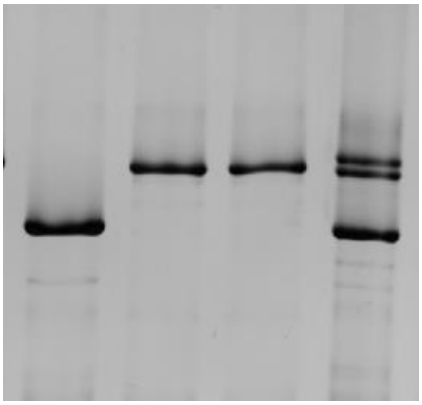

Figure 2: Sample image of silver-stained MHC bands. The left lane shows a fiber exhibiting MHC I isoform, the two middle bands exhibit MHC IIA isoform, and right lane contains a sample homogenate used to visualize all three (I, IIA, IIX) isoforms.

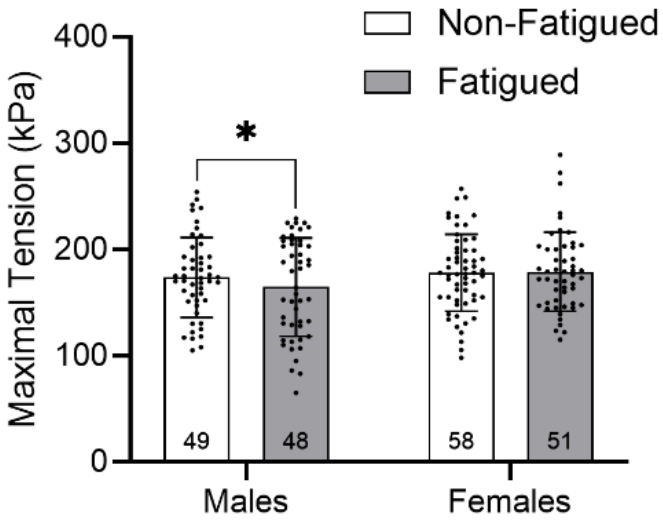

Figure 3: Active tension generation was assessed in MHC IIA fibers. There was no significant effect of training (p=0.219), biological sex (p=0.843), or fatigue condition (p=0.653) on active tension. Active tension was significantly reduced in fatigued fibers of males (p=0.013) but not females. Data are shown as mean ± SD.

Assessment of Passive Stretch Protocol: The difference between the measured stress and predicted stress, termed "missed stress", was calculated at each stretch step, for each fiber. Stress decay was greatest at SL=3.2-3.8 µm, suggesting the greatest potential for incomplete stress decay. At these lengths, measured stress was only different from predicted stress by 0.08-2.37%. Given this minimal variation, it is not likely that incomplete stress decay impacted the ability to draw meaningful conclusions from final measured stress, thus measured stress was used throughout.

Passive Stress: Passive stress was analyzed at each step of the passive stretch protocol. When all MHC IIA fibers were considered, passive stress was significantly different by fatigue (p=0.034 at SL=2.6 µm, p<0.01 at SL=2.8-3.8 µm), fatigue by training interactions (p= 0.049 at SL 2.6 µm, p= 0.038 at SL 2.8 µm, p= 0.028 at SL 3.0 µm, p= 0.023 at SL 3.2 µm, p= 0.017 at SL 3.4 µm, p= 0.013 at SL 3.6 µm, p=0.017 at SL 3.8 µm), and fatigue by sex interactions (p<0.01 at all SL, Figure 4A). When considering only non-fatigued fibers, passive stress was significantly higher in RT versus UT fibers at longer SL (p= 0.033 at SL 3.0 µm, p= 0.035 at SL 3.2 µm, p= 0.034 at SL 3.4 µm, p= 0.032 at SL 3.6 µm, p=0.034 at SL 3.8 µm, Figure 4B). There was no main effect of biological sex on passive stress in non-fatigued fibers, at any SL. In UT males (Figure 4C), passive stress was significantly lower in fatigued versus non-fatigued fibers at longer lengths (p= 0.032 at SL 3.0 µm, p= 0.018 at SL 3.2 µm, p= 0.018 at SL 3.4 µm, p= 0.010 at SL 3.6 µm, p<0.01 at SL 3.8 µm). In UT females (Figure 4D), passive stress was not significantly different by fatigue at any SL. Furthermore, in fibers from UT participants, the effect of fatiguing exercise on passive stress differed by biological sex at longer SL (p= 0.019 at SL 3.0 µm, p<0.01 at SL 3.2-3.8 µm). In RT males (Figure 4E), passive stress was significantly reduced by fatigue at all SL (p<0.01 at SL 2.6-3.8 µm) and the response of passive stress to fatigue was greater than that of UT males (interaction p= 0.018 at SL 2.6 µm, p<0.01at SL 2.8-3.0 µm, p= 0.010 at SL 3.2 µm, p<0.01 at SL 3.4-3.8 µm). In fibers from RT females (Figure 4F),

fatigue did not significantly affect passive stress at any SL, and the response of passive stress to fatiguing exercise was different from that of RT males at all SL ($p<0.01$ at SL 2.6-3.8 μm).

Passive Young's Modulus: Short Lengths. Analyses of passive modulus included only MHC IIA fibers. At short fiber lengths, passive modulus was significantly reduced by fatigue (19.5 ± 10.8 vs. 16.4 ± 8.3 kPa/%Lo, respectively, $p=0.006$, Figure 5A). The significant interaction between fatigue and training ($p=0.044$) prompted assessment of the effect of training on passive modulus at short lengths in non-fatigued and fatigued fibers, separately. As a result, passive modulus was significantly higher in RT versus UT non-fatigued fibers (22.6 ± 12.3 vs. 15.1 ± 6.1 kPa/%Lo, respectively, $p=0.031$) but not fatigued ($p=0.406$) fibers (Figure 5B). The interaction between fatigue and biological sex ($p<0.001$) was statistically significant, prompting post-hoc analysis via separate mixed models for males and females. These follow-up analyses revealed that passive modulus was significantly reduced by fatigue in males (23.4 ± 12.5 vs. 15.8 ± 9.2 kPa/%Lo, respectively, $p<0.001$) but not females (16.2 ± 7.9 vs. 16.9 ± 7.4 kPa/%Lo, respectively, $p= 0.380$). A significant fatigue x training interaction ($p=0.022$) in the male cohort prompted analysis of the fatigue effect in RT and UT males, separately. Passive modulus was significantly reduced by fatiguing exercise in fibers from RT (29.4 ± 13.3 vs. 19.1 ± 10.8 kPa/%Lo, respectively, $p <0.001$) and UT (15.4 ± 4.2 vs. 12.3 ± 5.3 kPa/%Lo, respectively, $p = 0.024$) males at short lengths (Figure 5C).

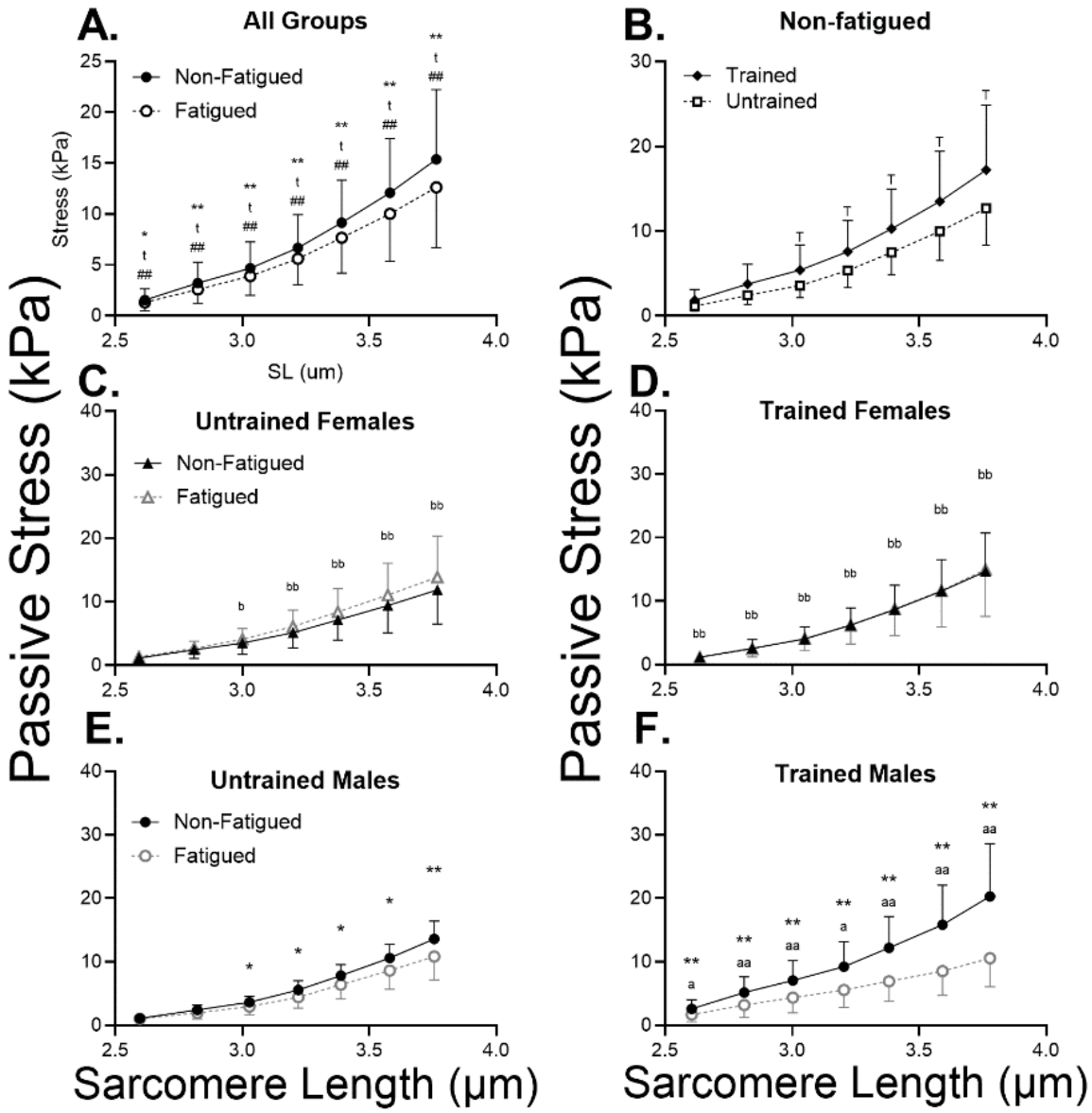

Figure 4: In the combined group, passive stress was significantly reduced at all sarcomere lengths, though the response was different by biological sex and training group **(A)** In non-fatigued fibers, passive stress was significantly higher in RT versus UT participants **(B)**. In UT participants, passive stress was significantly reduced by fatiguing exercise at SL=3.0-3.8 μm in males **(C)** but not females **(D)**, due to significant fatigue by sex interactions at these lengths. In RT participants, the effect of fatigue on passive stress was highly significant at all SL in males **(E)** but not in females **(F)**, due to the highly significant fatigue by sex interaction in this group. Furthermore, the response of passive stress to fatiguing exercise was different between RT and UT males. Data are shown as mean ± SD. Symbols indicate a significant effect of fatigue (* $p<0.05$ or ** $p<0.01$), fatigue by training interaction (^{t} $p<0.05$), fatigue by biological sex interaction ($^{\#}$ $p<0.05$ or $^{\#\#}p<0.01$), main effect of training ($^{T}p<0.05$), fatigue response different from that of UT (^{a} $p<0.05$ or ^{aa} $p<0.01$), fatigue response different from that of males (^{b} $p<0.05$ or ^{bb} $p<0.01$).

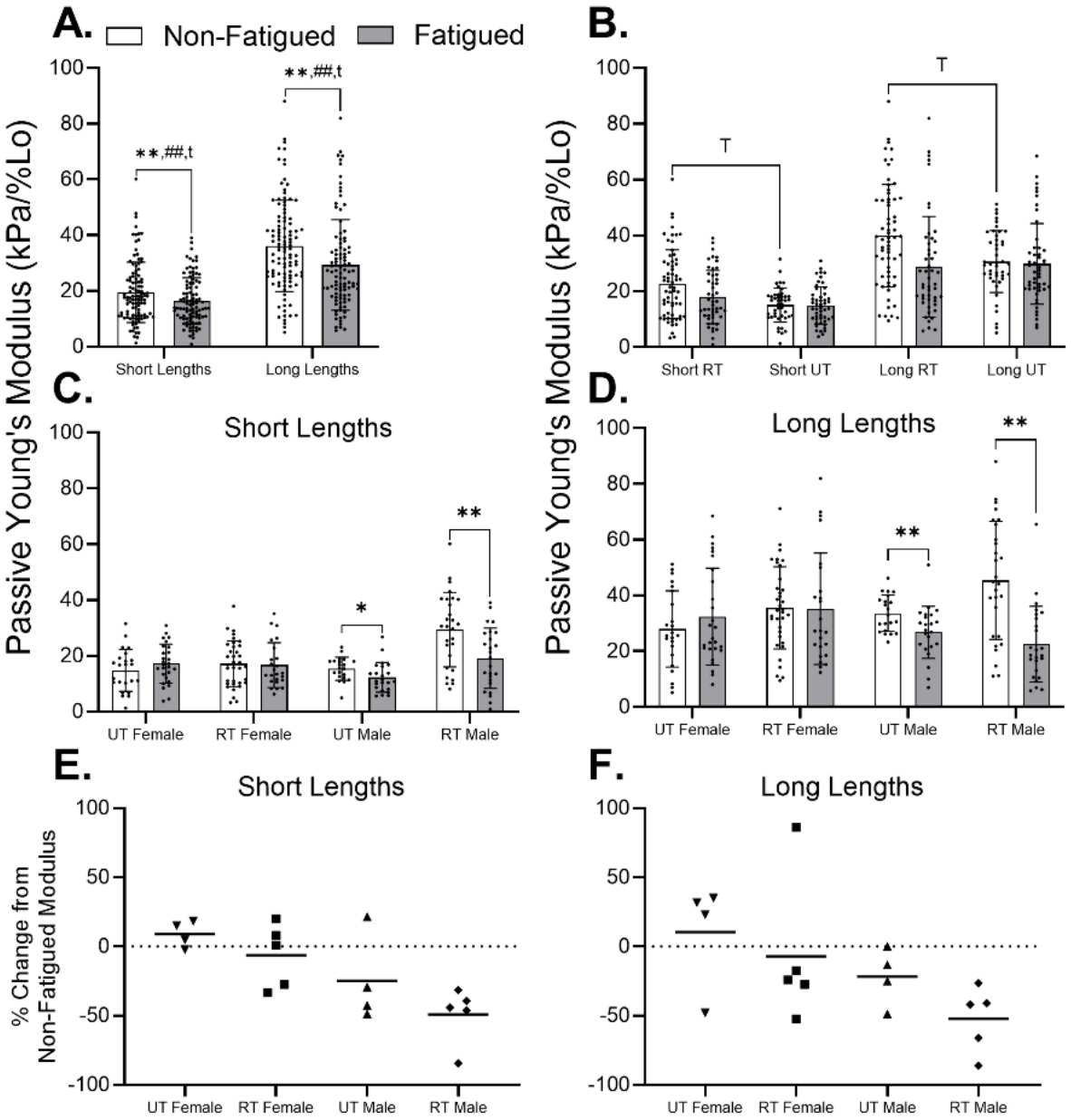

Figure 5: (A) Passive Young's Modulus was significantly reduced by fatiguing exercise at short and long lengths. Furthermore, the biological sex by fatigue and training by fatigue interactions were significant at short and long lengths. **(B)** In non-fatigued fibers, passive Young's Modulus was significantly greater in RT versus UT individuals at short and long lengths. At short **(C)** and long **(D)** SL, it becomes evident that reductions in passive modulus were driven by RT and UT males, but not females. On a per-individual basis, passive modulus was reduced in 9 of the 10 included males at short **(E)** and long **(F)** lengths. However, females exhibited little to no change in passive modulus at short lengths, and varied responses at long lengths. Data represent mean ± SD. Symbols indicate significant effect of fatigue (* $p<0.05$ or ** $p<0.01$), fatigue by training interaction (^{t} $p<0.05$), fatigue by biological sex interaction ($^{\#\#}$ $p<0.01$), or main effect of training (^{T} $p<0.05$).

Long Lengths. At long fiber lengths, passive modulus was significantly reduced by fatigue (36.1 ± 16.4 vs. 29.3 ± 16.2 kPa/%Lo, respectively, $p=0.004$, Figure 5A), and was significantly altered by interactions between biological sex and condition ($p<0.001$) and training and condition ($p=0.037$). Subsequent analyses revealed that training significantly increased passive modulus of non-fatigued (39.9 ± 18.4 vs. 30.6 ± 11.1 kPa/%Lo, respectively, $p=0.045$) but not fatigued ($p=0.925$) fibers (Figure 5B). Additionally, fatigue reduced passive modulus of fibers

from males (40.3 ± 17.4 vs. 24.6 ± 11.8 kPa/%Lo, respectively, p<0.001) but not females (p=0.296). Furthermore, the significant training x condition interaction in the male cohort revealed that passive modulus was significantly reduced by fatigue in RT (45.4 ± 21.2 vs. 22.6 ± 13.6 kPa/%Lo, respectively, p<0.001) and UT (33.6 ± 6.5 vs. 26.8 ± 9.3 kPa/%Lo, respectively, p=0.004) males at long lengths (Figure 5D). Figures 4E and 4F illustrate the individual responses, expressed as a percent difference between the passive modulus of non-fatigued fibers, and that of fatigued fibers. Although RT and UT males demonstrated reduced passive cellular modulus in fatigued versus non-fatigued fibers at short (Figure 5E) and long (Figure 5F) lengths, the response in females varied considerably by individual, especially at long lengths.

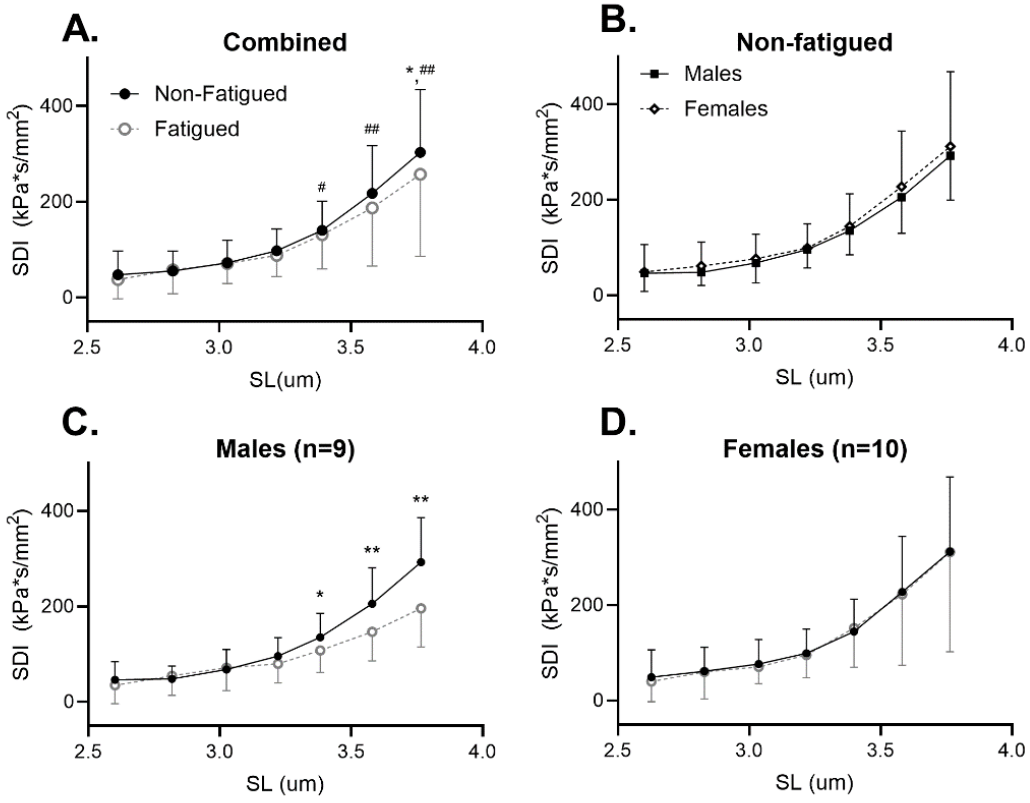

Figure 6: **(A)** In the combined dataset, neither biological sex nor training status had significant main effects on SDI at any SL. However, the biological sex by fatigue interaction was significant at SL=3.4 µm - 3.8µm, and fatigue significantly reduced SDI at SL=3.8 µm. **(B)** In non-fatigued fibers, there was no difference in SDI between males and females, at any SL. **(C)** Stress decay index was significantly reduced by fatiguing exercise at SL=3.4 µm - 3.8µm. **(D)** On the contrary, females did not exhibit changes in SDI resulting from fatiguing exercise at any SL. Data are shown as mean ± SD. Symbols indicate significant effect of fatigue (* p<0.05 or ** p<0.01) or fatigue by biological sex interaction ($^{\#}$ p<0.05 or $^{\#\#}$ p<0.01).

Stress Decay Index: There were no significant effects of biological sex (p= 0.657 at SL 2.6 µm, p= 0.437 at SL 2.8 µm, p= 0.968 at SL 3.0 µm, p= 0.530 at SL 3.2 µm, p= 0.193 at SL 3.4 µm, p= 0.419 at SL 3.6 µm, p=0.435 at SL 3.8 µm) or training (p= 0.452 at SL 2.6 µm, p= 0.500 at SL 2.8 µm, p= 0.752 at SL 3.0 µm, p= 0.429 at SL 3.2 µm, p= 0.269 at SL 3.4 µm, p= 0.706 at SL 3.6 µm, p=0.945 at SL 3.8 µm) on SDI at any SL. On the other hand, SDI was significantly reduced in fatigued versus non-fatigued fibers at SL 3.8 µm only (257.43 ± 171.75 vs. 303.08 ± 131.20 kPa*s/mm^2, p=0.034), but not at any other length (p= 0.079 at SL 2.6 µm, p= 0.656 at SL 2.8 µm, p= 0.704 at

SL 3.0 µm, p= 0.151 at SL 3.2 µm, p= 0.449 at SL 3.4 µm, p= 0.074 at SL 3.6 µm, Figure 6A). Furthermore, there were significant sex by fatigue interactions at SL = 3.4 µm (p=0.021), 3.6 µm (p=0.007), and 3.8 µm (p=0.001) but not at other SLs (p= 0.871 at SL 2.6 µm, p= 0.476 at SL 2.8 µm, p= 0.188 at SL 3.0 µm, p= 0.329 at SL 3.2 µm). As a result, the effect of fatigue on SDI was examined in males and females, separately, at these SLs. In non-fatigued fibers only, there were no differences in SDI between males and females, at any SL (p= 0.804 at SL 2.6 µm, p= 0.180 at SL 2.8 µm, p= 0.424 at SL 3.0 µm, p= 0.818 at SL 3.2 µm, p= 0.640 at SL 3.4 µm, p= 0.740 at SL 3.6 µm, p=0.902 at SL 3.8 µm, Figure 6B). In males, SDI was significantly reduced in fatigued versus non-fatigued fibers at SL = 3.2 µm (96.17 ± 38.49 versus 80.13 ± 39.91 kPa*s/mm2, respectively, p=0.027), SL = 3.4 µm (108.00 ± 46.54 versus 135.27 ± 50.31 kPa*s/mm^2, respectively, p=0.002), 3.6 µm (147.08 ± 61.32 versus 205.33 ± 75.27 kPa*s/mm2, respectively, p<0.001), and 3.8 µm (195.78 ± 81.11 versus 292.59 ± 92.99 kPa*s/mm2, respectively, p<0.001), but not at any other SLs (p= 0.133 at SL 2.6 µm, p= 0.257 at SL 2.8 µm, p= 0.189 at SL 3.0 µm, Figure 6C). However, fatigue had no effect on SDI at any SL in fibers from females (p= 0.326 at SL 2.6 µm, p= 0.781 at SL 2.8 µm, p= 0.469 at SL 3.0 µm, p= 0.698 at SL 3.2 µm, p= 0.394 at SL 3.4 µm, p= 0.564 at SL 3.6 µm, p=0.482 at SL 3.8 µm, Figure 6D).

To consider the underlying contributors to the fatigue-induced shift in SDI, we examined the measures that were used to calculate SDI: half-relaxation time, peak stress, and the magnitude of stress decay (peak stress – baseline stress). There were no significant differences in half-relaxation time due to fatiguing exercise, biological sex, or training at any SL (all p<0.05, Figure 7A). However, both peak stress and magnitude of stress decay were significantly different by fatigue, with significant interactions of biological sex by fatigue and training by fatigue. Specifically, peak stress was significantly different by fatigue (p=0.026 at SL=2.8 µm, p≤ 0.01 at SL=3.0-3.8 µm), fatigue by training interactions (p<0.01at SL 2.6, p=0.012 at SL 2.8 µm, p= 0.012 at SL 3.0 µm, p= 0.033 at SL 3.2 µm, p= 0.049 at SL 3.4 µm, p= 0.047 at SL 3.6 µm, p=0.026 at SL 3.8 µm), and fatigue by sex interactions (p=0.022 at SL=2.8 µm, p<0.01 at SL 3.0-3.8 µm, Figure 7B). Finally, the magnitude of stress decay was impacted by fatigue (p=0.030 at SL 3.4 µm, p=0.014 at SL 3.6 µm, p<0.01 at SL 3.8 µm), and the interaction of biological sex by fatigue (p=0.028 at SL 3.2 µm, p<0.01 at SL 3.4-3.8 µm) at long lengths, and by the interaction of training by fatigue at short lengths (p=0.023 at SL 2.6 µm, p=0.013 at SL 2.8 µm, p=0.042 at SL 3.0 µm, Figure 7C).

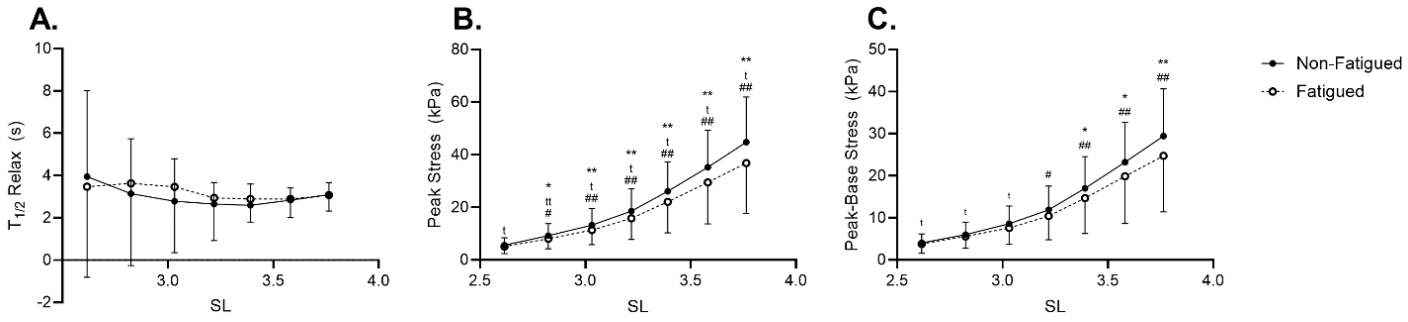

Figure 7: When considering the measures used to calculate SDI, half-relaxation time **(A)** is not impacted by fatiguing exercise. However, both peak stress **(B)** and the magnitude of stress decay **(C)** are reduced by fatiguing exercise with both measures demonstrating mediating effects of

biological sex and training status on the response to fatigue. Data are shown as mean ± SD. Symbols indicate significant effect of fatigue (* p<0.05 or ** p<0.01) fatigue by training interaction (^{t} p<0.05 or ^{tt} p<0.01), or fatigue by biological sex interaction ($^{\#}$ p<0.05 or $^{\#\#}$ p<0.01).

To test whether spontaneous actomyosin interactions while in relaxing (pCa 8.0) solution contributed to observed differences in SDI, fatigue differences in SDI were assessed in a subset of fibers, from 2 UT young males, were treated with 40mM of BDM. These BDM-treated fibers, SDI was significantly reduced in fatigued compared to non-fatigue fibers at SL = 3.4 µm (89.06 ± 19.52 versus 169.16 ± 66.95 kPa*s/mm2, respectively, p=0.009), 3.6 µm (115.40 ± 35.55 versus 260.22 ± 112.20 kPa*s/mm2, respectively, p=0.006), and 3.8 µm (197.54 ± 50.78 versus 425.61 ± 234.63 kPa*s/mm2, respectively, p=0.026, Figure 8), as was observed in non-treated fibers.

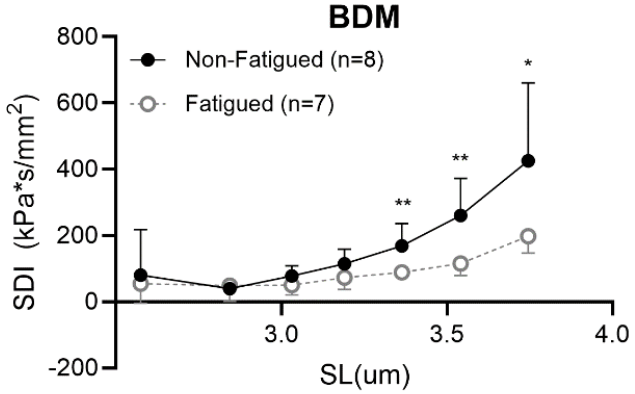

Figure 8: In BDM treated fibers from 2 UT males, fatigue induced differences in SDI persisted at SL 3.4-3.8 µm, suggesting that intracellular proteins other than myosin and actin contribute to this phenomenon. Data represent mean ± SD. Symbols indicate significant effect of fatigue (*, p<0.05 or **, p<0.01).

Tissue-level Measures: Due to the linearity of the stress-strain curve for tissue samples, passive Young's Modulus was quantified as the slope of the entire stress-strain curve for each sample studied. When the younger cohort was studied as a whole, there was no significant difference between modulus values of males and females (14.34 ± 9.67 vs. 25.91 ± 12.22 kPa/%Lo, respectively, p = 0.197) or of non-fatigued and fatigued samples (21.06 ± 11.67 vs. 23.93 ± 13.76 kPa/%Lo, respectively, p = 0.287). However, given the relatively limited sample in males versus females (26 vs. 58 bundles, respectively), a subsequent analysis tested the effect of fatigue condition on tissue passive modulus in females only. This sample was limited post-hoc by our desire to match bundle size across samples. While initially, sample size was matched across sex, we eliminated bundles from analyses that were 2 SD below or above or below the inclusive mean for CSA. This is due to recent evidence suggesting the dimension of tissue samples may influence passive modulus at the fibrillar and tissue level (Malakoutian *et al.*, 2021). Our restricted analysis revealed a modest but significant increase in passive modulus of the fatigued versus non-fatigued bundles (28.98 ± 12.85 vs. 23.57 ± 11.36 kPa/%Lo, p=0.036) in the female cohort but no difference in the males (NF: 15.13 ± 10.51, F: 13.42 ± 8.97 kPa/%Lo, p=0.735, Figure 9A). Notably, the same was found when a wider range of tissue sizes was included (data not shown). To assess whether cellular changes in passive modulus resulting from fatiguing exercise were associated with the same measures in CMT, average change in passive modulus were compared between fibers and CMT samples for each participant. Although values are clustered by biological sex,

and changes in fiber and CMT values with fatigue are consistent, the correlation between change in fiber modulus versus that of CMT was not significant (p=0.26, Figure 9B). Passive modulus was measured as the slope of the stress-strain curve produced by passive stretch of CMT from one RT female, before and after incubation in KI and KCl. Before treatment, passive modulus was significantly higher in fatigued versus non-fatigued CMT (30.78 ± 7.62 versus 23.59 ± 8.39 kPa/%Lo, respectively, p=0.025, Figure 9C). However, passive modulus following KI/KCl treatment was not different between fatigued (5.17 ± 3.13 kPa/%Lo) and non-fatigued (2.40 ± 1.88 kPa/%Lo) CMT (p=0.370). As anticipated, KI/KCl treatment significantly and dramatically reduced passive modulus of non-fatigued and fatigued fibers (p<0.001 for both).

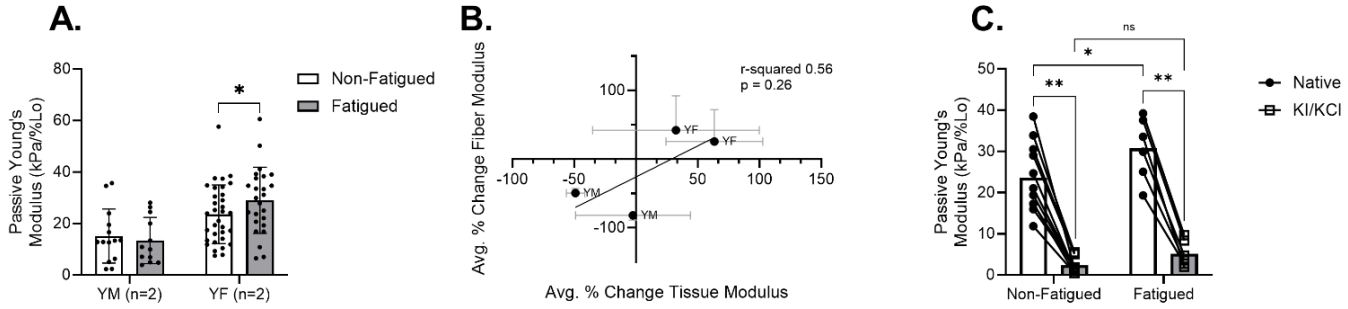

Figure 9: (A) Although tissue-level passive modulus was not affected by fatiguing exercise in the male cohort, it was significantly increased by fatiguing exercise in the female cohort (p=0.036). (B) The direction of change in passive modulus was similar between fibers and CMT for each participant, the correlation of change was insignificant. (B) Fatigue-induced differences in passive modulus were detected at the level of CMT, however, chemical elimination of intracellular contributors to passive modulus abolished the fatigue effect. Passive modulus was similarly reduced by treatment in fatigued and non-fatigued CMT. Each point represents one CMT sample, with lines connecting the pre-post treatment values. Symbols indicate fatigue difference (*, p<0.05 or **, p<0.001).

Discussion

Study sample. In the present group of participants, height, weight, and BMI were greater in males versus females (Table 1). Importantly, the step count and time spent in moderate activity per day was higher in the RT compared to UT participants (Table 1). What's more, measures of whole-muscle performance (Table 3) were higher in RT versus UT participants and in males versus females. However, there was no effect of biological sex or training on the duration of fatiguing exercise or the fatigue ratio, an index of the magnitude of fatigue (Table 3). Thus, it is unlikely that interactions between fatigue and biological sex or training are due to differences in the duration of fatiguing exercise or magnitude of in-vivo fatigue. Finally, although fiber-type distribution and fiber CSA differed across training and biological sex groups (Table 2), final analyses included only MHC IIA fibers and mechanics measures were reported normalized to CSA to minimize confounding effects on outcome measures. While limiting assessment to MHC IIA fibers somewhat limits our ability to make more broad generalizations about the applicability of our findings, we remain confident the phenomenon of fatigue-induced changes in muscle tissue mechanics reported here are durable across conditions. Indeed, inclusion of all measured fibers, regardless of fiber type (n = 423) added both statistical power and variability, such that conclusions related to the effect of fatiguing exercise on passive stress and Young's Modulus were not altered. However, variations by fiber type across conditions contributed significant variability that disrupted observed interactions between main effects of fatigue and training/sex. We sought to limit the potential for confounding interpretations based on different fiber pools

across groups by limiting our assessments by fiber type, to samples where MHC isoform was relatively equally represented across conditions (MHC IIA, see Table 2).

Cellular active mechanics. Active tension was not significantly different by biological sex or by training group. However, a significant fatigue by biological sex interaction revealed a modest yet significant reduction in active tension of fatigued versus non-fatigued fibers in males only (Figure 3) as has been previously observed (Privett *et al.*, 2021; Ricci *et al.*, 2023). One proposed explanation for this reduction is exercise induced PTM of sarcomere proteins involved in active contractile function. For example, slow skeletal myosin binding protein-C (ssMyBP-C), a thick filament regulatory protein that interacts with both the thick and thin filaments to regulate crossbridge formation (Yamamoto, 1986; Korte *et al.*, 2003; Robinett *et al.*, 2019) is phosphorylated by fatiguing exercise (Privett *et al.*, 2021; Ricci *et al.*, 2023). Whereas dephosphorylated ssMyBP-C is more likely to bind to both the thick and thin filaments, resulting in slowed crossbridge kinetics, phosphorylation releases this clutch-like mechanism, enhancing crossbridge kinetics (Colson, 2019; Robinett *et al.*, 2019). Therefore, it is plausible that accelerated crossbridge kinetics resulting from ssMyBP-C phosphorylation during fatiguing exercise may reduce force production. Though we can only speculate as to the mechanisms explaining reduced isometric tension of fatigued fibers in male participants, tension production in these fibers clearly demonstrates adequate function of all fibers included in the present analyses.

Chronic Training Increases Baseline Passive Stress and Young's Modulus at Longer Lengths. In non-fatigued fibers, passive stress (Figure 4B) and Young's modulus (Figure 5B) were higher in fibers from RT versus UT participants at longer SLs. This observation is consistent with previous work (Noonan *et al.*, 2020*a*), in which training was shown to modify cellular passive modulus in rodent skeletal muscle fibers in a training-modality-dependent manner. There is evidence that chronic training alters ECM-based stiffness in skeletal muscle (Kjær, 2004), yet this is unlikely to influence the cellular mechanics reported in this present study due to the use of chemically permeabilized skeletal muscle fibers, which no longer have intact ECM. Rather, it is more likely that intracellular proteins are responsible for the observed training effect on passive measures. The fact that training effects were observed at longer SLs (3.0-3.8μm), where overlap of thick and thin filaments is minimal, suggests that the sarcomere protein titin is at least partially involved. Differential expression of titin isoforms across participants have previously been reported (Fry *et al.*, 1997), presenting the possibility that training-induced shifts in titin isoform distribution may have contributed to the observed increase in passive stress or modulus in RT versus UT participants. Yet, existing literature does not support the notion of training-induced shifts in titin isoform (McGuigan *et al.*, 2003; Pellegrino *et al.*, 2016) or titin size (Noonan *et al.*, 2020*a*) in skeletal muscle. Nonetheless, 3 weeks of exercise training has been demonstrated to shift titin isoform in murine cardiac muscle (Hidalgo *et al.*, 2014) suggesting that the effect of exercise on titin isoform may be specific to training modality and muscle type. It is also possible that chronic training alters titin-based stiffness through changes to titin PTMs. Training-based differences in titin phosphorylation, a well-studied mediator of titin-based stiffness, have been observed in murine cardiac muscle (Hidalgo *et al.*, 2014). However, it is not yet known whether chronic training alters the phosphorylation background of titin in human skeletal muscle, and we did not report titin phosphorylation measures in the present study.

Although it is unclear how chronic training impacts skeletal muscle titin in humans, specifically, there is certainly a role for titin in skeletal muscle mechano-signaling and remodeling in response to exercise (Krüger & Kötter, 2016), supporting the notion that titin-based stiffness may adapt to a chronic training stimulus in order to better meet the demands of intense physical exercise.

Fatiguing Exercise Alters Cellular Passive Mechanics. In support of our initial hypothesis, fatiguing exercise significantly reduced both passive stress (Figure 4A) and Young's Modulus (Figure 5A) when all participants were considered collectively. Given that the effect of fatiguing exercise on passive stress and modulus was mediated by biological sex and training status, subsequent analyses examined training- and biological sex-based groups separately. As a result, it became clear that trained males had the most robust reduction in passive stress (Figure 4F) and modulus (Figure 5C-D) in fatigued versus non-fatigued fibers, yet untrained females exhibited a non-significant upward trend in passive stress (Figure 4C) and modulus (Figure 5D) in fatigued versus non-fatigued fibers. In all groups where a mean difference (even a non-significant one) in passive stress or modulus was observed between non-fatigued and fatigued fibers, the difference increased as SL increased. In fact, the difference in mean passive stress between fatigued and non-fatigued fibers was largest at longer SLs (~3.4μm and longer), where thick and thin filaments no longer overlap. Although the contribution of residual actomyosin interactions to cellular passive mechanical properties is possible, we have previously demonstrated that cellular passive modulus is still altered by fatiguing exercise in fibers treated with 2,3-butanedione monoxime (BDM), a myosin inhibitor, suggesting that residual crossbridge formation is not a primary mechanism of fatigue-induced changes to cellular passive mechanics (Privett *et al.*, 2024*a*). Rather, the fact that fatigue-induced differences are largest at longest lengths, where passive mechanics in permeabilized muscle fibers are predominantly titin-based, suggests that titin-based mechanisms may have contributed to these observations. Titin-based stiffness can be acutely regulated via PTM, and it is possible that exercise-induced small molecules such as inorganic phosphate (Müller *et al.*, 2014; Hamdani *et al.*, 2017), oxidative molecules (Alegre-Cebollada *et al.*, 2014), or heat shock proteins (Kötter *et al.*, 2014) bind to viscoelastic regions of titin during fatiguing exercise, thereby altering titin-based viscoelasticity.

We have previously reported altered titin phosphorylation following a single bout of fatiguing exercise (Privett *et al.*, 2024*a*), which may have implications for titin-based stiffness (Hamdani *et al.*, 2017). However, the specific response of titin-based stiffness to phosphorylation is highly dependent on the location at which the phosphorylation event occurs, as has been observed previously (Müller *et al.*, 2014). Separately, S-glutathionylation of cryptic binding sites of cardiac titin has been shown to inhibit titin Ig domain refolding, thereby reducing titin-based stiffness (Alegre-Cebollada *et al.*, 2014). In skeletal muscle, S-glutathionylation has been demonstrated to reduce passive force resulting from fiber stretch, yet the observed reductions were smaller than those observed in cardiac muscle (Watanabe *et al.*, 2020). However, oxidation events such as S-glutathionylation are not likely present in our sample due to the use of the antioxidant DTT in dissecting and relaxing solutions. Finally, it is possible that small HSPs generated during fatiguing exercise may bind to titin in a way that alters titin-based stiffness. Previous work reported the translocation of small HSPs, alphaβ-crystallin and HSP27, to the elastic regions of skeletal muscle titin (36). In the same study, the binding of these small HSPs in cardiac myocytes prevented acidification-based

aggregation of titin Ig domains and subsequent increases in titin-based stiffness. Our present study did not measure changes to titin PTMs, precluding the ability to draw conclusions regarding their contribution to the observed changes in passive stress and modulus. However, these passive measures were made in permeabilized single skeletal muscle fibers, suggesting the observed differences were at least in part due to a titin-based mechanism. Further studies in this area should seek to determine the where exercise-induced changes to titin phosphorylation occur along the titin protein (Privett *et al.*, 2024*a*) and should assess whether the binding of small HSPs to the elastic regions of skeletal muscle titin is altered by an acute bout of fatiguing exercise.

Biological Sex and Chronic Training Mediate the Effect of Fatiguing Exercise on Cellular Passive Stress and Young's Modulus. Neither the duration of fatiguing exercise nor the fatigue ratio differed by biological sex or training status; therefore, the sex- and training-based differences in response to fatiguing exercise are not likely explained by differences in performance of the fatiguing exercise itself (Table 3). Rather, the lack of a significant mean response in females was at least partially due to the variability among female participants (Figure 5E), especially at long lengths (Figure 5F). One potential explanation for this varied response might be sex-based differences in circulating levels of estrogen (Bell *et al.*, 2011, 2012; Ham *et al.*, 2020). Specifically, despite our efforts to minimize variability by collecting biopsy samples from the same point of the menstrual cycle (pre-follicular phase, n=5) or from participants using hormonal contraception (n=5), inter-individual differences in systemic estrogen may have contributed to differences in skeletal muscle mitochondrial function (Pellegrino *et al.*, 2022; Yoh *et al.*, 2023). Mitochondrial function can affect the concentration of heat shock proteins (Liu & Steinacker, 2001) and oxidative molecules such as glutathione (Marí *et al.*, 2009), both of which have the capacity to alter titin-based stiffness via PTM, in the sarcoplasm. Given the potential impact of varied blood estrogen concentration on intracellular mediators of skeletal muscle stiffness, future studies will seek to measure circulating estrogen concentration at the time of muscle biopsy.

The response of cellular passive mechanics was also mediated by training status. Although training-induced changes to skeletal muscle titin isoform are possible, there is no evidence for training-induced shifts in skeletal muscle titin in the literature (McGuigan *et al.*, 2003; Pellegrino *et al.*, 2016). However, training may modify the pattern of PTMs to titin. There is evidence that titin-based stiffness can be modified by phosphorylation (Hamdani *et al.*, 2017) and S-glutathionylation (Alegre-Cebollada *et al.*, 2014), yet there is no direct evidence suggesting that chronic training results in baseline changes to either. HSPs, on the other hand, have been demonstrated to increase in baseline expression following training (Morton *et al.*, 2009). Therefore, it is possible that HSPs exert a greater influence in the skeletal muscle of trained versus untrained young adults. For this reason, future studies should seek to measure HSP binding to titin in human VL samples.

Stress Decay Index. Although the incremental stretch protocol used here precludes the measurement of viscosity, per se, SDI is a useful proxy for assessing the impact of fatiguing exercise on VL viscoelasticity (Lim *et al.*, 2019). In the results reported here, there is a clear mediating effect of biological sex on the response of SDI to fatiguing exercise such that fatigue reduces SDI at longer SL in samples from males but not females (Figure 6). To interrogate the underlying contributors to fatigue-induced alteration to SDI, half-relaxation time, peak stress, and

magnitude of stress decay were analyzed (Figure 7). There was no effect of fatigue, biological sex, or training on half-relaxation time, suggesting that these factors did not impact the time course of stress decay. Rather, the peak stress and the magnitude of stress decay were both reduced in fatigued versus non-fatigued fibers, with mediating effects of training and/or biological sex on fatigue response in a length-dependent manner. In skeletal muscle myofibrils, viscoelastic behavior arises from titin immunoglobulin domain unfolding such that the amplitude of force decay increases as sarcomere length increases (Minajeva *et al.*, 2001), paralleling the results presented here (Figure 7C). The possibility that residual actomyosin binding interactions in our relaxing solution (pCa 8.0) may have contributed to the observed differences in SDI was considered. However, the effect of fatigue on SDI was still present in BDM-treated fibers (Figure 8), suggesting that actomyosin binding was unlikely to be a primary contributor to fatigue-induced differences in SDI. The present study design does not allow us to draw strong conclusions regarding the physiological importance of fatigue-induced changes to titin viscoelasticity to whole-muscle function. However, one previous study utilized a unique knock-out model targeting the PEVK region, a prominent contributor to cardiac viscoelasticity, to produce a 40% reduction in left ventricular chamber viscosity in the PEVK knock-out hearts (Chung *et al.*, 2011). Although it is important to acknowledge the potential muscle specificity of the mechanisms and physiological relevance of titin-based viscoelastic properties, this work highlights the potential role of titin in modulating whole-muscle viscoelasticity. As such, future studies should include methods to measure true viscosity of fatigued and non-fatigued muscle, perhaps in myofibrils to isolate the contributions of sarcomere proteins.

Contribution of intracellular proteins to tissue-level passive modulus. To consider the impact of altered cellular passive modulus on tissue-level measures following fatiguing exercise, CMT samples from one trained female were subjected to passive stretch measures (Figure 1) before and after treatment with KI and KCl to eliminate sarcomere thin and thick filaments, respectively. The removal of thick and thin filaments via KI/KCl is an established method that completely eliminates intracellular contributions to composite tissue stiffness (Ottenheijm *et al.*, 2012) in cardiac and skeletal muscle. Therefore, any remaining passive force measured following treatment is attributed to ECM. In the subset of CMT samples used for KI/KCl experiments, fatigued CMT exhibited higher passive modulus compared to non-fatigued CMT before treatment, similar to observations in single fibers from this same individual. This parallel response in fiber and CMT modulus to fatiguing exercise supports our interpretation that intracellular mediators of passive modulus contribute to passive mechanics at higher levels of organization, though we are unable to directly assess their relative contribution from the data presented here. In our KI/KCl assays, fatigue-induced differences in modulus were no longer evident following treatment to eliminate titin-based modulus (Figure 9C), suggesting that differences in fatigued versus non-fatigued passive modulus in CMT samples were dependent on intracellular mechanisms. Indeed, passive modulus following KI/KCl was dramatically reduced in all samples, highlighting the importance of intracellular mechanisms to CMT modulus in our preparation. Likewise, the correlation between relative difference in single fiber versus CMT passive modulus in fatigued versus non-fatigued sample was consistent with the idea that filamentous contributions to cellular stiffness may scale to CMT. However, these associations were not significant and are interpreted with some caution, given prior evidence that the inclusion of ECM (Mathewson *et al.*, 2014; Ward *et al.*, 2020) may override influences of the myofiber. Nevertheless,

previous studies of genetically modified murine muscle tissue have shown direct effects of titin on whole-muscle passive tension (Brynnel *et al.*, 2018), supporting the idea that alterations in titin mechanics may scale to the whole tissue level. Further study is required to determine how these changes scale with nonlinear mechanical properties when translating from in vitro cellular to in vivo tissue levels of organization (Ward *et al.*, 2020). With those caveats in mind, the data in the present manuscript contribute to a growing body of literature supporting the notion that intracellular mechanisms contribute to whole muscle tissue mechanics in vivo, encouraging further research into the potential magnitude and dynamic regulation of these effects.

Limitations

The present findings support earlier data (Privett *et al.*, 2024*a*) suggesting a sex-specific response to acute muscle fatigue that reduces viscoelasticity in males, but not females. These acute responses are observed regardless of the presence or absence of chronic effectors impacting viscoelasticity (physical training history; Figure 4B). Sex based differences in the dynamic response to acute physiological stressors is notable, but caution is warranted when attempting to extrapolate these findings to in vivo observations. Though we examined elastic modulus in CMT samples from a subset of volunteers and demonstrated the important role of fibrillar mechanics to tissue level behaviors (Figure 9C), we have not replicated our primary finding in CMT. Therefore, further experiments are required to explore how altered titin-based mechanics might impact muscle tissue that includes EMC and associated structures in vivo. Further, additional experiments are needed to clarify whether passive mechanics in permeabilized single fibers might reflect in vivo function when that function is critical for injury prevention or performance. Indeed, while a growing body of literature supports the notion that titin plays a critical role in stretch-shortening dynamics at the fiber level (Nishikawa *et al.*, 2013; Power *et al.*, 2013; Herzog, 2014; Herzog *et al.*, 2016; Nishikawa, 2016, 2020), it is not clear at present whether alterations observed here, under passive conditions, may impact performance during dynamic loading.

Conclusions

In conclusion, fatiguing exercise impacts cellular passive stress and Young's Modulus in a way that is mediated by training status and biological sex in young adults. Whereas trained and untrained young males demonstrated reduced passive stress and Young's Modulus in fatigued versus non-fatigued single fibers, neither trained nor untrained young females demonstrated a change in mean stress or Young's Modulus at any sarcomere length. However, a look at individual differences in mean Young's Modulus of fatigued versus non-fatigued fibers revealed that females exhibited a high degree of variability in the direction and magnitude of change in Young's Modulus. We speculate that inter-individual differences in circulating estrogen may have contributed to this variability; however, future studies will need to measure blood estrogen at time of study to support or refute this idea. Like passive stress and modulus, the effect of fatiguing exercise on cellular SDI was mediated by biological sex, with only males demonstrating significantly reduced SDI in fatigued versus non-fatigued fibers at SLs 3.4-3.8 μm due to changes in the magnitude of stress decay, rather than changes to the time course of stress decay. Finally, CMT assays suggest that although intracellular proteins appear to impact CMT passive modulus, their relative impact on the effect of fatiguing exercise on CMT passive mechanics is not yet clear.

Data availability statement
Supporting data in results are presented in the manuscript and included in figures. Additional data are available as supporting information published with the paper online.

Acknowledgements
The Authors wish to thank the volunteers for their invaluable contributions to our work. Additionally, thanks are due to Jordan Cooper, who provided valuable assistance in experimental assays and data analysis associated with the present study.

Funding
This research was supported by the Wu Tsai Human Performance Alliance and NIH R21AG077125-01A1.

Disclosures
The authors declare no competing interests, financial or otherwise.

Author Contributions
These experiments were conducted in the Muscle Cellular Biology Laboratory in the University of Oregon Human Physiology Department. G.E.P., A.W.R., K.W.N, and D.M.C. designed and performed experiments. G.E.P., A.W.R., K.W.N, and D.M.C. analyzed and interpreted study data and revised the manuscript. G.E.P. drafted the manuscript. D.M.C. conceived of and directed the study. All authors approved the final version of the manuscript and agree to be accountable for all aspects of the work in ensuring that questions related to the accuracy or integrity of any part of the work are appropriately investigated and resolved. All persons designated as authors qualify for authorship and all those who qualify for authorship are listed.

References

Aagaard P, Suetta C, Caserotti P, Magnusson SP & Kjær M (2010). Role of the nervous system in sarcopenia and muscle atrophy with aging: strength training as a countermeasure. *Scand J Med Sci Sports* **20,** 49–64.

Aas SN, Breit M, Karsrud S, Aase OJ, Rognlien SH, Cumming KT, Reggiani C, Seynnes O, Rossi AP & Toniolo L (2020). Musculoskeletal adaptations to strength training in frail elderly: a matter of quantity or quality? *J Cachexia Sarcopenia Muscle* **11,** 663–677.

Alegre-Cebollada J, Kosuri P, Giganti D, Eckels E, Rivas-Pardo JA, Hamdani N, Warren CM, Solaro RJ, Linke WA & Fernández JM (2014). S-Glutathionylation of Cryptic Cysteines Enhances Titin Elasticity by Blocking Protein Folding. *Cell* **156,** 1235–1246.

Allan CA & McLachlan RI (2004). Age-related changes in testosterone and the role of replacement therapy in older men. *Clin Endocrinol (Oxf)*. Available at: https://www.academia.edu/download/72156275/j.1365-2265.2004.02002.x20211010-19216-24fokt.pdf [Accessed September 3, 2024].

Andonian P, Viallon M, Le Goff C, de Bourguignon C, Tourel C, Morel J, Giardini G, Gergele L, Millet GP & Croisille P (2016). Shear-wave elastography assessments of quadriceps stiffness changes prior to, during and after prolonged exercise: a longitudinal study during an extreme mountain ultra-marathon. *PLoS One* **11,** e0161855.

Arendt EA, Agel J & Dick R (1999). Anterior Cruciate Ligament Injury Patterns Among Collegiate Men and Women. *J Athl Train* **34,** 86–92.

Azizi E & Roberts TJ (2010). Muscle performance during frog jumping: influence of elasticity on muscle operating lengths. *Proc R Soc B Biol Sci* **277,** 1523–1530.

Beckendorf L & Linke WA (2015). Emerging importance of oxidative stress in regulating striated muscle elasticity. *J Muscle Res Cell Motil* **36,** 25–36.

Bell DR, Blackburn JT, Norcorss MF, Ondrak KS, Hudson JD, Hackney AC & Padua DA (2012). Estrogen and muscle stiffness have a negative relationship in females. *Knee Surg Sports Traumatol Arthrosc* **20,** 361–367.

Bell DR, Blackburn JT, Ondrak KS, Hackney AC, Hudson JD, Norcross MF & Padua DA (2011). The effects of oral contraceptive use on muscle stiffness across the menstrual cycle. *Clin J Sport Med* **21,** 467–473.

Blackburn JT, Norcross MF & Padua DA (2011). Influences of hamstring stiffness and strength on anterior knee joint stability. *Clin Biomech* **26,** 278–283.

Blazevich AJ (2019). Adaptations in the passive mechanical properties of skeletal muscle to altered patterns of use. *J Appl Physiol* **126,** 1483–1491.

Bouillard K, Jubeau M, Nordez A & Hug F (2014). Effect of vastus lateralis fatigue on load sharing between quadriceps femoris muscles during isometric knee extensions. *J Neurophysiol* **111,** 768–776.

Brynnel A, Hernandez Y, Kiss B, Lindqvist J, Adler M, Kolb J, Van der Pijl R, Gohlke J, Strom J & Smith J (2018). Downsizing the molecular spring of the giant protein titin reveals that skeletal muscle titin determines passive stiffness and drives longitudinal hypertrophy. *Elife* **7,** e40532.

Bupha-Intr T, Oo YW & Wattanapermpool J (2011). Increased myocardial stiffness with maintenance of length-dependent calcium activation by female sex hormones in diabetic rats. *Am J Physiol-Heart Circ Physiol* **300,** H1661–H1668.

Burkholder TJ & Lieber RL (2001). Sarcomere length operating range of vertebrate muscles during movement. *J Exp Biol* **204,** 1529–1536.

Callahan DM & Kent-Braun JA (2011). Effect of old age on human skeletal muscle force-velocity and fatigue properties. *J Appl Physiol* **111,** 1345–1352.

Callahan DM, Tourville TW, Miller MS, Hackett SB, Sharma H, Cruickshank NC, Slauterbeck JR, Savage PD, Ades PA & Maughan DW (2015*a*). Chronic disuse and skeletal muscle structure in older adults: sex-specific differences and relationships to contractile function. *Am J Physiol-Cell Physiol* **308,** C932–C943.

Callahan DM, Tourville TW, Slauterbeck JR, Ades PA, Stevens-Lapsley J, Beynnon BD & Toth MJ (2015*b*). Reduced rate of knee extensor torque development in older adults with knee osteoarthritis is associated with intrinsic muscle contractile deficits. *Exp Gerontol* **72,** 16–21.

Campbell KS & Lakie M (1998). A cross-bridge mechanism can explain the thixotropic short-range elastic component of relaxed frog skeletal muscle. *J Physiol* **510,** 941–962.

Campbell MJ, McComas AJ & Petito F (1973). Physiological changes in ageing muscles. *J Neurol Neurosurg Psychiatry* **36,** 174–182.

de Campos D, Orssatto LBR, Trajano GS, Herzog W & Fontana H de B (2022). Residual force enhancement in human skeletal muscles: A systematic review and meta-analysis. *J Sport Health Sci* **11,** 94–103.

Casey A, Constantin-Teodosiu D, Howell S, Hultman E & Greenhaff PL (1996). Metabolic response of type I and II muscle fibers during repeated bouts of maximal exercise in humans. *Am J Physiol-Endocrinol Metab* **271,** E38–E43.

Cawthon PM, Fox KM, Gandra SR, Delmonico MJ, Chiou C-F, Anthony MS, Sewall A, Goodpaster B, Satterfield S & Cummings SR (2009). Do muscle mass, muscle density, strength, and physical function similarly influence risk of hospitalization in older adults? *J Am Geriatr Soc* **57,** 1411–1419.

Chalchat E, Gennisson J-L, Peñailillo L, Oger M, Malgoyre A, Charlot K, Bourrilhon C, Siracusa J & Garcia-Vicencio S (2020). Changes in the viscoelastic properties of the vastus lateralis muscle with fatigue. *Front Physiol* **11,** 307.

Chapman N, Whitting J, Broadbent S, Crowley-McHattan Z & Meir R (2018). Residual force enhancement in humans: a systematic review. *J Appl Biomech* **34,** 240–248.

Chidi-Ogbolu N & Baar K (2019). Effect of Estrogen on Musculoskeletal Performance and Injury Risk. *Front Physiol*. Available at: https://www.frontiersin.org/article/10.3389/fphys.2018.01834 [Accessed May 5, 2022].

Chung CS, Methawasin M, Nelson OL, Radke MH, Hidalgo CG, Gotthardt M & Granzier HL (2011). Titin Based Viscosity in Ventricular Physiology: An Integrative Investigation of PEVK-Actin Interactions. *J Mol Cell Cardiol* **51,** 428–434.

Collins BC, Laakkonen EK & Lowe DA (2019). Aging of the Musculoskeletal System: How the Loss of Estrogen Impacts Muscle Strength. *Bone* **123,** 137–144.

Colson BA (2019). What a drag!: Skeletal myosin binding protein-C affects sarcomeric shortening. *J Gen Physiol* **151,** 614–618.

Cross KM, Gurka KK, Saliba S, Conaway M & Hertel J (2013). Comparison of hamstring strain injury rates between male and female intercollegiate soccer athletes. *Am J Sports Med* **41,** 742–748.

Dalton SL, Kerr ZY & Dompier TP (2015). Epidemiology of Hamstring Strains in 25 NCAA Sports in the 2009-2010 to 2013-2014 Academic Years. *Am J Sports Med* **43,** 2671–2679.

D'Antona G, Pellegrino MA, Carlizzi CN & Bottinelli R (2007). Deterioration of contractile properties of muscle fibres in elderly subjects is modulated by the level of physical activity. *Eur J Appl Physiol* **100,** 603–611.

De Ste Croix MBA, Priestley AM, Lloyd RS & Oliver JL (2015). ACL injury risk in elite female youth soccer: Changes in neuromuscular control of the knee following soccer-specific fatigue. *Scand J Med Sci Sports* **25,** e531–e538.

Debold E (2012). Recent Insights into Muscle Fatigue at the Cross-Bridge Level. *Front Physiol*. Available at: https://www.frontiersin.org/article/10.3389/fphys.2012.00151 [Accessed April 27, 2022].

Debold EP, Fitts RH, Sundberg CW & Nosek TM (2016). Muscle Fatigue from the Perspective of a Single Crossbridge. *Med Sci Sports Exerc* **48,** 2270–2280.

Deitch JR, Starkey C, Walters SL & Moseley JB (2006). Injury Risk in Professional Basketball Players: A Comparison of Women's National Basketball Association and National Basketball Association Athletes. *Am J Sports Med* **34,** 1077–1083.

Doran P, Gannon J, O'Connell K & Ohlendieck K (2007). Aging skeletal muscle shows a drastic increase in the small heat shock proteins *α*B-crystallin/HspB5 and cvHsp/HspB7. *Eur J Cell Biol* **86,** 629–640.

Dowd KP, Harrington DM & Donnelly AE (2012). Criterion and Concurrent Validity of the activPAL^{TM} Professional Physical Activity Monitor in Adolescent Females. *PLOS ONE* **7,** e47633.

Dubois V, Laurent M, Boonen S, Vanderschueren D & Claessens F (2012). Androgens and skeletal muscle: cellular and molecular action mechanisms underlying the anabolic actions. *Cell Mol Life Sci* **69,** 1651–1667.

Ducomps C, Mauriège P, Darche B, Combes S, Lebas F & Doutreloux JP (2003). Effects of jump training on passive mechanical stress and stiffness in rabbit skeletal muscle: role of collagen. *Acta Physiol Scand* **178,** 215–224.

Dutta S, Tsiros C, Sundar SL, Athar H, Moore J, Nelson B, Gage MJ & Nishikawa K (2018). Calcium increases titin N2A binding to F-actin and regulated thin filaments. *Sci Rep* **8,** 14575.

Eby SF, Cloud BA, Brandenburg JE, Giambini H, Song P, Chen S, LeBrasseur NK & An K-N (2015). Shear wave elastography of passive skeletal muscle stiffness: Influences of sex and age throughout adulthood. *Clin Biomech* **30,** 22–27.

Ford GA, Dachman WD, Blaschke TF & Hoffman BB (1995). Effect of aging on beta 2-adrenergic receptor-stimulated flux of K+, PO4, FFA, and glycerol in human forearms. *J Appl Physiol* **78,** 172–178.

Franse CB, Rietjens JA, Burdorf A, Grieken A van, Korfage IJ, Heide A van der, Raso FM, Beeck E van & Raat H (2017). A prospective study on the variation in falling and fall risk among community-dwelling older citizens in 12 European countries. *BMJ Open* **7,** e015827.

Franssen C, Kole J, Musters R, Hamdani N & Paulus WJ (2017). α-B Crystallin Reverses High Diastolic Stiffness of Failing Human Cardiomyocytes. *Circ Heart Fail* **10,** e003626.

Frontera WR & Ochala J (2015). Skeletal muscle: a brief review of structure and function. *Calcif Tissue Int* **96,** 183–195.

Fry A c., Staron R s., James C b. l., Hikida R s. & Hagerman F c. (1997). Differential titin isoform expression in human skeletal muscle. *Acta Physiol Scand* **161,** 473–479.

Fukuda N, Wu Y, Nair P & Granzier HL (2005). Phosphorylation of titin modulates passive stiffness of cardiac muscle in a titin isoform-dependent manner. *J Gen Physiol* **125,** 257–271.

Gajdosik RL (2001). Passive extensibility of skeletal muscle: review of the literature with clinical implications. *Clin Biomech* **16,** 87–101.

Gannon J, Staunton L, O'Connell K, Doran P & Ohlendieck K (2008). Phosphoproteomic analysis of aged skeletal muscle. *Int J Mol Med* **22,** 33–42.

Gleim GW & McHugh MP (1997). Flexibility and Its Effects on Sports Injury and Performance: *Sports Med* **24,** 289–299.

Godt RE & Maughan DW (1977). Swelling of Skinned Muscle Fibers of the Frog.

González B, Negredo P, Hernando R & Manso R (2002). Protein variants of skeletal muscle regulatory myosin light chain isoforms: prevalence in mammals, generation and transitions during muscle remodelling. *Pflüg Arch - Eur J Physiol* **443,** 377–386.

Granzier HL, Hutchinson KR, Tonino P, Methawasin M, Li FW, Slater RE, Bull MM, Saripalli C, Pappas CT, Gregorio CC & Smith JE (2014). Deleting titin's I-band/A-band junction reveals critical roles for titin in biomechanical sensing and cardiac function. *Proc Natl Acad Sci* **111,** 14589–14594.

Granzier HL & Irving TC (1995). Passive tension in cardiac muscle: contribution of collagen, titin, microtubules, and intermediate filaments. *Biophys J* **68,** 1027–1044.

Ham S, Kim S, Choi H, Lee Y & Lee H (2020). Greater muscle stiffness during contraction at menstruation as measured by shear-wave elastography. *Tohoku J Exp Med* **250,** 207–213.

Hamdani N, Herwig M & Linke WA (2017). Tampering with springs: phosphorylation of titin affecting the mechanical function of cardiomyocytes. *Biophys Rev* **9,** 225–237.

Hamdani N, Krysiak J, Kreusser MM, Neef S, Dos Remedios CG, Maier LS, Krüger M, Backs J & Linke WA (2013). Crucial role for Ca2+/calmodulin-dependent protein kinase-II in regulating diastolic stress of normal and failing hearts via titin phosphorylation. *Circ Res* **112,** 664–674.

Hansen M & Kjaer M (2016). Sex hormones and tendon. *Metab Influ Risk Tendon Disord*139–149.

Hegarty PV & Hooper AC (1971). Sarcomere length and fibre diameter distributions in four different mouse skeletal muscles. *J Anat* **110,** 249.

Herzog J, Leonard TR, Jinha A & Herzog W (2015). Titin Hysteresis is Greater for Actively Lengthened Compared to Passively Lengthened Skeletal Muscle Sarcomeres. *Biophys J* **108,** 460a.

Herzog W (2014). The role of titin in eccentric muscle contraction. *J Exp Biol* **217,** 2825–2833.

Herzog W, Schappacher G, DuVall M, Leonard TR & Herzog JA (2016). Residual force enhancement following eccentric contractions: a new mechanism involving titin. *Physiology* **31,** 300–312.

Hidalgo C, Saripalli C & Granzier HL (2014). Effect of exercise training on post-translational and post-transcriptional regulation of titin stiffness in striated muscle of wild type and IG KO mice. *Arch Biochem Biophys* **552–553,** 100–107.

Hidalgo Carlos, Hudson Bryan, Bogomolovas Julius, Zhu Yi, Anderson Brian, Greaser Marion, Labeit Siegfried, & Granzier Henk (2009). PKC Phosphorylation of Titin's PEVK Element. *Circ Res* **105,** 631–638.

Hvid LG, Brocca L, Ørtenblad N, Suetta C, Aagaard P, Kjaer M, Bottinelli R & Pellegrino MA (2017). Myosin content of single muscle fibers following short-term disuse and active recovery in young and old healthy men. *Exp Gerontol* **87,** 100–107.

Hvid LG, Ørtenblad N, Aagaard P, Kjaer M & Suetta C (2011). Effects of ageing on single muscle fibre contractile function following short-term immobilisation. *J Physiol* **589,** 4745–4757.

Hvid LG, Suetta C, Aagaard P, Kjaer M, Frandsen U & Ørtenblad N (2013). Four days of muscle disuse impairs single fiber contractile function in young and old healthy men. *Exp Gerontol* **48,** 154–161.

Ismail C, Zabal J, Hernandez HJ, Woletz P, Manning H, Teixeira C, DiPietro L, Blackman MR & Harris-Love MO (2015). Diagnostic ultrasound estimates of muscle mass and muscle quality discriminate between women with and without sarcopenia. *Front Physiol* **6,** 302.

Johansson J, Morseth B, Scott D, Strand BH, Hopstock LA & Grimsgaard S (2021). Moderate-to-vigorous physical activity modifies the relationship between sedentary time and sarcopenia: the Tromsø Study 2015–2016. *J Cachexia Sarcopenia Muscle* **12,** 955–963.

Joumaa V, Rassier DE, Leonard TR & Herzog W (2008). The origin of passive force enhancement in skeletal muscle. *Am J Physiol-Cell Physiol* **294,** C74–C78.

Kennedy P, Barnhill E, Gray C, Brown C, van Beek EJR, Roberts N & Greig CA (2020). Magnetic resonance elastography (MRE) shows significant reduction of thigh muscle stiffness in healthy older adults. *GeroScience* **42,** 311–321.

Kernozek TW, Torry MR & Iwasaki M (2008). Gender differences in lower extremity landing mechanics caused by neuromuscular fatigue. *Am J Sports Med* **36,** 554–565.

Kitajima Y & Ono Y (2016). Estrogens maintain skeletal muscle and satellite cell functions. *J Endocrinol* **229,** 267–275.

Kjær M (2004). Role of Extracellular Matrix in Adaptation of Tendon and Skeletal Muscle to Mechanical Loading. *Physiol Rev* **84,** 649–698.

Klinge K, Magnusson SP, Simonsen EB, Aagaard P, Klausen K & Kjaer M (1997). The Effect of Strength and Flexibility Training on Skeletal Muscle Electromyographic Activity, Stiffness, and Viscoelastic Stress Relaxation Response. *Am J Sports Med* **25,** 710–716.

Konopka JA, Hsue LJ & Dragoo JL (2019). Effect of Oral Contraceptives on Soft Tissue Injury Risk, Soft Tissue Laxity, and Muscle Strength: A Systematic Review of the Literature. *Orthop J Sports Med* **7,** 2325967119831061.

Kooij V, Holewinski RJ, Murphy AM & Van Eyk JE (2013). Characterization of the cardiac myosin binding protein-C phosphoproteome in healthy and failing human hearts. *J Mol Cell Cardiol* **60,** 116–120.

Korte FS, McDonald KS, Harris SP & Moss RL (2003). Loaded Shortening, Power Output, and Rate of Force Redevelopment Are Increased With Knockout of Cardiac Myosin Binding Protein-C. *Circ Res* **93,** 752–758.

Kötter S, Unger A, Hamdani N, Lang P, Vorgerd M, Nagel-Steger L & Linke WA (2014). Human myocytes are protected from titin aggregation-induced stiffening by small heat shock proteins. *J Cell Biol* **204,** 187–202.

Krüger M & Kötter S (2016). Titin, a Central Mediator for Hypertrophic Signaling, Exercise-Induced Mechanosignaling and Skeletal Muscle Remodeling. *Front Physiol*. Available at: https://www.frontiersin.org/article/10.3389/fphys.2016.00076 [Accessed March 28, 2022].

Krüger M, Kötter S, Grützner A, Lang P, Andresen C, Redfield MM, Butt E, Dos Remedios CG & Linke WA (2009). Protein kinase G modulates human myocardial passive stiffness by phosphorylation of the titin springs. *Circ Res* **104,** 87–94.

Krüger M & Linke WA (2006*a*). Protein kinase-A phosphorylates titin in human heart muscle and reduces myofibrillar passive tension. *J Muscle Res Cell Motil* **27,** 435–444.

Krüger M & Linke WA (2006*b*). Protein kinase-A phosphorylates titin in human heart muscle and reduces myofibrillar passive tension. *J Muscle Res Cell Motil* **27,** 435–444.

Krysiak J, Unger A, Beckendorf L, Hamdani N, von Frieling-Salewsky M, Redfield MM, Dos Remedios CG, Sheikh F, Gergs U & Boknik P (2018). Protein phosphatase 5 regulates titin phosphorylation and function at a sarcomere-associated mechanosensor complex in cardiomyocytes. *Nat Commun* **9,** 1–14.

Kubo K & Ikebukuro T (2019). Changes in joint, muscle, and tendon stiffness following repeated hopping exercise. *Physiol Rep*; DOI: 10.14814/phy2.14237.

Kubo K, Kanehisa H & Fukunaga T (2003). Gender differences in the viscoelastic properties of tendon structures. *Eur J Appl Physiol* **88,** 520–526.

Kubo K, Kanehisa H, Kawakami Y & Fukunaga T (2001). Effects of repeated muscle contractions on the tendon structures in humans. *Eur J Appl Physiol* **84,** 162–166.

Lai S, Collins BC, Colson BA, Kararigas G & Lowe DA (2016). Estradiol modulates myosin regulatory light chain phosphorylation and contractility in skeletal muscle of female mice. *Am J Physiol-Endocrinol Metab* **310,** E724–E733.

Lanza IR, Larsen RG & Kent-Braun JA (2007). Effects of old age on human skeletal muscle energetics during fatiguing contractions with and without blood flow. *J Physiol* **583,** 1093–1105.

Leonard TR, DuVall M & Herzog W (2010). Force enhancement following stretch in a single sarcomere. *Am J Physiol-Cell Physiol* **299,** C1398–C1401.

LeWinter MM & Granzier HL (2014). Cardiac Titin and Heart Disease. *J Cardiovasc Pharmacol* **63,** 207–212.

Lexell J, Taylor C & Sjostrom M (1988). What is the cause of the ageing atrophy? Total number, size and proportion of different fiber types studied in whole vastus lateralis muscle from 15- to 83-year-old men. *J Neurol Sci* **84,** 275–294.

Lexell J & Taylor CC (1991). Variability in muscle fibre areas in whole human quadriceps muscle: effects of increasing age. *J Anat* **174,** 239–249.

Lieber RL & Binder-Markey BI (2021). Biochemical and structural basis of the passive mechanical properties of whole skeletal muscle. *J Physiol* **599,** 3809–3823.

Lim J-Y, Choi SJ, Widrick JJ, Phillips EM & Frontera WR (2019). Passive force and viscoelastic properties of single fibers in human aging muscles. *Eur J Appl Physiol* **119,** 2339–2348.

Linke WA & Grützner A (2008). Pulling single molecules of titin by AFM—recent advances and physiological implications. *Pflüg Arch-Eur J Physiol* **456,** 101–115.

Linke WA & Hamdani N (2014). Gigantic business: titin properties and function through thick and thin. *Circ Res* **114,** 1052–1068.

Liu Y & Steinacker JM (2001). Changes in skeletal muscle heat shock proteins: pathological significance. *Front Biosci* **6,** D12–D25.

Lynch GS & Ryall JG (2008). Role of β-Adrenoceptor Signaling in Skeletal Muscle: Implications for Muscle Wasting and Disease. *Physiol Rev* **88,** 729–767.

Magnusson SP (1998). Passive properties of human skeletal muscle during stretch maneuvers. *Scand J Med Sci Sports* **8,** 65–77.

Mair SD, Seaber AV, Glisson RR & Garrett WE (1996). The Role of Fatigue in Susceptibility to Acute Muscle Strain Injury. *Am J Sports Med* **24,** 137–143.

Malakoutian M, Theret M, Yamamoto S, Dehghan-Hamani I, Lee M, Street J, Rossi F, Brown SHM & Oxland TR (2021). Larger muscle fibers and fiber bundles manifest smaller elastic modulus in paraspinal muscles of rats and humans. *Sci Rep* **11,** 18565.

Marcucci L, Bondì M, Randazzo G, Reggiani C, Natali AN & Pavan PG (2019). Fibre and extracellular matrix contributions to passive forces in human skeletal muscles: An experimental based constitutive law for numerical modelling of the passive element in the classical Hill-type three element model. *PLoS One* **14,** e0224232.

Marcucci L & Reggiani C (2020). Increase of resting muscle stiffness, a less considered component of age-related skeletal muscle impairment. *Eur J Transl Myol*.

Marí M, Morales A, Colell A, García-Ruiz C & Fernández-Checa JC (2009). Mitochondrial Glutathione, a Key Survival Antioxidant. *Antioxid Redox Signal* **11,** 2685–2700.

Mathewson MA, Chambers HG, Girard PJ, Tenenhaus M, Schwartz AK & Lieber RL (2014). Stiff muscle fibers in calf muscles of patients with cerebral palsy lead to high passive muscle stiffness. *J Orthop Res* **32,** 1667–1674.

Matzkin E & Garvey K (2019). Sex Differences in Common Sports-Related Injuries. *NASN Sch Nurse* **34,** 266–269.

McGuigan MR, Sharman MJ, Newton RU, Davie AJ, Murphy AJ & McBride JM (2003). Effect of explosive resistance training on titin and myosin heavy chain isoforms in trained subjects. *J Strength Cond Res* **17,** 645–651.

Meyer GA & Lieber RL (2011). Elucidation of extracellular matrix mechanics from muscle fibers and fiber bundles. *J Biomech* **44,** 771–773.

Miller MS, Bedrin NG, Ades PA, Palmer BM & Toth MJ (2015). Molecular determinants of force production in human skeletal muscle fibers: effects of myosin isoform expression and cross-sectional area. *Am J Physiol-Cell Physiol* **308,** C473–C484.

Miller MS, Callahan DM & Toth MJ (2014). Skeletal muscle myofilament adaptations to aging, disease, and disuse and their effects on whole muscle performance in older adult humans. *Front Physiol* **5,** 369.

Miller MS, VanBuren P, LeWinter MM, Braddock JM, Ades PA, Maughan DW, Palmer BM & Toth MJ (2010). Chronic heart failure decreases cross-bridge kinetics in single skeletal muscle fibres from humans. *J Physiol* **588,** 4039–4053.

Miller MS, VanBuren P, LeWinter MM, Lecker SH, Selby DE, Palmer BM, Maughan DW, Ades PA & Toth MJ (2009). Mechanisms underlying skeletal muscle weakness in human heart failure: alterations in single fiber myosin protein content and function. *Circ Heart Fail* **2,** 700–706.

Minajeva A, Kulke M, Fernandez JM & Linke WA (2001). Unfolding of titin domains explains the viscoelastic behavior of skeletal myofibrils. *Biophys J* **80,** 1442–1451.

Mongold SJ, Ricci AW, Hahn ME & Callahan DM (2022). Skeletal Muscle Compliance and Echogenicity in Resistance-Trained and Nontrained Women. *J Strength Cond Res*10–1519.

Morrison S, Colberg SR, Parson HK, Neumann S, Handel R, Vinik EJ, Paulson J & Vinik AI (2016). Walking-induced fatigue leads to increased falls risk in older adults. *J Am Med Dir Assoc* **17,** 402–409.

Morse C, Spencer J, Hussain A & Onambélé-Pearson G (2013). The effect of the oral contraceptive pill on the passive stiffness of the human gastrocnemius muscle in vivo. *J Musculoskelet Neuronal Interact* **13,** 97–104.

Morse CI (2011). Gender differences in the passive stiffness of the human gastrocnemius muscle during stretch. *Eur J Appl Physiol* **111,** 2149–2154.

Morton JP, Kayani AC, McArdle A & Drust B (2009). The Exercise-Induced Stress Response of Skeletal Muscle, with Specific Emphasis on Humans: *Sports Med* **39,** 643–662.

Moss RL (1979). Sarcomere length-tension relations of frog skinned muscle fibres during calcium activation at short lengths. *J Physiol* **292,** 177–192.

Müller AE, Kreiner M, Kötter S, Lassak P, Bloch W, Suhr F & Krüger M (2014). Acute exercise modifies titin phosphorylation and increases cardiac myofilament stiffness. *Front Physiol* **5,** 449.

Münster S, Jawerth LM, Leslie BA, Weitz JI, Fabry B & Weitz DA (2013). Strain history dependence of the nonlinear stress response of fibrin and collagen networks. *Proc Natl Acad Sci* **110,** 12197–12202.

Myer GD, Ford KR, Paterno MV, Nick TG & Hewett TE (2008*a*). The effects of generalized joint laxity on risk of anterior cruciate ligament injury in young female athletes. *Am J Sports Med* **36,** 1073–1080.

Myer GD, Ford KR, Paterno MV, Nick TG & Hewett TE (2008*b*). The Effects of Generalized Joint Laxity on Risk of Anterior Cruciate Ligament Injury in Young Female Athletes. *Am J Sports Med* **36,** 1073–1080.

Neubauer O, Sabapathy S, Ashton KJ, Desbrow B, Peake JM, Lazarus R, Wessner B, Cameron-Smith D, Wagner K-H & Haseler LJ (2014). Time course-dependent changes in the transcriptome of human skeletal muscle during recovery from endurance exercise: from inflammation to adaptive remodeling. *J Appl Physiol* **116,** 274–287.

Nishikawa K (2016). Eccentric contraction: unraveling mechanisms of force enhancement and energy conservation. *J Exp Biol* **219,** 189–196.

Nishikawa K (2020). Titin: a tunable spring in active muscle. *Physiology* **35,** 209–217.

Nishikawa KC, Monroy JA, Powers KL, Gilmore LA, Uyeno TA & Lindstedt SL (2013). A molecular basis for intrinsic muscle properties: implications for motor control. In *Progress in Motor Control*, pp. 111–125. Springer.

Noonan AM, Mashouri P, Chen J, Power GA & Brown SH (2020*a*). Training Induced Changes to Skeletal Muscle Passive Properties Are Evident in Both Single Fibers and Fiber Bundles in the Rat Hindlimb. *Front Physiol* **11,** 907.

Noonan AM, Mazara N, Zwambag DP, Weersink E, Power GA & Brown SH (2020*b*). Age-related changes in human single muscle fibre passive elastic properties are sarcomere length dependent. *Exp Gerontol* **137,** 110968.

Noonan AM, Zwambag DP, Mazara N, Weersink E, Power GA & Brown SH (2020*c*). Fiber Type and Size as Sources of Variation in Human Single Muscle Fiber Passive Elasticity. *J Biomech Eng*.

Ottenheijm CA, Voermans NC, Hudson BD, Irving T, Stienen GJ, Van Engelen BG & Granzier H (2012). Titin-based stiffening of muscle fibers in Ehlers-Danlos Syndrome. *J Appl Physiol* **112,** 1157–1165.

Paroo Z, Dipchand ES & Noble EG (2002). Estrogen attenuates postexercise HSP70 expression in skeletal muscle. *Am J Physiol-Cell Physiol* **282,** C245–C251.

Paulo JA, McAllister FE, Everley RA, Beausoleil SA, Banks AS & Gygi SP (2015). Effects of MEK inhibitors GSK1120212 and PD0325901 in vivo using 10-plex quantitative proteomics and phosphoproteomics. *Proteomics* **15,** 462–473.

Pavan P, Monti E, Bondí M, Fan C, Stecco C, Narici M, Reggiani C & Marcucci L (2020). Alterations of Extracellular Matrix Mechanical Properties Contribute to Age-Related Functional Impairment of Human Skeletal Muscles. *Int J Mol Sci* **21,** 3992.

Pedersen TH, Nielsen OB, Lamb GD & Stephenson DG (2004). Intracellular Acidosis Enhances the Excitability of Working Muscle. *Science* **305,** 1144–1147.

Pellegrino A, Tiidus PM & Vandenboom R (2022). Mechanisms of Estrogen Influence on Skeletal Muscle: Mass, Regeneration, and Mitochondrial Function. *Sports Med* **52,** 2853–2869.

Pellegrino J, Ruby BC & Dumke CL (2016). Effect of plyometrics on the energy cost of running and MHC and titin isoforms. *Med Sci Sports Exerc* **48,** 49–56.

Piasecki M, Ireland A, Jones DA & McPhee JS (2016*a*). Age-dependent motor unit remodelling in human limb muscles. *Biogerontology* **17,** 485–496.

Piasecki M, Ireland A, Piasecki J, Stashuk DW, Swiecicka A, Rutter MK, Jones DA & McPhee JS (2018). Failure to expand the motor unit size to compensate for declining motor unit numbers distinguishes sarcopenic from non-sarcopenic older men. *J Physiol* **596,** 1627–1637.

Piasecki M, Ireland A, Stashuk D, Hamilton-Wright A, Jones DA & McPhee JS (2016*b*). Age-related neuromuscular changes affecting human vastus lateralis. *J Physiol* **594,** 4525–4536.

Pinnell RAM, Mashouri P, Mazara N, Weersink E, Brown SHM & Power GA (2019). Residual force enhancement and force depression in human single muscle fibres. *J Biomech* **91,** 164–169.

Plubell DL, Wilmarth PA, Zhao Y, Fenton AM, Minnier J, Reddy AP, Klimek J, Yang X, David LL & Pamir N (2017). Extended multiplexing of tandem mass tags (TMT) labeling reveals age and high fat diet specific proteome changes in mouse epididymal adipose tissue. *Mol Cell Proteomics* **16,** 873–890.

Power GA, Makrakos DP, Rice CL & Vandervoort AA (2013). Enhanced force production in old age is not a far stretch: an investigation of residual force enhancement and muscle architecture. *Physiol Rep*; DOI: 10.1002/phy2.4.

Power GA, Rice CL & Vandervoort AA (2012). Increased residual force enhancement in older adults is associated with a maintenance of eccentric strength. *PloS One* **7,** e48044.

Prado LG, Makarenko I, Andresen C, Krüger M, Opitz CA & Linke WA (2005). Isoform diversity of giant proteins in relation to passive and active contractile properties of rabbit skeletal muscles. *J Gen Physiol* **126,** 461–480.

Privett GE, Needham KW, Ricci AW, Mongold SJ & Callahan DM (2021). Protein Kinase A Modifies Skeletal Muscle Contractile Function Via Modification Of Mybp-C: 386. *Med Sci Sports Exerc* **53,** 121.

Privett GE, Ricci AW, David LL, Wiedenfeld Needham K, Tan YH, Nakayama KH & Callahan DM (2024*a*). Fatiguing exercise reduces cellular passive Young's modulus in human vastus lateralis muscle. *Exp Physiol*EP092072.

Privett GE, Ricci AW, Ortiz-Delatorre J & Callahan DM (2024*b*). Predicting Myosin Heavy Chain Isoform from Post-Dissection Fiber Length in Human Skeletal Muscle Fibers. *Am J Physiol-Cell Physiol*; DOI: 10.1152/ajpcell.00700.2023.

Ricci A, Privett G, Needham K & Callahan D (2023). Acute fatigue induces paradoxical increases in velocity and power in a sex and myosin isoform dependent manner. *Physiology* **38,** 5734486.

Rivas-Pardo JA, Eckels EC, Popa I, Kosuri P, Linke WA & Fernández JM (2016). Work Done by Titin Protein Folding Assists Muscle Contraction. *Cell Rep* **14,** 1339–1347.

Robinett JC, Hanft LM, Geist J, Kontrogianni-Konstantopoulos A & McDonald KS (2019). Regulation of myofilament force and loaded shortening by skeletal myosin binding protein C. *J Gen Physiol* **151,** 645–659.

Romani WA & Russ DW (2013). Acute effects of sex-specific sex hormones on heat shock proteins in fast muscle of male and female rats. *Eur J Appl Physiol* **113,** 2503–2510.

Ryall JG, Schertzer JD & Lynch GS (2007). Attenuation of age-related muscle wasting and weakness in rats after formoterol treatment: therapeutic implications for sarcopenia. *J Gerontol A Biol Sci Med Sci* **62,** 813–823.

Salcan S, Bongardt S, Barbosa DM, Efimov IR, Rassaf T, Krüger M & Koetter S (2020). Elastic titin properties and protein quality control in the aging heart. *Biochim Biophys Acta BBA-Mol Cell Res* **1867,** 118532.

Sarvazyan A, Rudenko O, Aglyamov S & Emelianov S (2014). Muscle as a molecular machine for protecting joints and bones by absorbing mechanical impacts. *Med Hypotheses* **83,** 6–10.

Schiaffino S & Reggiani C (2011). Fiber Types in Mammalian Skeletal Muscles. *Physiol Rev* **91,** 1447–1531.

Siracusa J, Charlot K, Malgoyre A, Conort S, Tardo-Dino P-E, Bourrilhon C & Garcia-Vicencio S (2019). Resting muscle shear modulus measured with ultrasound shear-wave elastography as an alternative tool to assess muscle fatigue in humans. *Front Physiol* **10,** 626.

Stevens JA (2005). Gender differences for non-fatal unintentional fall related injuries among older adults. *Inj Prev* **11,** 115–119.

Straight CR, Ades PA, Toth MJ & Miller MS (2018). Age-related reduction in single muscle fiber calcium sensitivity is associated with decreased muscle power in men and women. *Exp Gerontol* **102,** 84–92.

Strickler T, Malone T & Garrett WE (1990). The effects of passive warming on muscle injury. *Am J Sports Med* **18,** 141–145.

Stromberg DD & Wiederhielm CA (1969). Viscoelastic description of a collagenous tissue in simple elongation. *J Appl Physiol* **26,** 857–862.

Stupka N, Lowther S, Chorneyko K, Bourgeois JM, Hogben C & Tarnopolsky MA (2000). Gender differences in muscle inflammation after eccentric exercise. *J Appl Physiol* **89,** 2325–2332.

Suetta C, Haddock B, Alcazar J, Noerst T, Hansen OM, Ludvig H, Kamper RS, Schnohr P, Prescott E & Andersen LL (2019). The Copenhagen Sarcopenia Study: lean mass,

strength, power, and physical function in a Danish cohort aged 20–93 years. *J Cachexia Sarcopenia Muscle* **10,** 1316–1329.

Suetta C, Hvid LG, Justesen L, Christensen U, Neergaard K, Simonsen L, Ortenblad N, Magnusson SP, Kjaer M & Aagaard P (2009). Effects of aging on human skeletal muscle after immobilization and retraining. *J Appl Physiol* **107,** 1172–1180.

Tarnopolsky MA, Pearce E, Smith K & Lach B (2011). Suction-modified Bergström muscle biopsy technique: Experience with 13,500 procedures. *Muscle Nerve* **43,** 716–725.

The UniProt Consortium (2023). UniProt: the Universal Protein Knowledgebase in 2023. *Nucleic Acids Res* **51,** D523–D531.

Thorstensson A & Karlsson J (1976). Fatiguability and Fibre Composition of Human Skeletal Muscle. *Acta Physiol Scand* **98,** 318–322.

Tonino P, Kiss B, Strom J, Methawasin M, Smith JE, Kolb J, Labeit S & Granzier H (2017). The giant protein titin regulates the length of the striated muscle thick filament. *Nat Commun* **8,** 1041.

Tudor-Locke C, Burkett L, Reis JP, Ainsworth BE, Macera CA & Wilson DK (2005). How many days of pedometer monitoring predict weekly physical activity in adults? *Prev Med* **40,** 293–298.

Udaka J, Ohmori S, Terui T, Ohtsuki I, Ishiwata S, Kurihara S & Fukuda N (2007). Disuse-induced Preferential Loss of the Giant Protein Titin Depresses Muscle Performance via Abnormal Sarcomeric Organization. *J Gen Physiol* **131,** 33–41.

Wang Y, Li X, Li Z, Li M, Zhu J & Zhang D (2018). Changes in degradation and phosphorylation level of titin in three ovine muscles during postmortem. *Int J Food Sci Technol* **53,** 913–920.

Wang Y, Li X, Zhang D, Li Z, Xu B & Zhu J (2023). Effect of titin phosphorylation on degradation of titin from skeletal muscles. *Food Sci Hum Wellness* **12,** 1184–1191.

Ward SR, Winters TM, O'Connor SM & Lieber RL (2020). Non-linear scaling of passive mechanical properties in fibers, bundles, fascicles and whole rabbit muscles. *Front Physiol*.

Watanabe D, Lamboley CR & Lamb GD (2020). Effects of S-glutathionylation on the passive force–length relationship in skeletal muscle fibres of rats and humans. *J Muscle Res Cell Motil* **41,** 239–250.

Watsford ML, Murphy AJ, McLachlan KA, Bryant AL, Cameron ML, Crossley KM & Makdissi M (2010). A Prospective Study of the Relationship between Lower Body Stiffness and Hamstring Injury in Professional Australian Rules Footballers. *Am J Sports Med* **38,** 2058–2064.

Willems MET & Huijing PA (1994). Heterogeneity of mean sarcomere length in different fibres: effects on length range of active force production in rat muscle. *Eur J Appl Physiol* **68,** 489–496.

Wilson GJ, Wood GA & Elliott BC (1991). The relationship between stiffness of the musculature and static flexibility: an alternative explanation for the occurrence of muscular injury. *Int J Sports Med* **12,** 403–407.

Wilson JM & Flanagan EP (2008). The Role of Elastic Energy in Activities with High Force and Power Requirements: A Brief Review. *J Strength Cond Res* **22,** 1705–1715.

Witvrouw E, Mahieu N, Danneels L & McNair P (2004). Stretching and Injury Prevention. *Sports Med*7.

Wood LK, Kayupov E, Gumucio JP, Mendias CL, Claflin DR & Brooks SV (2014). Intrinsic stiffness of extracellular matrix increases with age in skeletal muscles of mice. *J Appl Physiol* **117,** 363–369.

Wu Y, Bell SP, Trombitas K, Witt CC, Labeit S, LeWinter MM & Granzier H (2002). Changes in Titin Isoform Expression in Pacing-Induced Cardiac Failure Give Rise to Increased Passive Muscle Stiffness. *Circulation* **106,** 1384–1389.

Wu Y, Cazorla O, Labeit D, Labeit S & Granzier H (2000). Changes in Titin and Collagen Underlie Diastolic Stiffness Diversity of Cardiac Muscle. *J Mol Cell Cardiol* **32,** 2151–2161.

Yamaguchi T, Arai H, Katayama N, Ishikawa T, Kikumoto K & Atomi Y (2007). Age-Related Increase of Insoluble, Phosphorylated Small Heat Shock Proteins in Human Skeletal Muscle. *J Gerontol Ser A* **62,** 481–489.

Yamamoto K (1986). The binding of skeletal muscle C-protein to regulated actin. *FEBS Lett* **208,** 123–127.

Yamasaki R, Wu Y, McNabb M, Greaser M, Labeit S & Granzier H (2002). Protein Kinase A Phosphorylates Titin's Cardiac-Specific N2B Domain and Reduces Passive Tension in Rat Cardiac Myocytes. *Circ Res* **90,** 1181–1188.

Yoh K, Ikeda K, Horie K & Inoue S (2023). Roles of estrogen, estrogen receptors, and estrogen-related receptors in skeletal muscle: regulation of mitochondrial function. *Int J Mol Sci* **24,** 1853.

Young RB, Bridge KY & Strietzel CJ (2000). Effect of electrical stimulation on β-adrenergic receptor population and cyclic AMP production in chicken and rat skeletal muscle cell cultures. *Vitro Cell Dev Biol - Anim* **36,** 167.

Zimmerman SD, Thomas DP, Velleman SG, Li X, Hansen TR & McCormick RJ (2001). Time course of collagen and decorin changes in rat cardiac and skeletal muscle post-MI. *Am J Physiol-Heart Circ Physiol* **281,** H1816–H1822.